

We had previously been working with a magnesium zirconate system for a rocket engine application which looked promising. We married this magnesium zirconate coating with a bond coat of nickel-aluminide materials which provided a much improved system over the old Rockide Z process. This magnesium process was substantiated in the JT11D-20 program and became the jet engine industry standard.

Magnesium zirconate is effective both as a thermal barrier and as a wear resistant coating. As a thermal barrier it is applied to burner cans, burner-to-turbine transition ducts, selected turbine parts, afterburner liners, flame holders and nozzle flap seals. For wear resistance it is applied to the afterburner nozzle synchronizing ring, afterburner combustion duct, burner pressure probes and burner can clamps.

Tungsten carbide coatings were specially developed to produce an acceptable blend hard enough to resist wear yet not brittle enough to be susceptible to cracking. These coatings are applied to compressor blade midspan shrouds.

Two unique specifications were created for chromium carbide coatings to be applied to bearing compartment sealing parts. These coatings must be hard enough to resist wear while constantly being rubbed by a carbon seal yet ductile enough to not crack under the temperatures generated by this rubbing.

Plasma and thermal spray equipment, a means for applying ceramic coating, had only been introduced to the jet engine industry a few years earlier. Pratt & Whitney soon became a leader in this infant thermal spray coating technology. We worked directly with the only two known equipment manufacturing companies in existence at that time to develop a plasma gun that would produce coating densities greater than 85%. We also worked with new bond coat materials for the ceramic that would provide both oxidation and thermal resistance at elevated temperatures. Surface preparation prior to the bond coat was developed. Parameters for the plasma gun such as amperage, voltage, primary and secondary inert gas flow rates, stand off distances and gun travel rates were established. No automation existed at that time and we were operator dependent on gun travel speed to provide an acceptable coating without burning up the hardware. It was quite a challenge for the young Materials Engineers to optimize hand held energy with temperatures equivalent to the sun's. We were creating plasma energy utilizing helium, argon and hydrogen with temperatures of 20,000°F. Dwell time of the ceramic particles within this ionized gas stream were micro-seconds. The actual coating process was quick. We were coating liners up to 52 inches in diameter in just a short period of time. During this investigation/development period we evaluated various experimental coating materials to provide oxidation and thermal shock resistance.

New methods of automation have since been introduced for plasma coating. It is now a computer controlled process that provides a reliable method for depositing a wide variety of wear resistant coatings in addition to ceramic coatings. New repair methods utilizing the plasma technology have been established and are used in JT11D-20 engine maintenance.

### 4.3 Problems

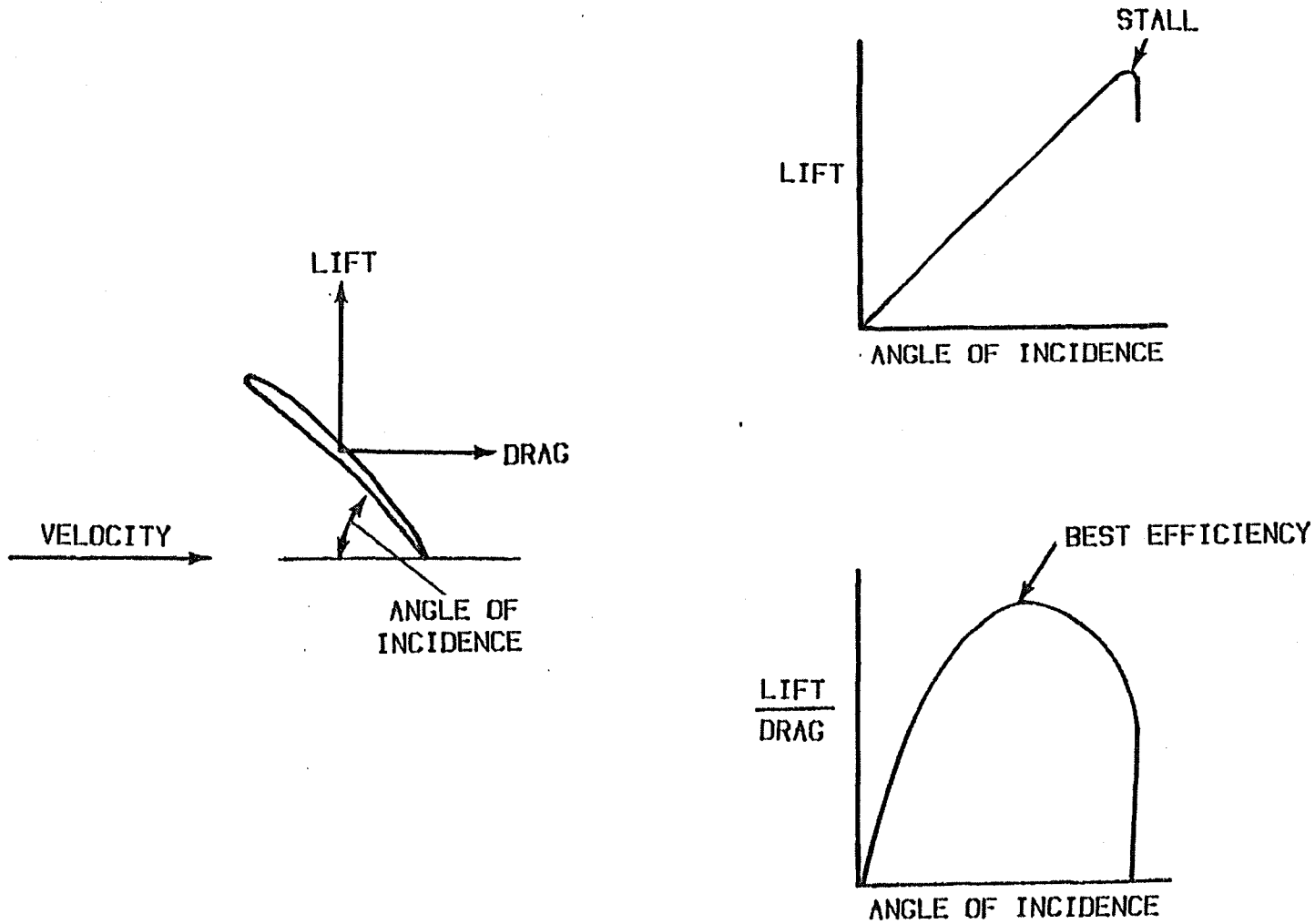
Several production problems never before encountered were experienced. We had to learn how to form sheet metal from materials which previously had been used only for forging turbine blades. Once we had achieved this, we had to learn how to weld it successfully. Disks, shafts, and other components also had to be fabricated from high-strength, temperature-resistant turbine blade-like materials to withstand temperatures and stresses encountered. There was not a single part, down to the last cotter key, that could be made from the same materials as used on previous engines. Other problems were substandard material properties in sheets and forgings of new alloys never before processed in these forms or quantities, delays in procurement of turbine blades and vanes to meet the stringent quality standards required for operation at high turbine inlet temperature. Problems of this sort always arise in early production engines whenever major advances in materials technology are made. The introduction of titanium into production engines is an earlier example of this phenomenon: the engine development process alone frequently does not answer all of the fabrication and quality control problems that must be solved early in the production cycle if reliable and durable engines are to be obtained.

### 4.4 High Temperature Materials Are Expensive

In engines designed for subsonic or supersonic dash operations, Titanium is considered to be a relatively expensive material. In an engine designed to operate continuously at compressor inlet temperatures up to 800°F, Titanium must be replaced both in the rotor and static structure by more expensive high temperature alloys. An example of the increased material costs may be found in the first stage Astroloy turbine disk forgings, which originally cost \$8,300 (in 1962 dollars) compared to \$250.00 for AMS 5616 disk forgings used in JT3D engines. These high temperature alloys are not only more expensive as raw material, but also require more time to machine and to fabricate. However, anytime a new material is introduced it is more expensive until its production becomes routine. Functional components such as controls and pumps are also more expensive than for previous engines because of the increased accuracy requirements for the new wider range of flight conditions and more expensive materials that are more difficult to fabricate.

FIGURE 1.

# AERODYNAMICS OF A SINGLE AIRFOIL



-18-

323

## 5. JT11D-20 CYCLE SELECTION

At high supersonic flight speeds, high inlet temperature causes the following problems in a conventional turbojet engine.

- A single-spool, fixed-geometry compressor runs out of surge margin.
- The combination of high inlet temperature and limited turbine temperature gives lower cycle efficiency. This reduces thrust and increases fuel consumption.
- Compressor efficiency deteriorates because the front stages of the compressor are stalled. This also reduces thrust and increases fuel consumption.
- Compressor blades may be subjected to high stress from the combination of high rotational speed and flutter from stall in the front stages.
- The combination of high turbine temperature and high temperature surrounding the engine results in cooling problems for the afterburner duct.

The JT11D-20 bleed bypass engine cycle eliminates these problems or reduces their severity.

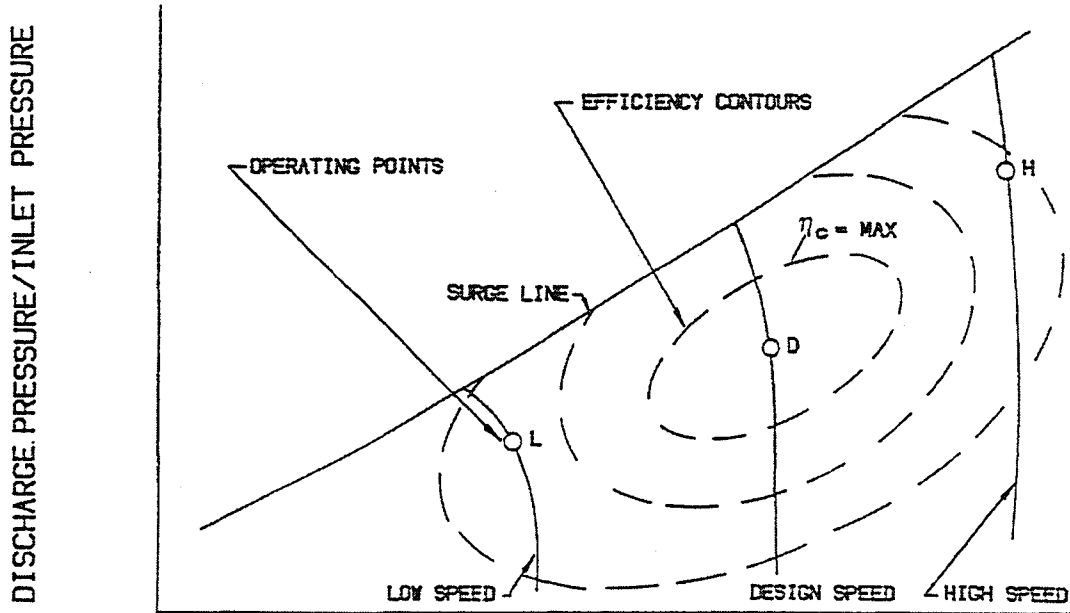
### 5.1 Compressor

5.1.1 Stage Matching When an isolated airfoil is tested in a wind tunnel, the lift increases with angle of incidence until the airfoil stalls when there is a sharp drop in lift as shown in Figure 11. The optimum lift-to-drag ratio, which can be considered as the most efficient operating point of the airfoil, occurs at an intermediate incidence between zero incidence and stall.

When airfoils are placed in a cascade to form the rotor or stator of a compressor stage they usually have a larger incidence range before stall than an isolated airfoil of the same shape and there is three dimensional flow induced by centrifugal force and tip effects.

FIGURE 12

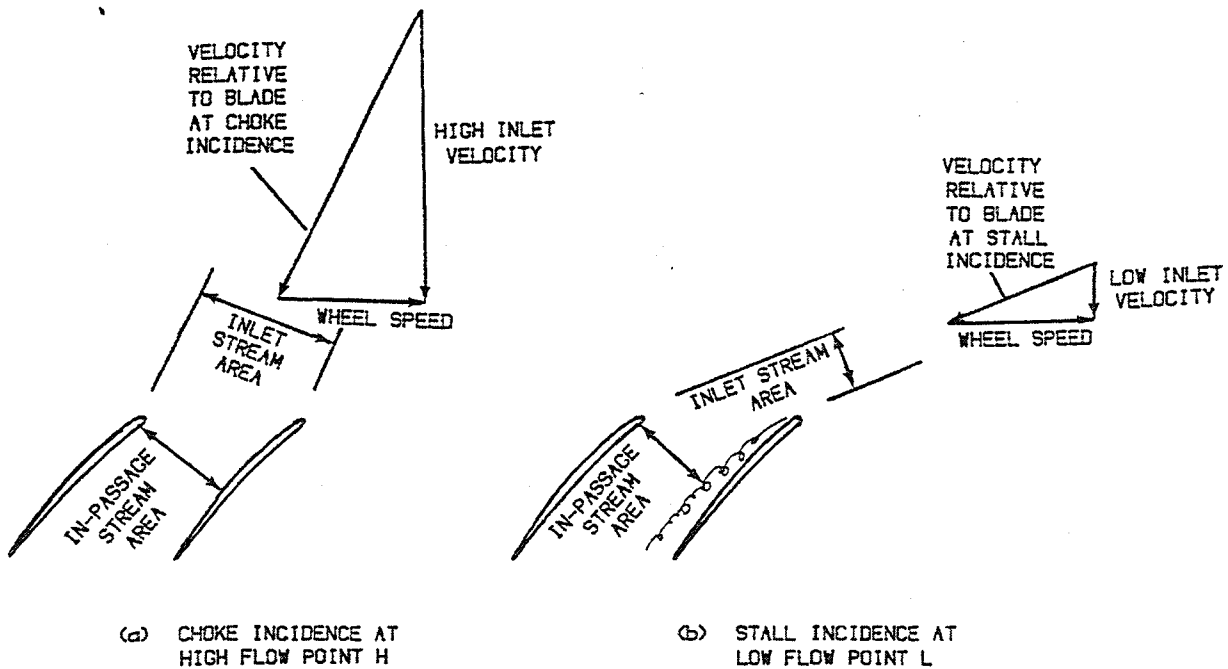
TYPICAL COMPRESSOR MAP



CORRECTED INLET AIRFLOW

FIGURE 13

CHOKE AND STALL OF COMPRESSOR BLADES



5

Compressor performance is usually presented on a compressor map. Figure 12 shows a typical compressor map for an axial-flow multistage compressor. The pressure ratio between inlet and discharge pressures is presented as a function of corrected airflow at constant values of rotor speed. Efficiency contours (dashed lines) show the ratio of work output to ideal work. The airfoil incidence increases as pressure ratio is increased along a constant speed line. After some airfoils in the compressor reach stall incidence, a sector of the flowpath can have reverse flow. This is called rotating stall because the sector rotates, usually at half compressor speed. A more violent type of flow instability is called surge. When surge occurs, the entire flow in the compressor is reversed. The surge line on a compressor map shows the limit of stable operation.

Three typical engine operating points are shown on Figure 12: "L", "D", and "H". Point L is a low corrected airflow condition that might occur at high flight Mach number. Point H is a high corrected airflow condition that corresponds to maximum power. Point D, between these extremes, represents the design point or maximum efficiency condition. It is a compromise between the requirements of L and H. At the design point the airfoils, (compressor blades and vanes) are at near optimum incidence and the flow areas are sized for this design corrected airflow.

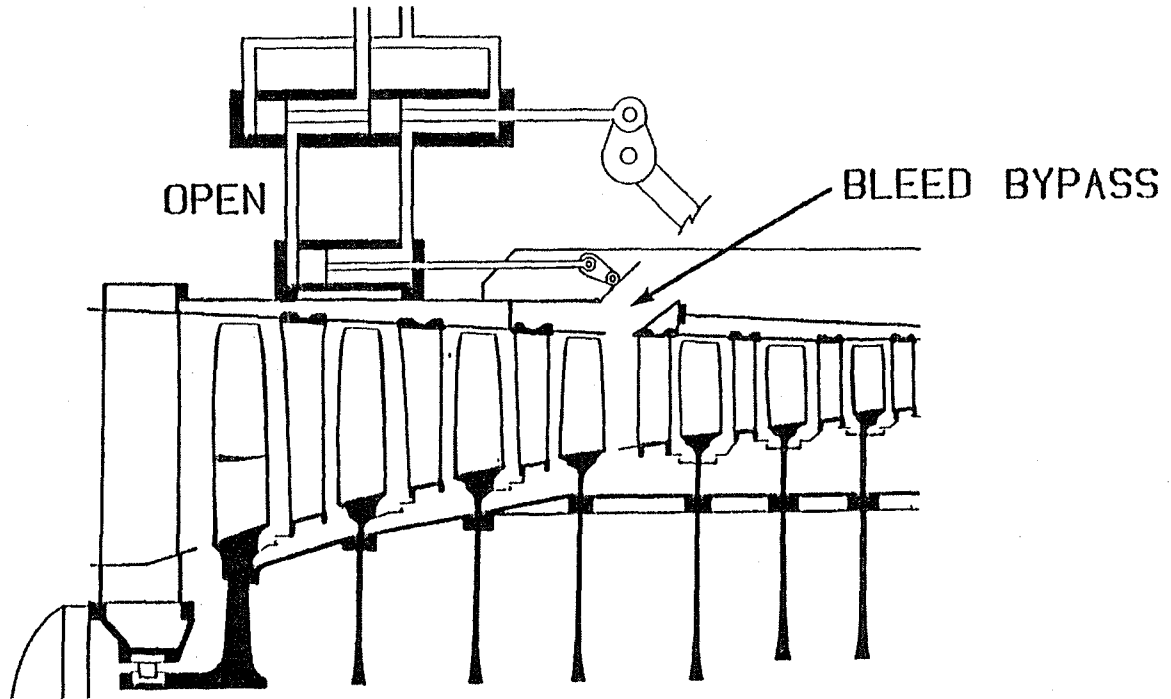
At the high corrected flow of point H, the airflow is restricted by the front stages of the compressor, which are said to be choked. In contrast, at the low corrected flow of point L, the reduction in flow is greater than the reduction of wheel speed. Consequently the inlet velocity is reduced relative to the rotational velocity. This moves the angle of incidence relative to the blade to stall. The difference between choke and stall incidence, and the respective velocity diagrams is illustrated by the exaggerated sketch in Figure 13. The difference between choke and stall incidence, is less than  $10^\circ$  for typical compressor airfoils. At choke incidence, it can be seen that the inlet stream area is larger than the in-passage stream area, consequently flow is restricted. Conversely, at stall incidence, the inlet stream area is less than the area between the blades. This results in diffusion and separation from the suction surface of the blade.

When the front stages of the compressor are choked, not only is flow restricted but more compression per stage is accomplished at H than at D because of the higher rotational speed of the blades. Therefore, in the rear stages, the density is higher, consequently, the axial velocity is lower than design, and the incidence on the rear stages move towards stall. Conversely, when the front stages of the compressor are stalled, less compression per stage is accomplished at L. The density in the rear stages is lower, the axial velocity higher and the rear stages move towards choke incidence.

The bleed bypass is located aft of the 4th compressor rotor, as shown in Figure 14. Opening this bleed permits more air to pass through the front stages. This unstalls them. Consequently, they operate more efficiently and the compressor has more surge margin.

FIGURE 14

BLEED BYPASS LOCATION

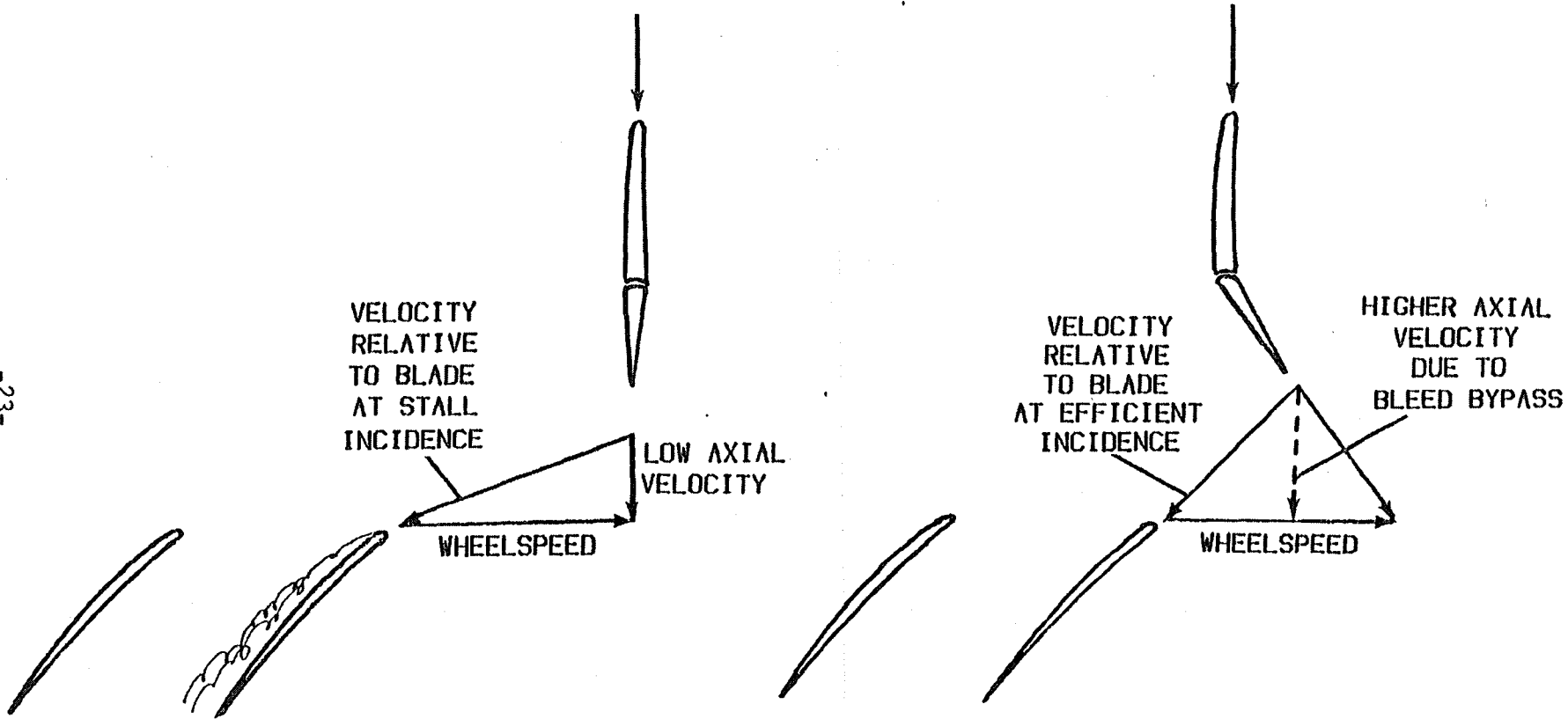


-22-

32M

COMBINATION OF BLEED BYPASS AND CAMBERED INLET GUIDE VANES ELIMINATES FIRST STAGE STALL

-23-



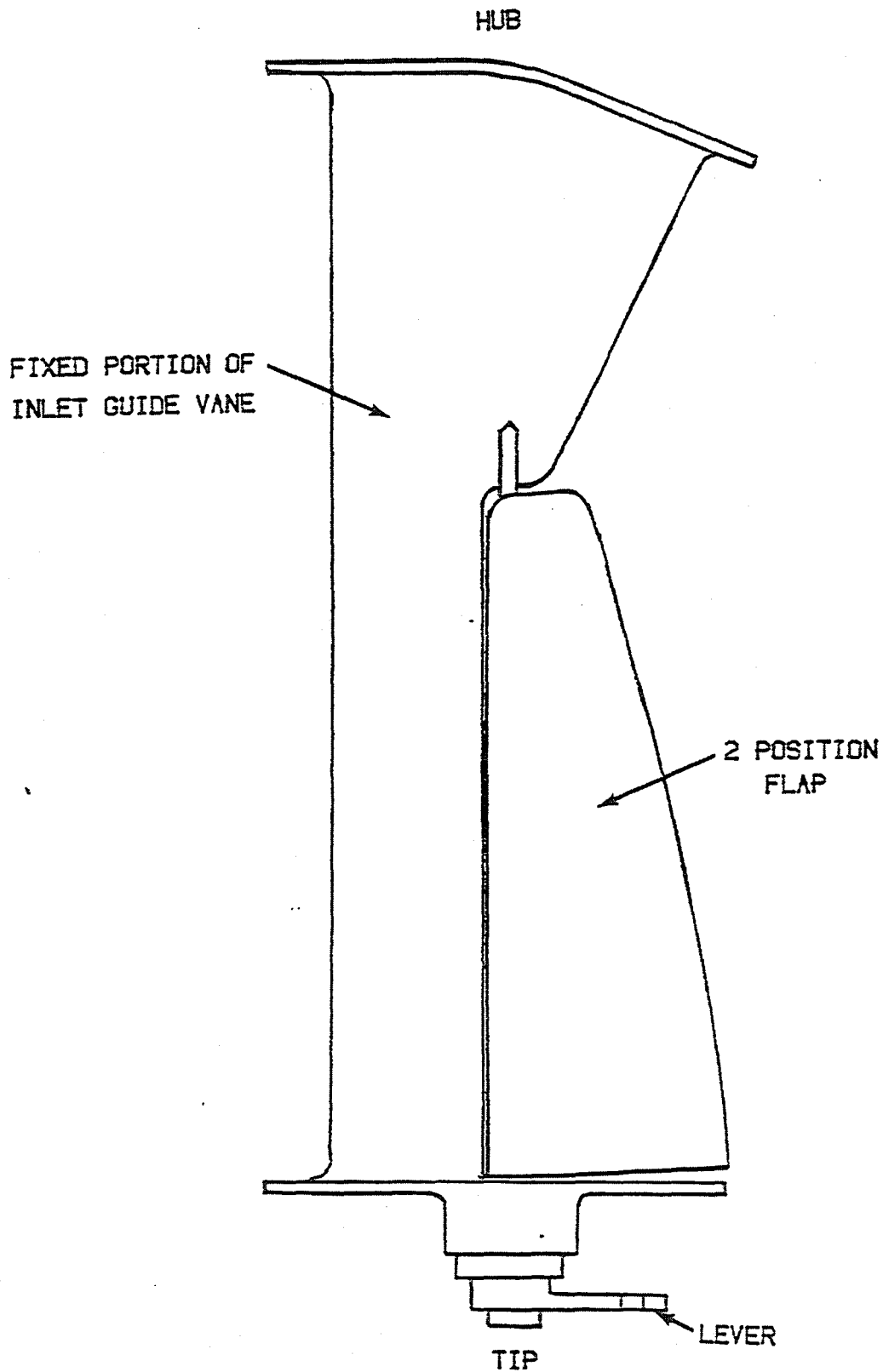
- (a) ● LOW AXIAL VELOCITY
- AXIAL INLET GUIDE VANE

- (b) ● HIGHER AXIAL VELOCITY DUE TO BLEED BYPASS
- CAMBERED INLET GUIDE VANE

328



**FIGURE 16**  
**VARIABLE CAMBER INLET GUIDE VANE**



### 5.1.2 Variable Camber Inlet Guide Vanes

Early JT11D-20 engines had permanently cambered inlet guide vanes to give best high Mach number performance (point L on Figure 12). An axial inlet guide vane gave more airflow and more thrust for transonic flight (point H on Figure 12). A two-position, variable-camber, inlet guide vane enables high performance at both operating conditions. Figure 15 illustrates the improved incidence match when the inlet guide vane is cambered for high Mach number, low-corrected flow operation. This improved incidence match improves both compressor efficiency and surge margin, and eliminates blade flutter at low corrected rotor speed.

Tests were run on several flap configurations to optimize subsonic airflow, supersonic flutter tolerance, and supersonic cruise efficiency. It was found that the best flap configuration was one that provided several degrees of pre-swirl at the tip and no swirl at the hub. The selected configuration has a flap of decreasing chord toward the hub as shown in Figure 16.

A variable camber inlet guide vane has the following advantages compared to a variable incidence guide vane:

- Better incidence match to engine inlet air
- Fixed portion of vanes used for bearing support and to accommodate oil pipes for bearing lubrication.

5.1.3 Airfoils The Mach number relative to the blades had been subsonic over the entire span in previous compressors. The higher rotational speeds and higher flow per unit area of this compressor resulted in Mach numbers significantly higher than 1.0. This meant that the blade passages contained shocks. Previous airfoil shapes had been NACA 400 or 65 series, which worked well at lower Mach numbers, but created strong shocks at high Mach numbers. Cascade testing had shown that circular-arc mean-camber line shapes had significantly lower losses than 65 series when the Mach number exceeded 0.8. As a result, circular-arc airfoils were used in the front 4 stages of the JT11D-20 compressor.

### 5.2 Increased Supersonic Thrust

Several approaches to the problem of increasing thrust in supersonic flight were investigated.

A brute force approach may be to build a larger compressor-engine combination; however a larger engine is heavier and the extra frontal area results in drag penalties. Both of these reduce range or payload.

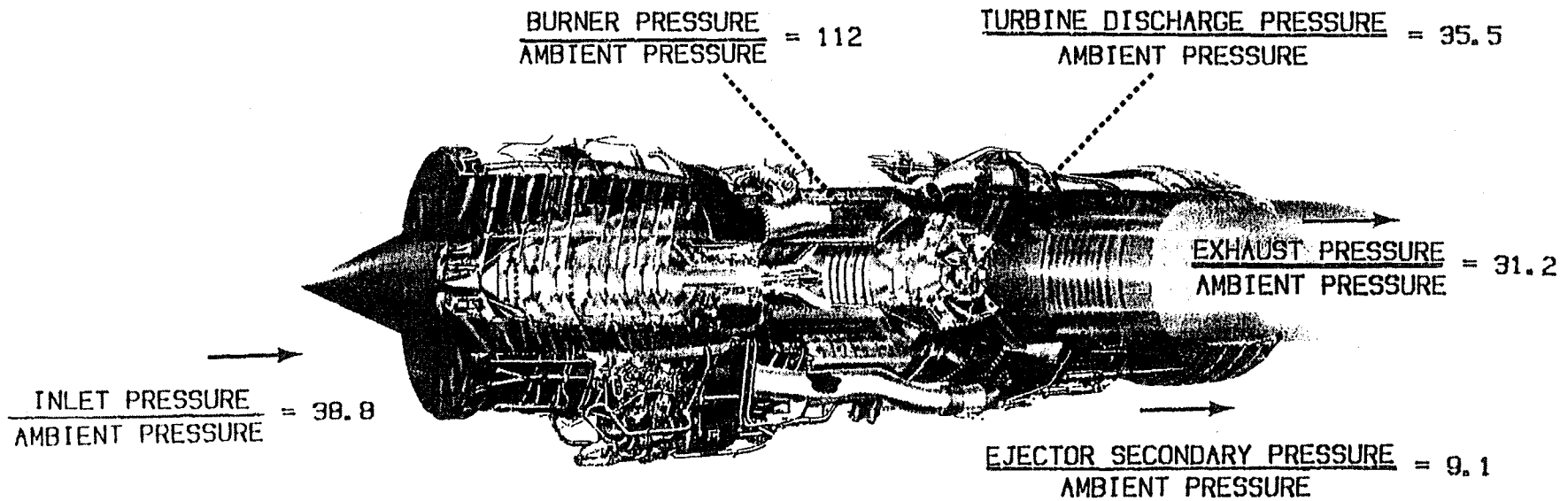
A second approach is to pre-cool the air entering the compressor by evaporating a liquid injected into the inlet. Water-alcohol solutions are often suggested. This scheme is called pre-compressor cooling and has three disadvantages. (1) The liquid consumption of the engine (fuel plus coolant) is high, which increases aircraft take-off weight. (2) The front stage compressor blades and vanes are subjected to impact by liquid droplets, which erodes them, and (3) smoke is often produced as a combustion product.

A third approach is to rotate the stator vanes mechanically to improve the air angles in both the front and rear stages. (As discussed in

FIGURE 17

TOTAL PRESSURES IN THE ENGINE AND NACELLE  
DURING SUPERSONIC CRUISE

---



Section 5.1.2, this approach was partially adopted during development with addition of a variable camber inlet guide vane). However, the turbine still provides a restriction against increased flow; so thrust increase due to variable stators is limited.

A fourth approach is to bypass the entire turbojet and utilize the afterburner as a ramjet. This configuration, known as a turbo-ramjet, is large and heavy because it must have the capacity to pass about equal corrected volume either through the turbojet or around it. Furthermore, the combustion efficiency is low relative to a turbojet. Again, this solution was partially adopted with the bleed bypass cycle which ducts part of the inlet air around the gas generator, but most of the air goes through the core engine. This conserves frontal area and heats the air for more efficient combustion.

The solution selected for this application is a variable cycle engine called the bleed bypass cycle. The JT11D-20 engine is an afterburning turbojet engine for takeoff and transonic flight, a low bypass ratio augmented turbofan for supersonic acceleration, it approximates a ramjet during high speed supersonic cruise and is a low bypass ratio turbofan during subsonic loiter.

Pressures throughout the engine are shown for supersonic cruise operation in Figure 17. The pressure at the nozzle exit is 80% of the pressure at the engine inlet. This pressure loss is typical of ramjet operation; in contrast to the pressure rise through the engine that is typical of turbojet operation. The high pressure ratio from inlet total pressure to ambient pressure (38.8:1) shows the importance of sealing the inlet. The primary exhaust nozzle pressure ratio (31.2:1) illustrates the need for an efficient nozzle. The secondary air pressure ratio 9.1:1 provides significant thrust from the secondary air.

### 5.3 Bleed Bypass Cycle

The bleed bypass cycle ducts air from the compressor middle stages into the afterburner, thus bypassing the flow restriction that exists in the rear compressor stages during supersonic flight, or subsonic flight at low power, and therefore improving airfoil incidence. This bleed air enters the afterburner at the same static pressure as the main flow and is heated in the afterburner during supersonic flight, so the bleed air produces almost as much thrust/lb of air as the main flow which passes through the rear compressor, burner and turbine.

The problems indicated earlier are solved or relieved as follows:

5.3.1 Surge Margin Increase obtained by opening the bleeds is 25% of the original surge margin during supersonic cruise. This surge margin increase is a combination of higher surge line due to better incidence matching and the lower operating line obtained by opening the bleeds.

5.3.2 Performance Improves With Bleed Bypass Engine - Figure 18 shows performance increments of the bleed bypass cycle compared to the same engine without the bypass bleed operating at the same rotor speed at a supersonic cruise Mach number (3+). The bleed bypass cycle gives 22% more airflow and 19% increase in net thrust. The net thrust increment from

FIGURE 18

## PERFORMANCE BENEFITS OF BLEED BYPASS CYCLE

### Bleeds Open Increment From Bleeds Closed Performance

Airflow <sup>1</sup>	+ 22%
Max Net Thrust <sup>1,2</sup>	+ 19%
Max Installed <sup>1,2,3</sup> Net Thrust	+ 47%
Installed Cruise <sup>1,3,4</sup> Fuel Consumption	-20%

---

<sup>1</sup> Constant Rotor Speed

<sup>2</sup> Constant Afterburner Exit Temperature

<sup>3</sup> Same Inlet And Nacelle, Surplus Air Spilled Through Forward Bypass

<sup>4</sup> At Cruise Thrust

bleeds closed performance is slightly lower than the airflow increment because the bleed bypass cycle has a lower exhaust pressure than the equivalent turbojet. This lower pressure is the result of higher pressure drop through the turbine, because the bleed air bypasses turbine, combined with pressure loss through the bleed bypass ducts.

The installed net thrust is the net thrust minus inlet drag. Inlet drag includes additive drag, spillage drag and inlet bleed drag. The comparison shown on Figure 18 assumes that the inlet and nacelle are sized for the bleed bypass engine and that the increased bleed required to match the inlet to the lower airflow of the turbojet engine is discharged through the forward bypass doors. The result of this bleed drag is to give a dramatic 47% installed thrust advantage for the bleed bypass engine.

When both engines are operated at the installed thrust level required for cruise flight the bypass bleed engine has a 20% advantage in fuel consumption, over the turbojet.

The performance advantage of the bleed bypass cycle is contingent on the assumptions used in the comparison: different assumptions will result in a different comparison. Key assumptions are discussed below.

Both engine cycles are assumed to operate at same afterburner exit temperature at maximum thrust. The bleed bypass cycle has bypass air to cool the outer afterburner duct while the turbojet cycle uses hotter turbine discharge air. Consequently, the bleed bypass cycle can operate to a higher afterburner temperature than a turbojet cycle without over-temperaturing the afterburner duct and nacelle at the high Mach numbers where the nacelle air surrounding the afterburner is hot. Conversely, if duct temperature and nacelle temperatures are not limiting, the turbojet can achieve higher average afterburner exit temperatures than a bleed bypass cycle because the gas near the walls is hotter and the afterburner efficiency of the turbojet is slightly higher.

Another key set of assumptions is the inlet and nacelle are sized for the bleed bypass cycle and that surplus inlet air is discharged through the forward bypass. An inlet designed for a turbojet engine would probably have a smaller capture area. This would reduce or eliminate the surplus inlet air penalty. But the inlet forebody drag is higher with a smaller capture area since the engine inlet diameter is the same for both cycles.

The penalty for taking the surplus air on board would be less if the air were discharged through the ejector rather than discharged through the forward bypass. Discharging the air through the ejector is only practical if there is sufficient room in the nacelle to duct surplus air to the ejector. More secondary airflow would also reduce the efficiency of the primary gas expansion.

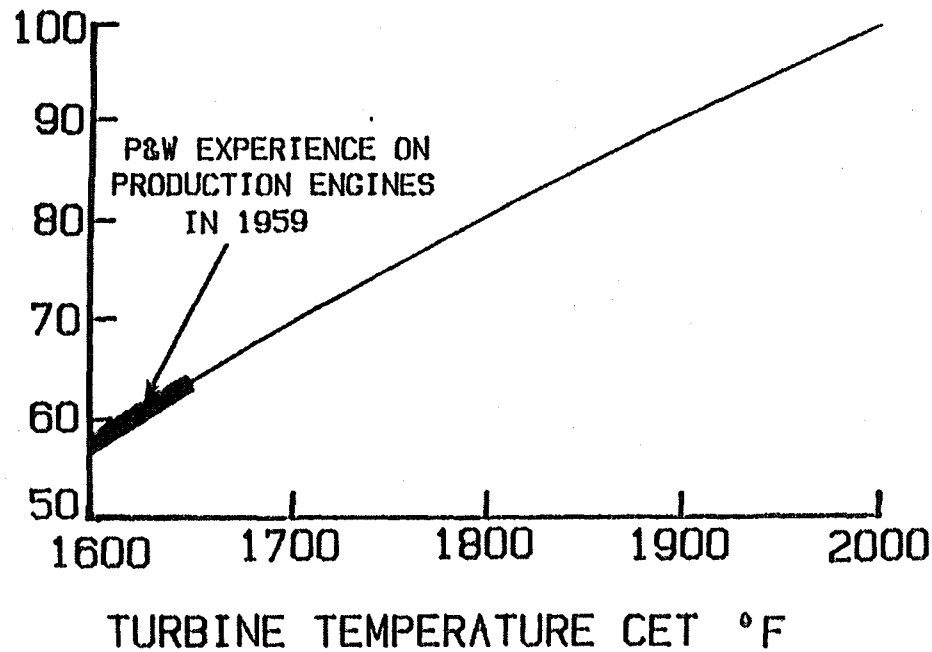
If the installed performance comparison were made with an inlet, nacelle and surplus air discharge optimized for each engine cycle then the installed net thrust advantage of the bleed bypass cycle would be greater than the net thrust advantage (19%) but less than the installed net thrust advantage shown in Figure 18 (47%).

FIGURE 19

# TURBINE TEMPERATURE REQUIREMENT FOR FLIGHT AT MACH 3+

---

INSTALLED  
NET THRUST  
% MAX



3  
5

5.3.3 Compressor Efficiency is increased by improving the angle of incidence to compressor airfoils in two areas. The first is in the front stages which operate more efficiently. Due to this improved performance the air is compressed more in the front stages, which in turn "unchokes" the rear stages when the bypass is opened.

5.3.4 Blade-Vane Fatigue caused by operating in stall is eliminated as stall is eliminated by opening the bypass bleeds.

5.3.5 Afterburner Cooling-the relatively cool bleed bypass air is discharged along the afterburner duct ahead of the afterburner liner, as shown on Figure 47. Consequently, bleed bypass air is used for afterburner cooling when the bleed bypass is open.

#### 5.4 Maximum Turbine Temperature

Maximum turbine temperature is an important driver in engine cycle selection. Higher turbine temperature results in more thrust/lb of airflow. Thrust/lb of airflow is particularly important for a supersonic application. Lower airflow means smaller engine and nacelle diameters and a smaller inlet and consequently less drag and lower thrust requirement. Higher turbine temperature also permits higher engine pressure ratio and operation to higher compressor inlet temperature. The SR71 mission requires operation to high compressor inlet temperature.

The engine thrust is sized at take-off for commercial aircraft and some military aircraft. For the SR71 aircraft, however, take-off is not a sizing point. Critical regimes for thrust sizing are transonic acceleration and high altitude supersonic cruise. The turbine temperature of production engines in 1959 would not give the required thrust for either transonic acceleration or supersonic cruise thrust. Figure 19 shows that P&W's turbine temperature experience in 1959 would only give about 60% of the JT11D-20 engine thrust at Mach 3+. This lower thrust level would decrease cruise altitude by about 11,000 ft and would result in 67% higher pressures in the engine and inlet and higher loads on the airframe.

The rapid thrust fall off when turbine temperature decreases, shown in Figure 19, is due to jet area constraint. Maximum afterburning during supersonic operation is close to maximum jet area. When turbine temperature is reduced at constant airflow there is a larger pressure drop across the turbine and the pressure in the afterburner is decreased. When maximum jet area is reached exhaust temperature has to be reduced, as afterburner pressure is reduced, in order to avoid suppressing rotor speed and airflow. Reduction in exhaust temperature and the reduction in exhaust pressure both reduce thrust. A combustor exit temperature (CET) of 2000°F was selected for the JT11D-20 engine cycle.

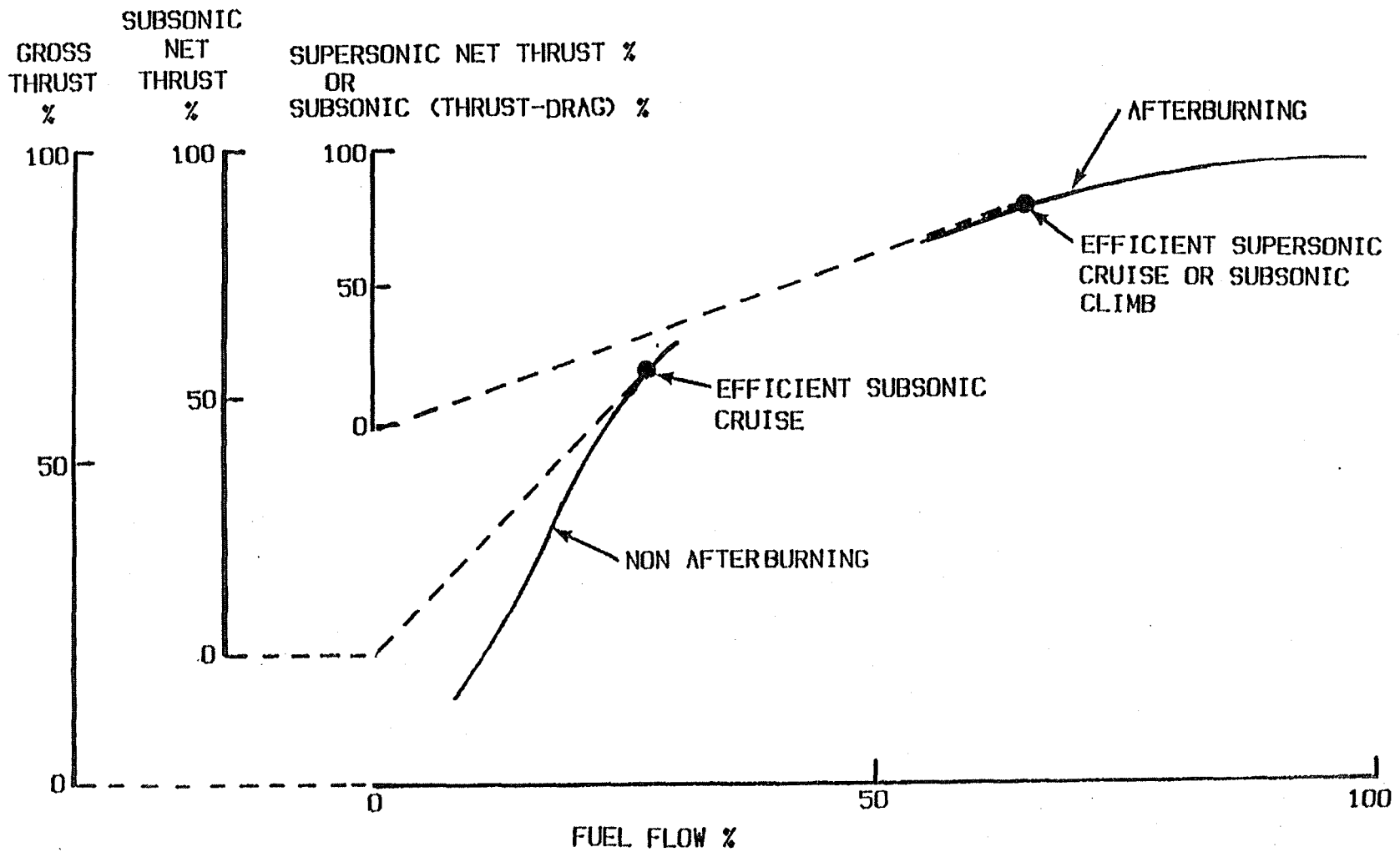
#### 5.5 Continuous Afterburning

Another feature of the JT11D-20 engine is the use of continuous afterburning for supersonic cruise. Afterburning increases thrust at the expense of increasing fuel flow. However, afterburning can be a



FIGURE

# AFTERBURNING GIVES BEST SUPERSONIC FUEL CONSUMPTION FOR THE JT11D-20 ENGINE



-32-

339

fuel-efficient mode of operation for a mission like the SR71 and an engine limited to the JT11D-20 turbine temperature, as shown below.

Figure 20 shows the relation between fuel flow and thrust of the JT11D-20 engine during sea level operation. The curve has been presented in terms of relative values to make it applicable over the flight envelope. There are three vertical scales. The outer scale shows gross thrust. The center scale shows net thrust (gross thrust minus ram drag) where the ram drag is the penalty for taking airflow on board at a subsonic cruise Mach number. The inner scale has two labels: "supersonic net thrust" reflects the higher ram drag at supersonic cruise speed while "subsonic net thrust minus drag" is the propulsive force available for climb or acceleration at some operating condition where the aircraft drag is assumed to be equal to the difference between the supersonic and subsonic ram drags. The best fuel efficiency is the highest value of propulsive force divided by fuel flow. This can be defined by a line from the origin to the highest point of the curve (the dashed lines on Figure 20). For subsonic cruise this occurs non-afterburning. However, afterburning gives the best fuel efficiency for both climb and supersonic cruise.

The Breguet range equation shows:

CRUISE RANGE is proportional to:  $\left(\frac{\text{NET THRUST}}{\text{FUEL FLOW}}\right) (\text{VELOCITY}) \left(\frac{\text{LIFT}}{\text{DRAG}}\right)$

For the example shown in Figure 20, subsonic cruise at Mach 0.8, 36,000 ft. altitude and supersonic cruise at Mach 3, 80,000 ft. altitude:

SUBSONIC CRUISE RANGE is proportional to:  $956 \left(\frac{\text{LIFT}}{\text{DRAG}}\right)_{\text{SUBSONIC}}$

SUPERSONIC CRUISE RANGE is proportional to:  $2190 \left(\frac{\text{LIFT}}{\text{DRAG}}\right)_{\text{SUPERSONIC}}$

Consequently, although the afterburning supersonic fuel flow is 2.4 times the subsonic fuel flow, this fuel flow penalty is offset by increased thrust and increased velocity so the supersonic range will be greater than the subsonic range if the supersonic lift/drag ratio is more than 44% of the subsonic lift/drag ratio. In addition to providing best fuel consumption for this engine cycle, afterburning also provides the additional thrust required to climb to and operate at the high cruise altitude.

### 5.7 Other Applications

In addition to the SR71 application, modifications to the JT11D-20 engine cycle were studied for applications with nuclear, hydrogen and methane fuels. A variation of the engine was also studied for a supersonic transport engine. None of these applications progressed beyond the study phase.

## 6. CONTROL SYSTEM

### 6.1 Control Parameters

The primary controllers are jet area, main fuel flow and afterburner fuel flow, as shown in Figure 21. In the JT11D-20 engine each controller is

**FIGURE 21**

**JT11D-20 PRIMARY CONTROL PARAMETERS**

<u>CONTROLLERS</u>	<u>SCHEDULED PARAMETERS (OPEN LOOP)</u>	<u>FEEDBACK PARAMETERS (CLOSED LOOP)</u>	<u>ENGINE SAFETY AND PERFORMANCE PARAMETERS</u>
JET AREA		ROTOR SPEED	{ Rotor Speed { Airflow { Surge Margin
MAIN FUEL FLOW	$\left( \frac{\text{MAIN FUEL FLOW}}{\text{BURNER PRESSURE}} \right)$	TURBINE EXIT TEMPERATURE	{ Turbine Inlet Temperature { Thrust
AFTERBURNER FUEL FLOW	$\left( \frac{\text{AFTERBURNER FUEL FLOW}}{\text{BURNER PRESSURE}} \right)$		{ Thrust { Afterburner Temperature { Screech

**FIGURE 22**

**JT11D-20 CONTROL SCHEDULES**

ROTOR SPEED		f (INLET TEMPERATURE)
MAIN FUEL CONTROL	$\left( \frac{\text{MAIN FUEL FLOW}}{\text{BURNER PRESSURE}} \right)$	f $\left( \begin{matrix} \text{ROTOR SPEED} \\ \text{INLET TEMPERATURE} \\ \text{BURNER PRESSURE} \end{matrix} \right)$
AFTERBURNER FUEL CONTROL	$\left( \frac{\text{AFTERBURNER FUEL FLOW}}{\text{BURNER PRESSURE}} \right)$	f (INLET TEMPERATURE)
TURBINE EXIT TEMPERATURE		f (INLET TEMPERATURE)
BLEED BYPASS		f $\left( \begin{matrix} \text{ROTOR SPEED} \\ \text{INLET TEMPERATURE} \end{matrix} \right)$
INLET GUIDE VANE CAMBER		f $\left( \begin{matrix} \text{ROTOR SPEED} \\ \text{INLET TEMPERATURE} \end{matrix} \right)$
START BLEEDS		f $\left( \begin{matrix} \text{ROTOR SPEED} \\ \text{INLET TEMPERATURE} \end{matrix} \right)$

independent of the other controllers. Jet area is modulated by a closed-loop control to obtain the required rotor speed and, therefore, to indirectly control airflow and surge margin. Open-loop control of main fuel flow is scheduled by the hydromechanical control to obtain the required value of main fuel flow to burner pressure ratio, which approximates the main burner fuel/air ratio and controls turbine inlet temperature. An electronic control provides vernier closed-loop control of turbine inlet temperature by sensing turbine exit temperature. Open-loop control of afterburner fuel flow is scheduled by the afterburner control to obtain the required value of afterburner fuel flow to main burner pressure ratio, which approximates afterburner fuel/air ratio and indirectly controls thrust and afterburner temperature and avoids afterburner screech. During a snap acceleration, the power lever moves into the afterburning region while the engine is still at low power. Afterburner fuel flow is inhibited until rotor speed accelerates to 85% of the scheduled value to prevent premature afterburning from back pressuring the turbine and slowing rotor acceleration.

These independent control loops have the disadvantage that action of each controller upsets the equilibrium of the other controllers. For example, consider pulling back the power lever to reduce thrust during afterburning operation. The afterburner control reduces afterburner fuel flow. This reduces thrust but also reduces afterburner pressure, increases the pressure drop across the turbine, reduces turbine discharge temperature and increases rotor speed. The main fuel flow is increased and jet area is reduced to re-establish the scheduled values of turbine discharge temperature and rotor speed, respectively. Each controller continues to disturb the other controllers in successively smaller increments until a new equilibrium point is reached. In contrast, a modern multi-variable control would simultaneously reduce afterburner fuel flow and jet area so that rotor speed and turbine temperature are not affected by this power lever transient. One multi-variable feature that was incorporated into the JT11D-20 control is opening the jet area when the afterburner is lit to minimize disturbance to the speed and turbine temperature controls.

In addition to the three primary, continuously variable, controllers there are two-position controllers that open and close the bleed bypass, camber and uncamber the inlet guide vanes and open and close the start bleeds, as shown in Figure 22. Figure 22 also shows that all the control schedules are functions of inlet temperature and that the majority of the schedules are also a function of rotor speed.

## 6.2 Control Constraints

In every engine control there are constraints to protect the engine and ensure satisfactory operation. The major constraints in the JT11D-20 control are shown in Figure 23. Maximum main burner fuel/air ratio is limited to prevent turbine over-temperature during transients. Maximum afterburner fuel/air ratio is limited to prevent screech and to prevent inefficient afterburner operation. Minimum fuel air ratio is limited in both the main burner and the afterburner to prevent blowout. Maximum rotor speed is limited for rotor structural integrity. Minimum rotor speed is limited above Mach 1.6 to maintain the constant airflow required

FIGURE 23

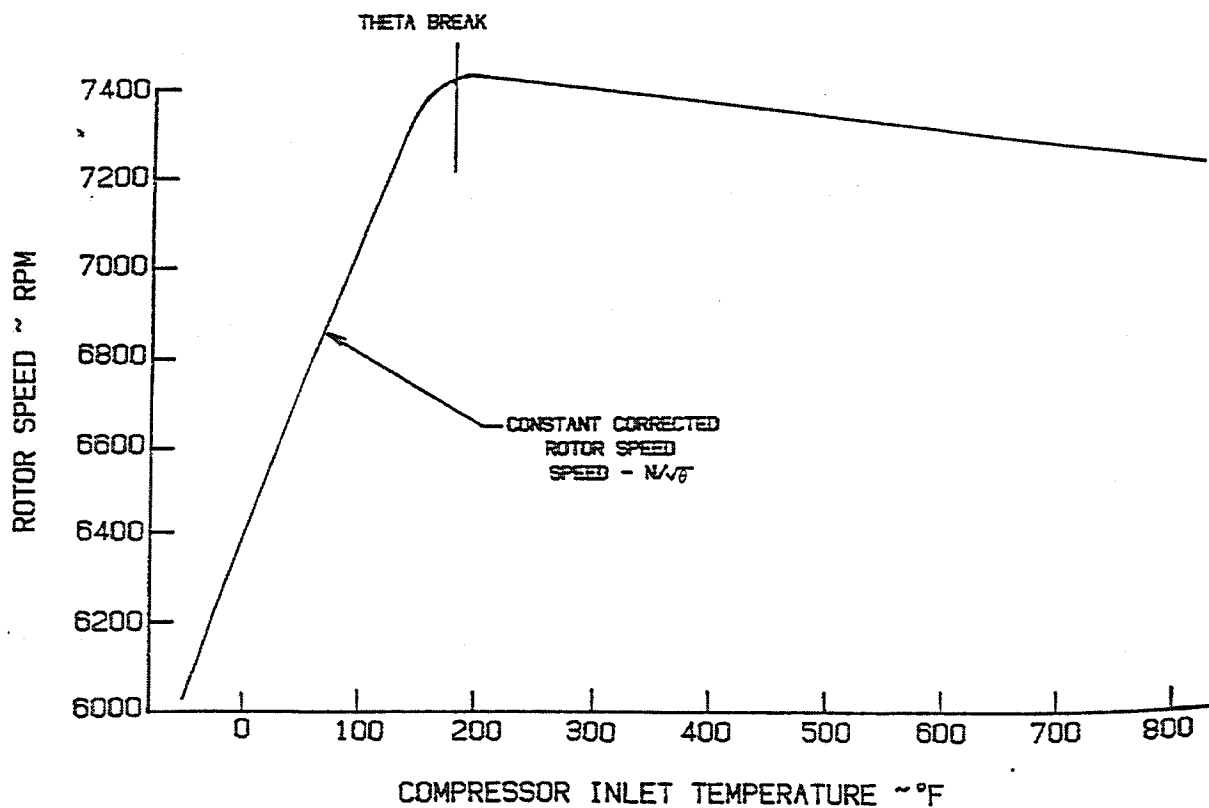
CONTROL CONSTRAINTS

CONSTRAINT

- MAXIMUM FUEL/AIR RATIO
- MINIMUM FUEL/AIR RATIO
- MAXIMUM ROTOR SPEED
- MINIMUM ROTOR SPEED ABOVE MACH 1.6
- MAXIMUM BURNER PRESSURE

FIGURE 24

JT11D-20 ROTOR SPEED SCHEDULE



by the inlet. Maximum burner pressure is limited to limit engine stresses. Maximum fuel temperature at the inlet to the engine is limited so the fuel will not deposit varnish on the inside of the fuel system or, at higher temperatures, plug lines and orifices with carbon deposits.

### 6.3 Airflow Control

In supersonic flight, the aircraft inlet has both external compression from an oblique shock and internal compression from a stabilized normal shock. If the engine airflow demand is greater than the inlet supply then the normal shock is sucked back towards the engine, ram recovery is reduced and inlet pressure distortion is increased. If the engine airflow becomes less than the inlet supply then the shock moves forward. If the shock moves forward beyond the throat then it abruptly moves outside the cowl lip (inlet unstart), both airflow and ram recovery are sharply reduced and inlet variable geometry has to be reset before the inlet can be started again.

Engine-airflow matching and control is very important for this type of inlet, consequently, the engine control maintains an airflow schedule by operating to the rotor speed/compressor inlet temperature schedule shown in Figure 24. This schedule is maintained to low engine power by automatic feedback control of exhaust nozzle area. For example, when afterburner fuel flow is reduced the nozzle closes to maintain the scheduled rotor speed.

The "Theta Break" shown on Figure 24 is the compressor inlet temperature at which the speed schedule transitions from constant corrected rotor speed to a rotor speed schedule selected to give the best compromise between inlet airflow matching, engine performance and engine durability.

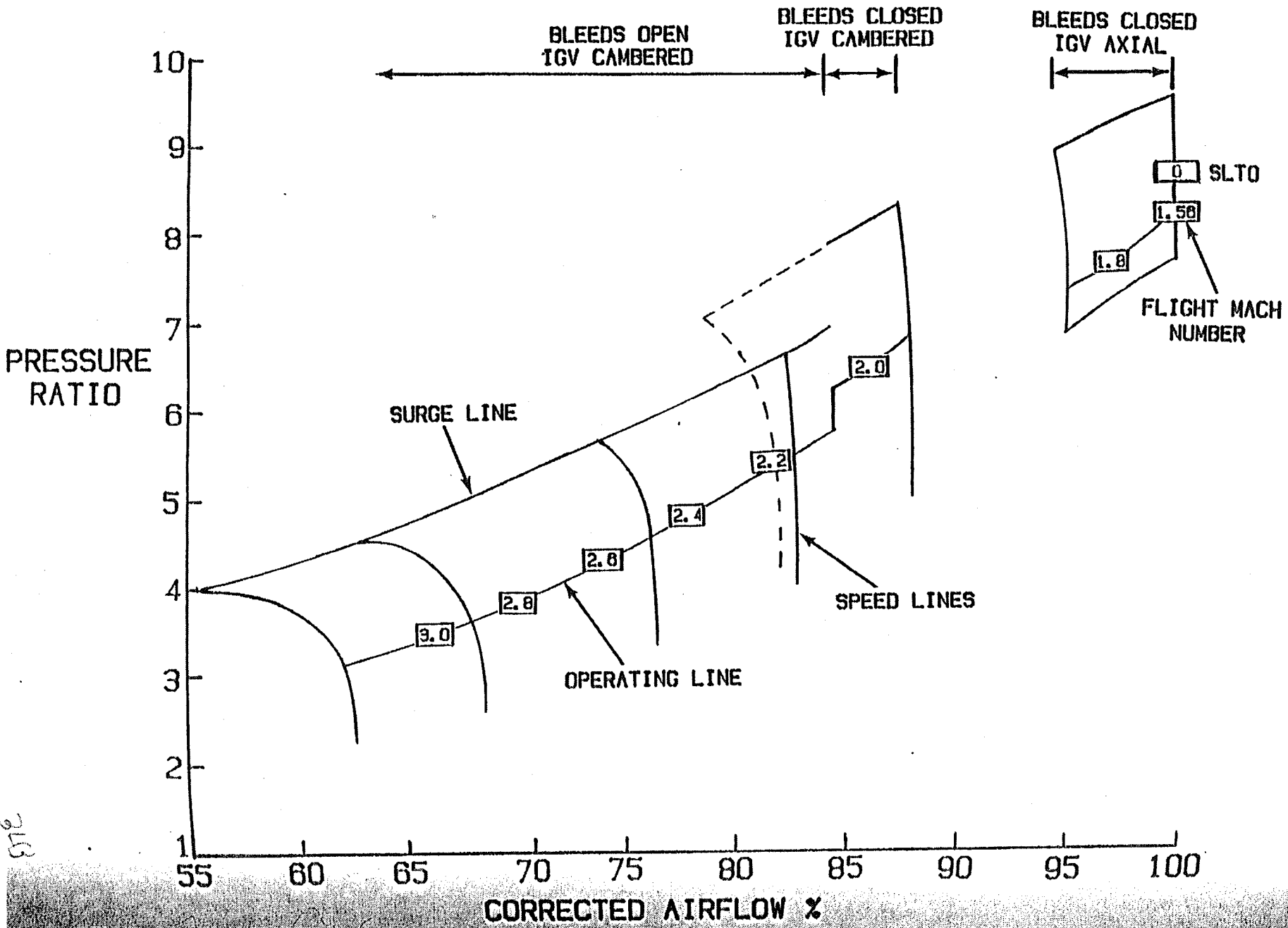
JT11D-20 engine operating points are shown on a compressor map in Figure 25 at maximum thrust. There is a discontinuity in airflow when the inlet guide vane is cambered and a discontinuity in the operating line when the bleed bypass is opened. Both of these cause a discontinuity in thrust. Hysteresis is built into the control schedules to prevent thrust cycling at a constant power lever angle.

While engine control schedules and variable geometry match the inlet airflow supply as far as possible, the final inlet-engine airflow matching is done by variable geometry and bleeds in the inlet. During static operation at take-off the engine requires more airflow than the inlet can supply and sucks down the nacelle below ambient pressure. The inlet spike is moved to the forward position (Figure 26) to provide the maximum inlet throat area. Reverse flow through the center body bleed and forward bypass doors provides additional airflow to the engine. Suck-in doors provide ventilation to the engine nacelle and prevent hot exhaust gas from being recirculated to the engine inlet. Blow-in-doors in the ejector and the closed position of the nozzle exit minimize over-expansion of the exhaust stream that causes thrust loss.

At high supersonic speeds the inlet spike is in the aft position and controlled so the oblique shock is close to the cowl lip (Figure 27). Cowl bleed air stabilizes the terminal normal shock and then is ducted to the ejector and contributes to thrust. Aft bypass doors, just ahead of

FIGURE

OPERATING POINTS ON A JT11L 20 COMPRESSOR MAP



872

**FIGURE 26**

**AIRFLOW MANAGEMENT WITH A STATIC AIRCRAFT**

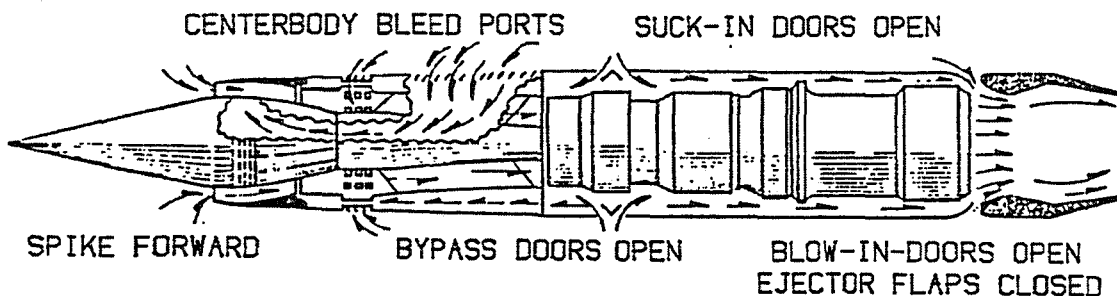


**FIGURE 27**

**AIRFLOW MANAGEMENT AT HIGH SUPERSONIC SPEED**

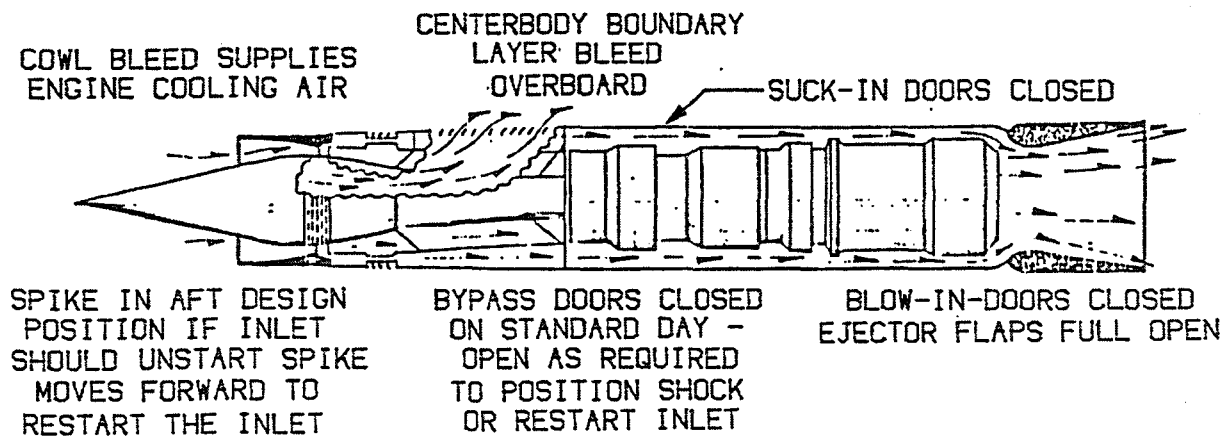
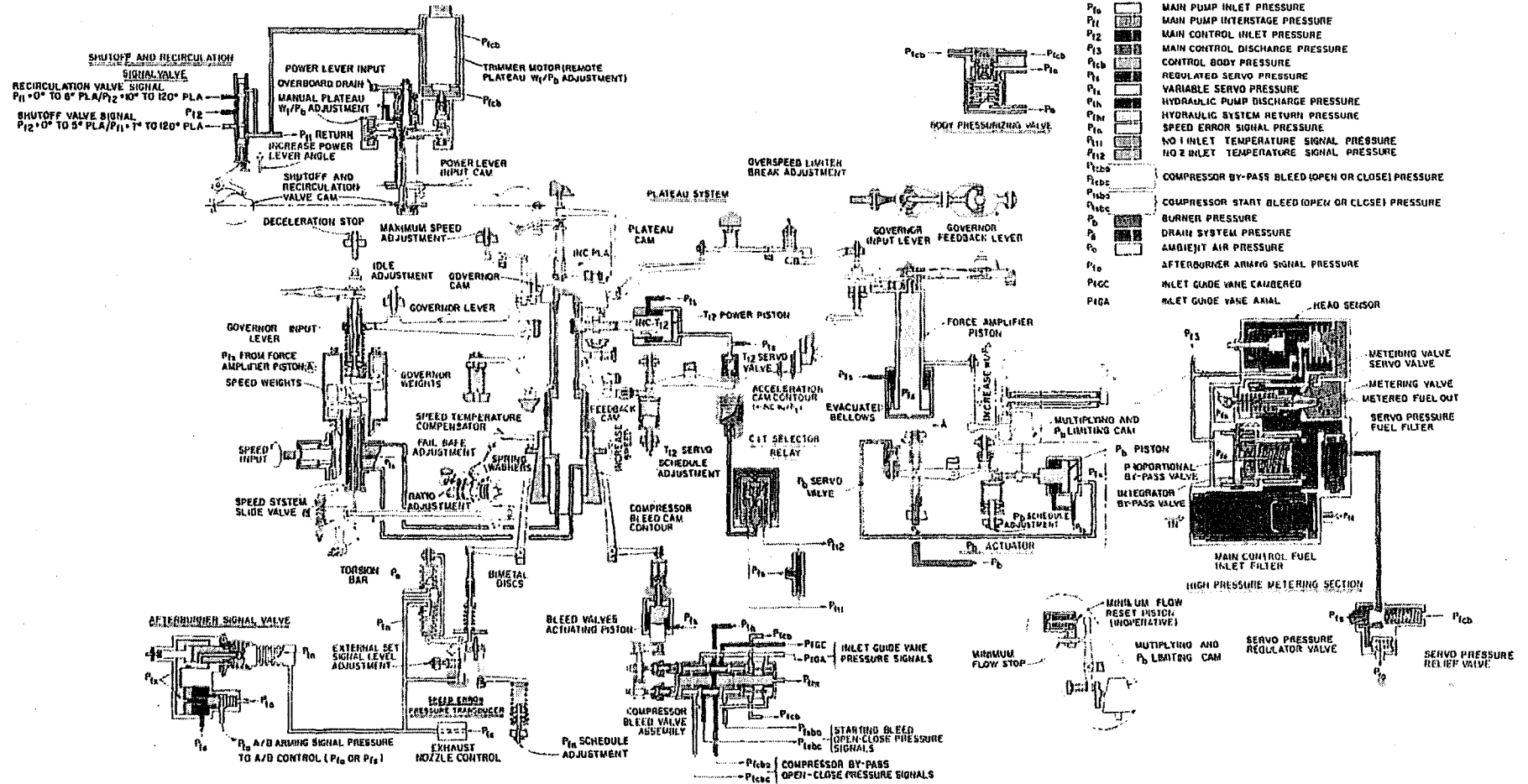




FIGURE 28

**SCHEMATIC DIAGRAM OF THE MAIN FUEL CONTROL**



315

the engine inlet, duct surplus inlet air to the ejector. The combination of engine airflow control, cowl bleed and aft bypass doors provides a close match between inlet supply and engine airflow demand on a standard day. Forward bypass doors provide vernier adjustment of airflow matching using closed-loop control to position the terminal normal shock. The ejector blow-in-doors are closed at high supersonic speed and the nozzle exit is in the fully open position to provide thrust augmentation.

#### 6.4 Main Fuel Control

The JT11D-20 main fuel control is more than a fuel metering unit. It also generates signals to control the compressor bleeds, fuel shutoff, fuel manifold dump, afterburner permission, and exhaust nozzle position. This unit, because of its importance to the success of the program, was constantly in the limelight. It is a hydromechanical control consisting of many cams, levers, rotating spool valves and springs as shown by the schematic diagram, Figure 28.

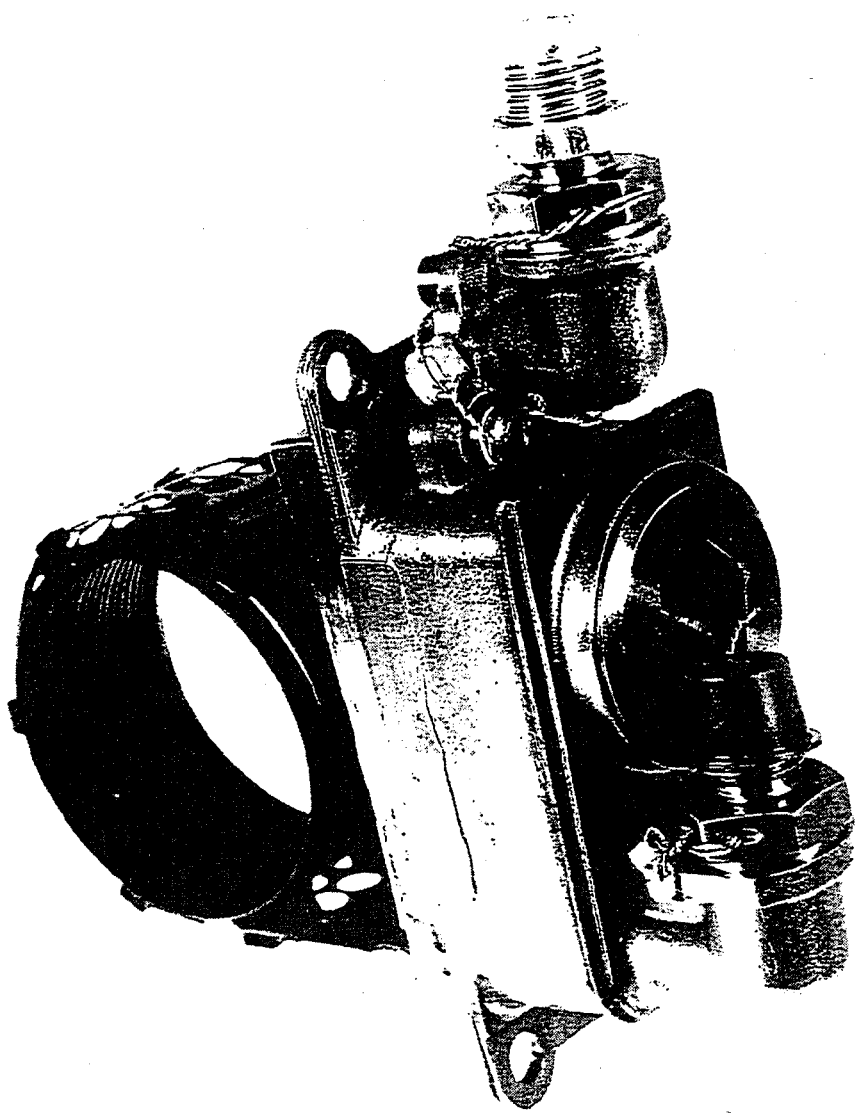
##### 6.4.1 Design Requirements

The fuel and control system components on an engine designed for continuous operation at high Mach number are subjected to much higher fuel and environmental temperatures than the systems on subsonic commercial engines or on military engines with supersonic dash capability, unless the system includes a substantial heatshield and cool fuel or other means of refrigeration. Providing an artificially cooled atmosphere or cool fuel was not possible in the SR71 aircraft because of limited heat sink capability. Consequently the JT11D-20 fuel system was designed to operate in the high temperature environment with hot fuel. In the JT11D-20 engine development, the environmental temperatures can exceed 800°F and the fuel temperatures range from 350°F at the fuel system inlet to nearly 600°F at the fuel nozzles. This combination of elevated fuel and environmental temperatures precludes the use of aluminum in component housings. Stainless steel was required to provide the necessary strength and corrosion resistance.

In addition to having to operate at the high temperatures, the components also were required to operate under subzero conditions. Thus, for these supersonic engine components, the temperature range over which operation was required was increased by several hundred percent over that required of the components on subsonic engines:

Steel components moving in a steel housing over a wide temperature range with the fuel as the only lubricant required development of surface treatments, clearances and accommodation for thermal distortion. At the elevated temperatures encountered in supersonic flight the normal aviation kerosenes possess negligible lubricity. In the development of the JT11D-20 components it was found necessary to provide lubricating additives in the fuel to overcome the persistent sticking of moving parts and excessive wear in the pumping elements. By an intensive program with new materials, new processes, and alternative mechanical designs, involving thousands of hours of experimental testing, these mechanical problems peculiar to this new flight regime were solved, and some reduction in the quantity of fuel lubricity additive was later possible.

FIGURE 29  
HYDROMECHANICAL INLET TEMPERATURE SENSOR



With the wide temperature ranges encountered in operation of high Mach number engines such as the JT11D-20, thermal expansion of the component parts makes it difficult to maintain the required accuracy. For example, the high temperatures encountered during operation affected springs, altering their rates and force. Thermal growth of metering elements required compensation. Again, research and development of new materials and new designs were required to overcome the problems.

Superimposed on these environmental and operational extremes, the fuel and control system components were required to operate to a much greater degree of accuracy than previous systems. Control modes compatible with the demands of the supersonic inlet and control were, of necessity, more complex. Inaccuracies in fuel metering, distribution, or pressure control produced severe consequences in engine performance, engine durability and engine/inlet flow stability.

Another requirement for the fuel system components on the JT11D-20 engine was the extremely high ratio of maximum fuel flow to minimum fuel flow (turndown ratio). This gave rise to more acute problems in the fuel pumps, the metering controls, and the fuel nozzles. Variable-area nozzles had to be developed, both for the main burner and the afterburner. Temperature rise in the pumps at the low fuel flows associated with aircraft descent became so high that recirculation back to the aircraft tank was required.

6.4.2 Problem due to Thermal Transients - Two control suppliers were used in the program. The first controls had computing functions and fulcrum points anchored to the housing. It worked well in a cold environment with cold fuel and in a hot environment with hot fuel; but the combination of cold fuel and hot environment and an increasing temperature transient resulted in turbine temperatures below the scheduled value. Such an environment is produced during climb and acceleration to the cruise Mach number. The falloff in turbine temperature with these early controls was sufficiently severe that the trim of turbine temperature could not compensate for the falloff. Thrust was significantly reduced by the low turbine temperature and as a result the aircraft could not obtain the cruise Mach number during early flights.

This problem was fixed on the first control by insulating the exterior of the control from the nacelle environment. However, the insulation made the control heavier and more difficult to maintain.

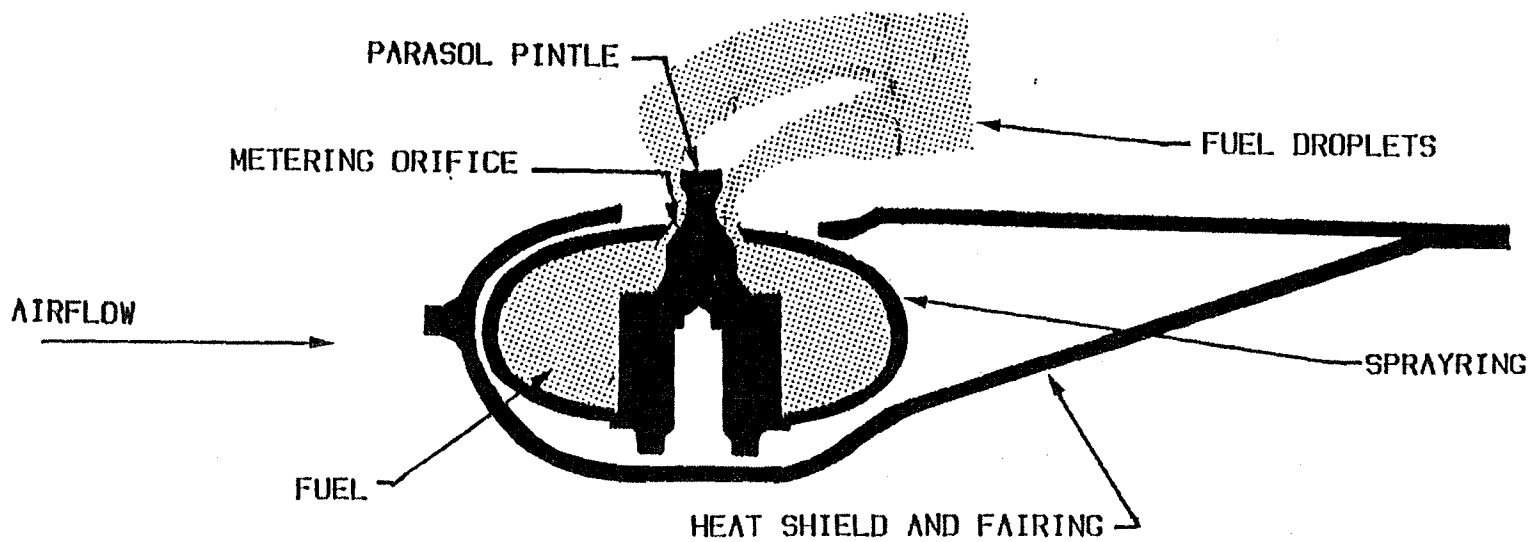
The second control supplier had a control that had been designed for and used on the B-70, one of the few beneficial items coming from that program that originally was supposed to "lead the way". This control had computing functions isolated from the case, consequently, turbine temperature falloff was not experienced. This second control did not require insulation and is incorporated in the engine Bill of Materials.

## 6.5 TEMPERATURE SENSOR

Every control parameter is a function of inlet temperature as shown in Figure 22, consequently, loss of the inlet temperature sense is loss of control. The hydromechanical temperature sensor, shown in Figure 29, consists of a gas filled tube, which converts increasing temperature into

FIGURE

JT11D-20 VARIABLE AREA SPRAYING



-44-

309

increasing pressure. The failure mode is leakage of sensor gas when the sensed pressure becomes equal to compressor inlet pressure. The charging pressure was increased from the charging pressure used in previous engine controls to ensure that a sensor failure always resulted in a pressure reduction. Initial controls had only a single temperature sensor. This was replaced by dual temperature sensors with select-high-pressure logic which gives fail-operational capability.

#### 6.6 MAIN FUEL PUMP

Due to fuel temperatures beyond anything that had been experienced up to that time and the accompanying low lubricity of the fuel, all fuel system component developments were experiences into the unknown. This was nowhere more so than in the main fuel pump. The first attempt at making the main fuel pump was to use gear pump technology from earlier programs and fabricate the housing from pre-formed steel sheet stock. This proved to be so difficult that a second supplier was brought in with a different approach to making the housing (cast steel).

A centrifugal boost stage followed by two redundant gear stages in parallel and a cast housing was selected as the production configuration. Although successful in operation and durability--there have been no in-flight failures--the housing is still unique, as proven in the late 70's when new castings were needed. We could not get anyone in the U.S. to pour this special metal and ended up going to England to have them poured.

#### 6.7 AFTERBURNER FUEL SYSTEM

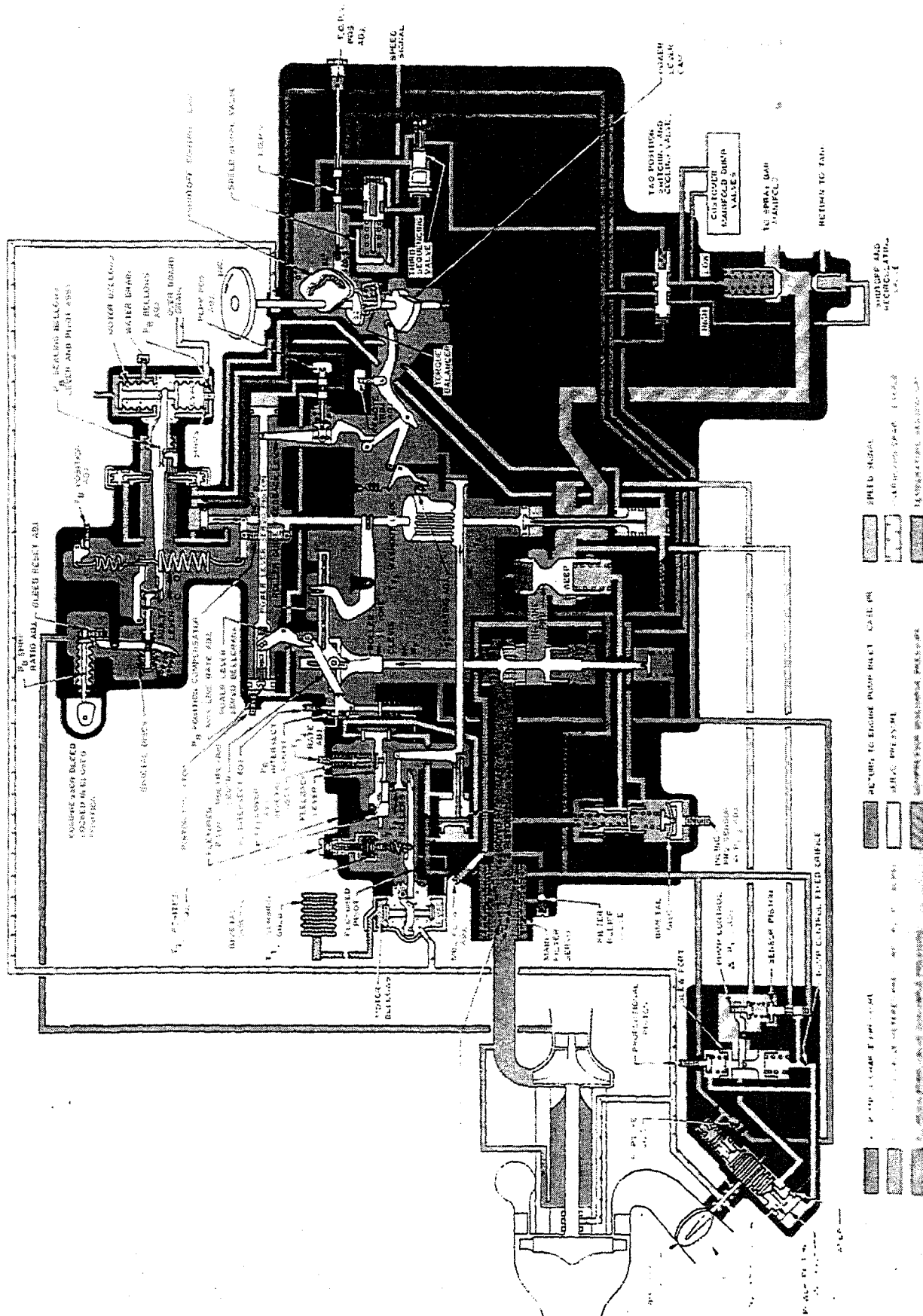
Earlier gas turbine afterburner fuel systems and earlier models of the JT11D-20 engine utilized a fuel metering system that distributed afterburner fuel through a series of fixed orifice area sprayrings. The afterburner turndown ratio required by the mission was such that a fixed orifice, sized to give the maximum fuel flow rate, gave very poor atomization and poor afterburner efficiency at low fuel flow. To maintain the required high afterburner efficiency the turndown ratio was achieved by switching on and off different zones of fuel flow.

Development of the afterburner fuel control to provide the "zoning" with the precision required was a demanding task. When a zone was not in use the spraybars were emptied to avoid coking of the fuel. When a new zone was activated it had to filled and the fuel flow to the operating zones had to be cut back at the same time that filling was complete. If these two events do not coincide there is a discontinuity in thrust and a disturbance to other control functions including airflow.

This sequencing problem was eliminated by a variable area spray ring that permitted a single zone afterburner. The variable area spray ring increases the orifice flow area as the pressure inside the elliptical tube increases (see Figure 30). This allows efficient metering and distribution of fuel over the more than 25 to 1 turndown ratio required over the flight envelope.

FIG. 31

SCHEMATIC DIAGRAM OF AFTER-BURNER FUEL CONTROL



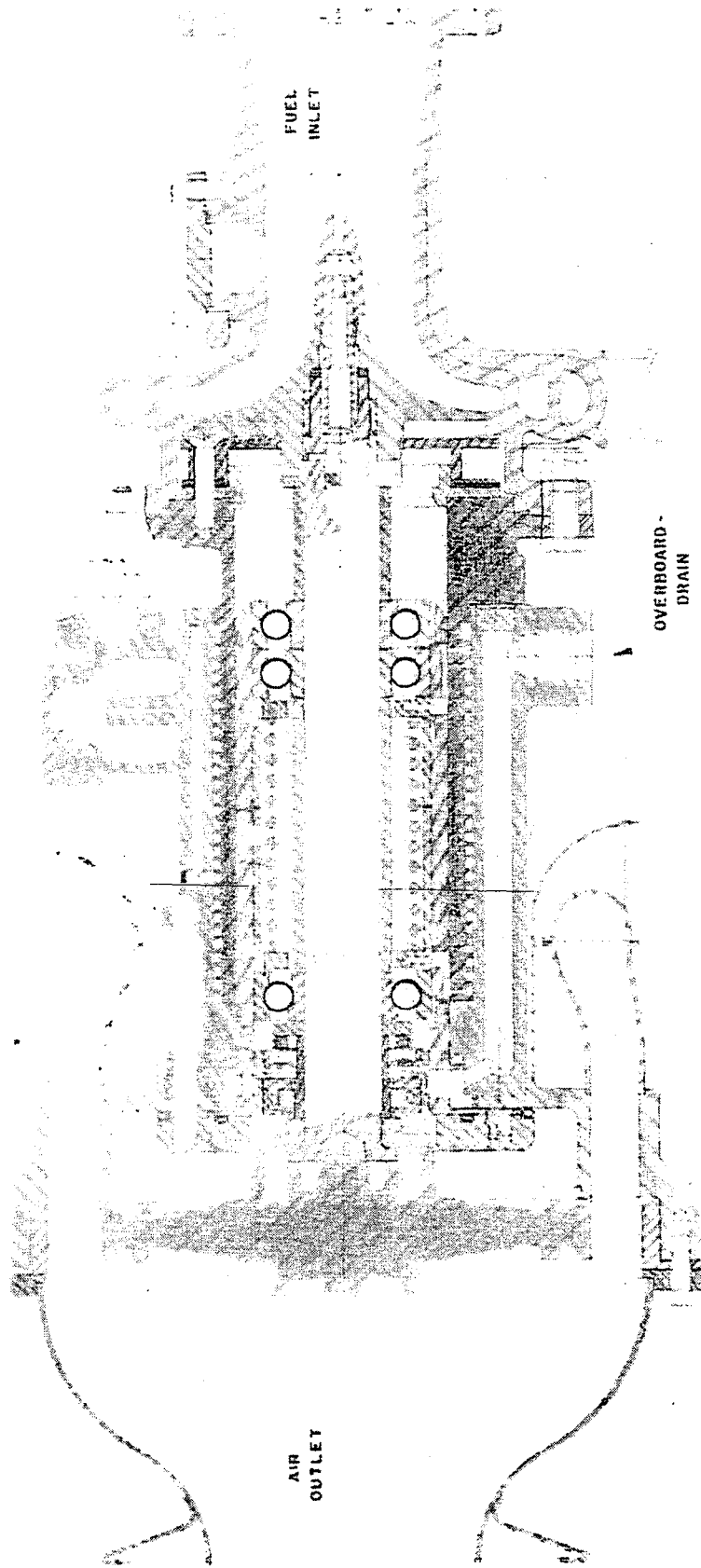
351

A schematic diagram of the single zone, hydromechanical afterburner fuel control is shown in Figure 31.



FIGURE 2

AFTERBURNER FUEL PUMP



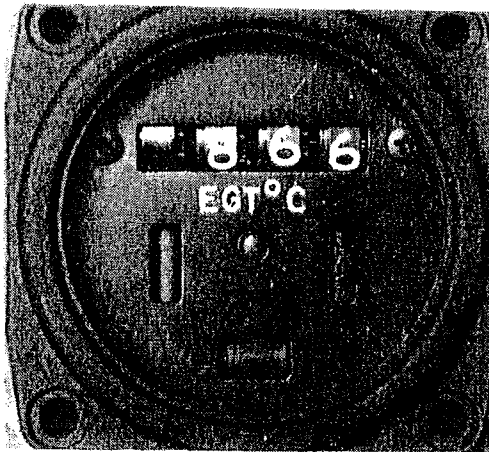
TP-C9  
PUMP-FUEL  
TURBINE DRIVEN

## 6.8 AFTERBURNER FUEL PUMP

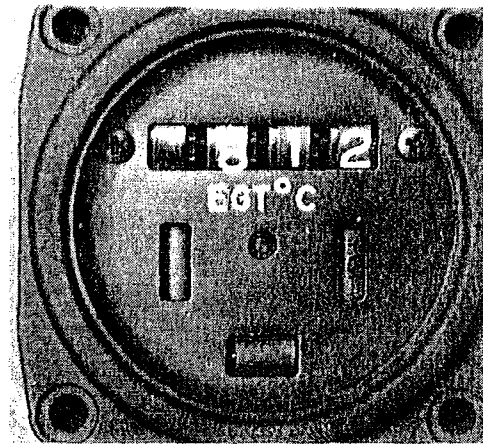
The afterburner fuel pump is a centrifugal pump driven by a gas turbine that is powered by compressor discharge air, Figure 32. This configuration was chosen to avoid fuel overheating during periods when the afterburner was off, such as descent from cruise. Other earlier engines used gear driven fuel pumps which were acceptable for a subsonic engine or with short term supersonic operation where the tank fuel would not heat up. Since the SR-71 operates steady state at speeds that lead to high tank fuel temperatures (engine fuel inlet temperature 300°F+), parasitic heat generated by a gear driven pump could not be tolerated. A compressor discharge bleed air driven pump was the solution. One example of cooperation between P&W and Lockheed is that the afterburner pump turbine is also used as the environmental control system drive turbine (one design, two uses).

FIGURE 33

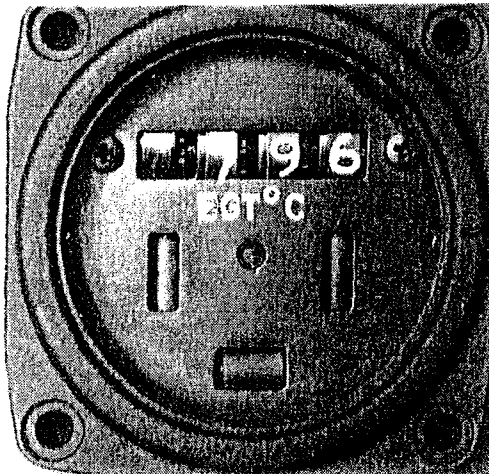
TURBINE TEMPERATURE GAGE OPERATING MODES



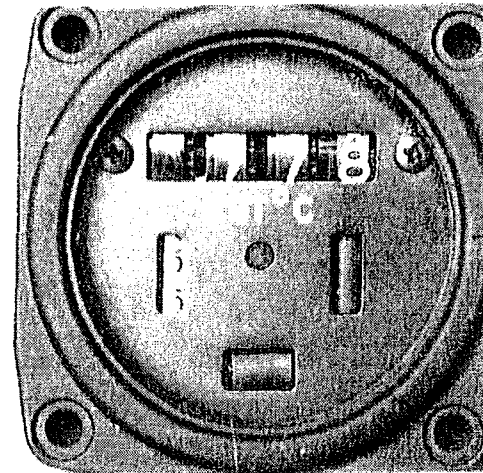
DERICHMENT ENERGIZED



TEMPERATURE OVER LIMIT



OPERATION NORMAL



TEMPERATURE UNDER LIMIT

## 6.9 ELECTRICAL/ELECTRONICS

The high temperature low pressure, environment of the SR-71 limits the use of engine mounted or nacelle located electrical systems or electrically powered devices.

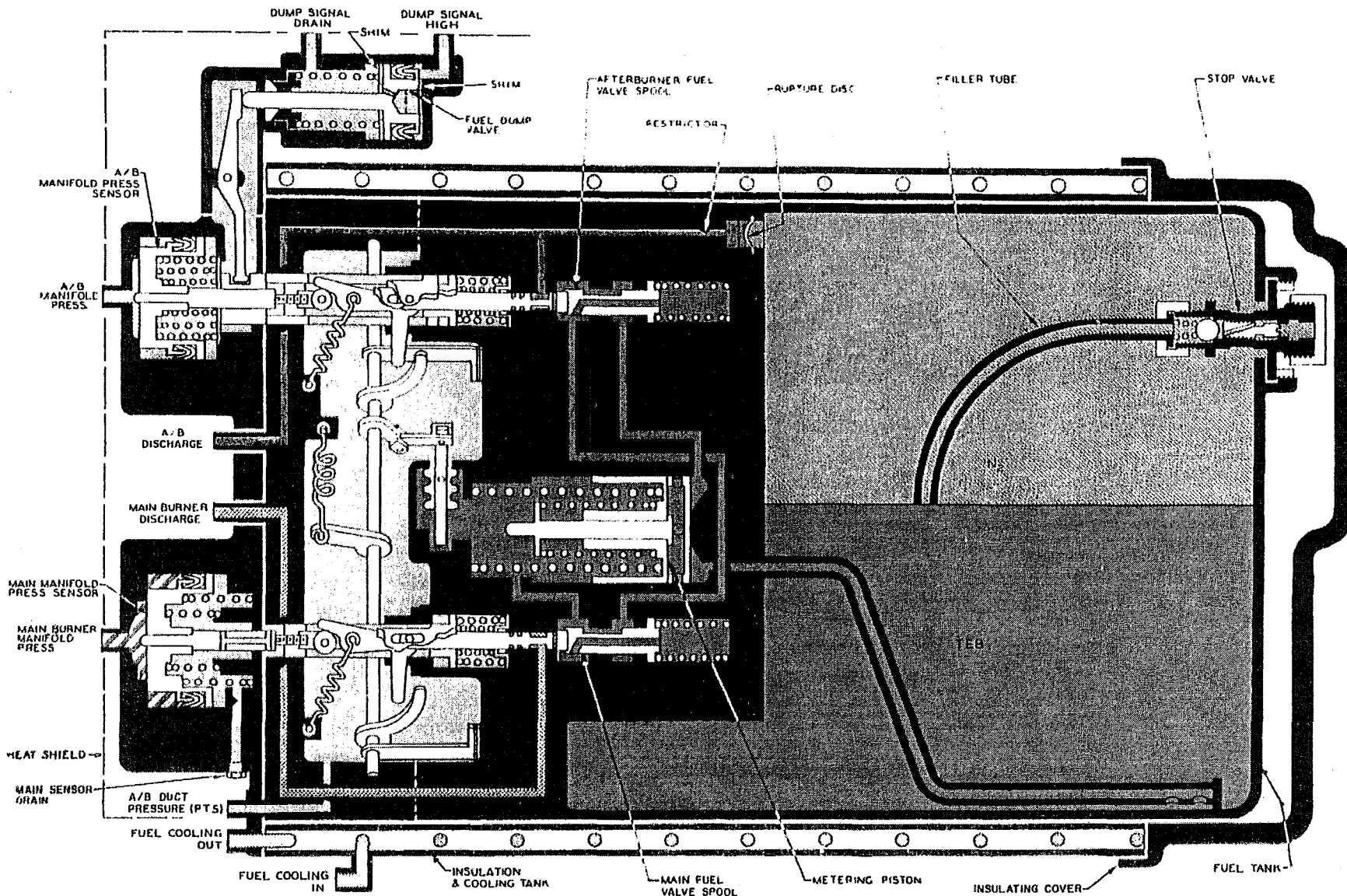
Initially the electrically powered devices on the engine consisted of a fuel cooled (400°F+) motor mounted on the main fuel control and limited engine instrumentation such as oil pressure and temperature, turbine exhaust gas temperature, exhaust nozzle area, and engine speed. Later an electrically powered solenoid was added.

From the very beginning, we knew that we could not pre-schedule engine fuel as precisely as necessary to maximize gas generator power while not over-temperaturing the turbine. A remote trim device was included that would allow the pilot to change turbine exhaust temperature through the electric motor mounted on the main fuel control. The pilot was provided with a curve of turbine exhaust temperature versus engine inlet temperature to make the required manual adjustments. However, unexpectedly sharp atmospheric changes were encountered. These, in combination with the speed of the aircraft, resulted in changes too fast for the pilot to handle and demanded excessive attention. By the time the pilot read the engine inlet temperature and adjusted the turbine exhaust temperature the inlet temperature had changed. This caused either low performance or turbine over-temperature and some inlet unstarts (highly reduced inlet airflow) .

An analog electronic trim on fuel flow was developed that uses close-loop feedback of turbine exhaust gas temperature. The computer portion of the control is mounted in the cooled electronic bay of the aircraft. Error in turbine temperature is computed as a function of compressor inlet temperature. The fuel trim is mounted on the main fuel control and consists of a pulse modulated motor. For over-temperature, turbine temperature is trimmed down fast continuously. Trim up is done slowly in pulses that become of shorter duration as the set point is reached. Dead zone is provided to prevent hunting. When error is within the limits to which temperatures can be sensed, dead zone prevents the control from trimming. The combination of pulse modulation and dead zone gives a fast-acting, stable control. The exhaust gas temperature with this system seldom deviates by more than 10°C from nominal.

The digital turbine exhaust gas temperature readout and override manual trim were retained. Color coded signals are provided in addition to the digital readout as shown in Figure 33. No color signals show normal operation. A yellow signal indicates low temperature while red signals over-temperature or loss of electrical power, depending on the position of the signal.

# FIGURE 4 CHEMICAL IGNITION SYSTEM



- |                           |                |                  |                     |                            |
|---------------------------|----------------|------------------|---------------------|----------------------------|
| PT 5                      | TEB            | COOLING FUEL     | MAIN BURNER IGNITER | DUMP SIGNAL DRAIN          |
| A/B MANIFOLD PRESS SENSOR | N <sub>2</sub> | DUMP SIGNAL HIGH | AFTERBURNER IGNITER | MAIN BURNER MANIFOLD PRESS |

-52-

359

If an inlet unstarts at high supersonic airspeed there is a decrease in airflow available to the engine of such magnitude that minimum fuel flow will cause turbine over-temperature. To prevent turbine damage, a solenoid valve in the fuel system is opened when the sensed turbine temperature is more than 50°C above the schedule. This solenoid valve, called a derich valve, diverts fuel from the main fuel nozzles to prevent over-temperature with an unstarted inlet.

Within the engine compartment, electrical wiring is encased in solid steel sheaths and insulated with a magnesium oxide powder. This is necessary to prevent "leakage" at the very low nacelle pressures present at cruise condition.

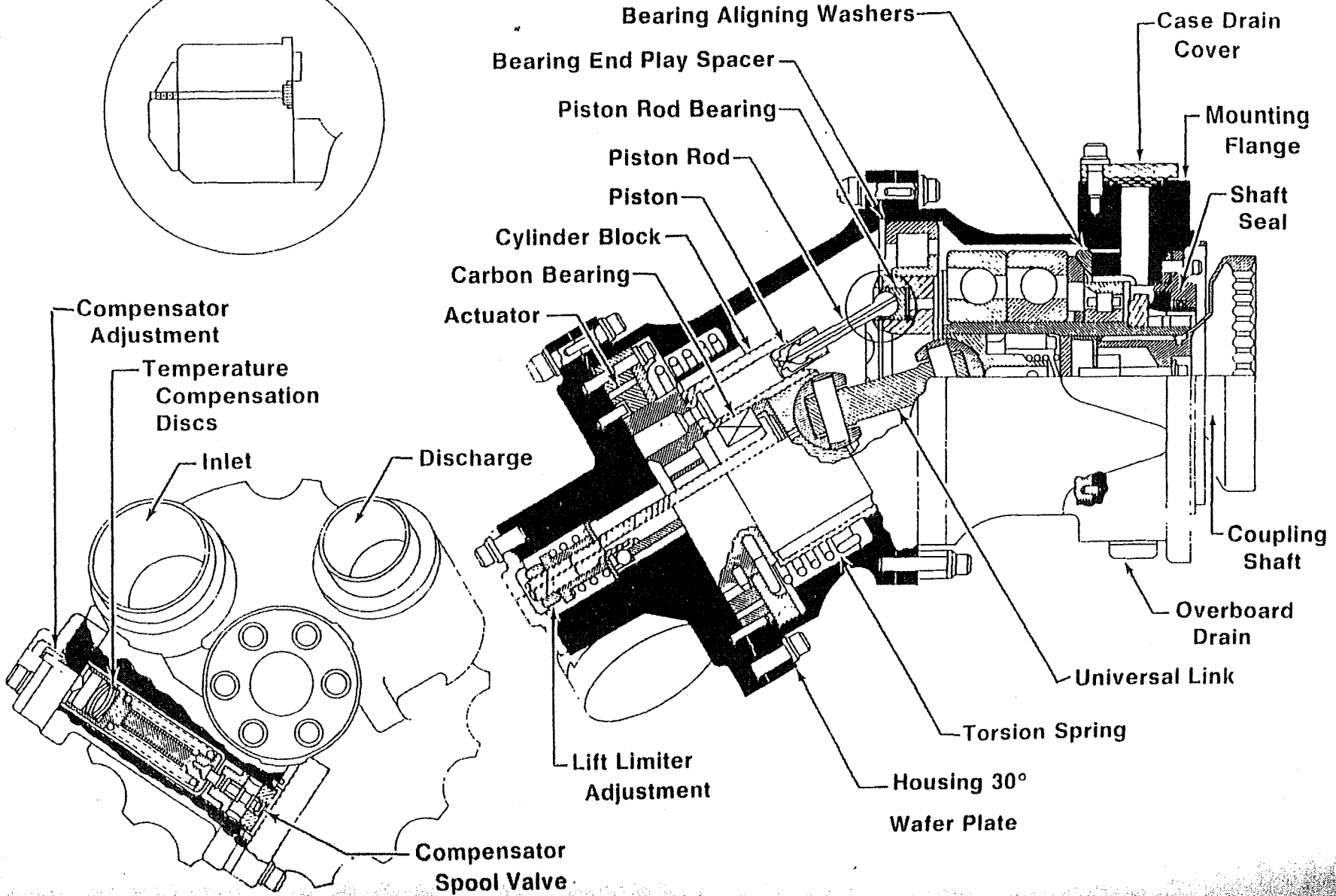
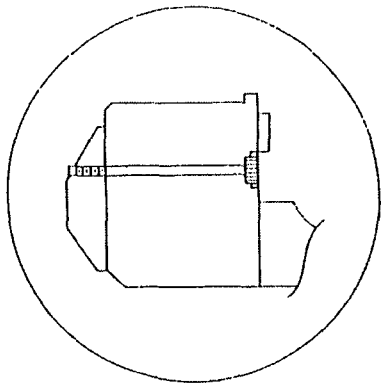
#### 6.10 IGNITION SYSTEM

High energy is required to ignite a fuel-air mixture at the low pressures experienced at high altitude. Because of the extreme difficulty in implementing high temperature, high energy electrical systems, the engine ignition system uses the pyrophoric fluid triethyl borane (TEB) that had been explored as a fuel in a prior program. This required the development of a Chemical Ignition System (CIS) that would meter TEB into the burner for both ground and air starting both the main engine and the afterburner. Therefore, a multiple delivery system, inert in itself, but capable of operating throughout the flight envelope was developed, see Figure 34. To assure an inert system, gaseous nitrogen is used to pressurize a tank. Gaseous nitrogen also powers a piston that delivers a specific amount of TEB to the main engine burner or afterburner regardless of engine operating condition. One concern that accompanied the selection of TEB as the ignition fluid was what to do in case of an aircraft mishap that precluded normal disassembly procedures. One solution pursued was to depressurize the tank by shooting with steel piercing bullets. This proceeded to the point where a pressurized chemical ignition unit was "shot" at the P&W development test site to develop fire suppression techniques while being filmed with high speed film. Concurrent with this effort, a "crash recovery" vehicle was planned by Lockheed that incorporated a "killer" cannon and fire suppression equipment. This piece of equipment was not developed. Crash recovery as it involved the CIS ended up not being an issue.

One development problem that plagued us throughout the early CIS development was plugging of the probe where TEB was injected into the burners. A number of attempts were made to air purge and fuel purge probes of different sizes and shapes. The solution ultimately selected was to continuously "drip" fuel into the TEB plumbing line near the CIS which assured purging of the plumbing and probe. This, however, was not without certain risks in that, if the fuel drip were too little, the fuel would evaporate and cake up and if it were too much it would cause a "hot" streak in the burner. An acceptable level to prevent all problems was found.

FIGURE 35

# JT11D-20 HYDRULIC PUMP



FA

359

A catalytic ignition system is provided in the afterburner. This catalytic igniter acts as a back-up to relight the afterburner if TEB has been exhausted. The catalytic igniter is not relied on as the sole means of ignition because high temperature is required for catalytic ignition. The catalytic igniter works well when the power lever is advanced into afterburning from intermediate thrust but may cause delay leading to "hard" lights during a snap acceleration from idle thrust.

#### 6.11 HYDRAULIC SYSTEM

Earlier models used compressor discharge pressure as the power to vary the exhaust nozzle area. These models were designed to operate for short periods of time at Mach 3, not cruise. The need for a continuously modulated (variable area) nozzle for climb to and cruise at Mach 3+, meant a more efficient power source was required. After considerable "soul searching", it was decided to control jet area with a hydraulic system powered by a variable displacement piston pump (like the airplane hydraulic system). A cross section of this hydraulic pump is shown in Figure 35.

Conventional hydraulic fluid is not suitable for the high-temperature environment of the exhaust nozzle actuators. Since cooling the hydraulic system uses scarce heat sink capacity, it was decided to use engine fuel as the hydraulic fluid. Another advantage of fuel is a very large reservoir: a leak in the hydraulic system could result in loss of control if the hydraulic reservoir is depleted during a long flight. The pressure originally selected was 3000 psi but was subsequently reduced to 1900 psi when operational testing proved that adequate response could be achieved at the lower pressure level. Developing this system required development of material combinations for pistons, piston bearings, metering plates, drive splines and special housing bolts that could absorb the high frequency fatigue of the pistons pressure pulses. Another development required was a "muffler" in the pump discharge to lessen the high pressure pulses that caused "dither" in the nozzle and fatigue (to failure) in high pressure plumbing. Since the pump has a "modulating delivery" capability it only uses significant power when the exhaust nozzle is actuated. Minimal power is used to maintain pressure during steady state operation. The systems powered by hydraulics include overboard bleeds, compressor bleeds and exhaust nozzle.

Two problems arose: first, no high pressure hydraulic pump had ever been developed to a primary propulsion system level of reliability even with low temperature, high lubricity hydraulic fluid; in this case an engine level of reliability was required from a high pressure pump using hot fuel. The fuel was not only hot but the newly developed special fuel had no lubricity. A small amount of fluorocarbon was added to allow the airframe and engine pumps and servos to work. Second, the hydraulic actuators must operate without seizure or leaking in a 1200°F environment with 1900 psi fuel. Both of these problems were solved, but only after thousands of hours of hot bench testing and hundreds of hours of engine testing were devoted to their solution.



FIGURE 36

## NEW CONTROL FEATURES PIONEERED ON JT11D - 20 ENGINE

---

- ADAPTIVE SPEED CONTROL CIRCUIT
- ELECTRONIC PULSE MODULATED TURBINE TEMPERATURE CONTROL
- TECHNOLOGY DEMONSTRATION OF FULL AUTHORITY DIGITAL ELECTRONIC CONTROL
- DEADZONE TO OBTAIN STABILITY AT HIGH GAIN
- ENGINE CONTROL MOUNTED IN AIRCRAFT ELECTRONICS BAY
- AIRFLOW CONTROL
- REDUNDANT SENSORS AND COMPONENTS
- CHEMICAL IGNITION OF MAIN-BURNER AND AFTERBURNER
- CATALYTIC IGNITION FOR AFTERBURNER RELIGHT

The engine hydraulic system was developed to have equal life to the one used in the airplane which operates on conventional hydraulic fluid at much lower temperature.

#### 6.12 NEW CONTROL FEATURES PIONEERED ON THE JT11D-20 ENGINE

The features of the JT11D-20 control system shown in Figure 36 were designed and developed in response to new mission and environmental requirements and therefore advanced the state-of-the art in controls.

The engine rotor speed control has gains which change over the flight envelope to adapt the control to the wide range of environmental conditions. This gain variation gave the required combination of fast response and stable operation over the flight envelope.

Electronic engine controls had been tried on previous engines and found to be unreliable, probably because the then state-of-the art in electronics could not tolerate the high vibration and high temperature environment surrounding an engine. Because hydromechanical controls were not sufficiently accurate for this application and manual trim was not satisfactory, a limited authority electronic trim control was studied. A prototype electronic analog control was built into the turbine exhaust gas temperature gage and flight tested. The success of the flight demonstration resulted in the development of the production analog control which is mounted in the aircraft electronics bay. This control was satisfactory and reliable; consequently, an electronic supervisory control, again with limited authority, was designed for the next generation of engines. Successful operation of a supervisory control on the initial F100 engine model led to the present state-of-the-art full-authority digital electronic control mounted on the engine.

The JT11D-20 engine was tested on a sea level test stand with a programmable full authority digital electronic control mounted in a trailer. These tests showed the feasibility of full authority digital electronic controls.

Prior to 1959, hysteresis or dead zone in a control was avoided because it implied lack of control precision. In the JT11D-20 control, and in particular, in the electronic supervisory control, it was found that placing a dead zone around the set point, in which no control action takes place, prevents hunting and overshoot and allows rapid response while maintaining stability. Dead zone is always beneficial in a control if it is within the accuracy of the sensors. Dead zone can also apply in management and in personal life: when it is not clear which direction to take the best approach is usually to do nothing.

Redundant compressor inlet temperatures and redundant main fuel pumps were incorporated together with fail-operational logic.

Fuel temperature management was required because fuel is the main heat sink while the maximum temperature the fuel can reach is limited by decomposition. Whenever possible, the hot fuel was burned in the engine rather than being returned to the fuel tank.

FIGURE 37

## CONTROL LESSONS LEARNED

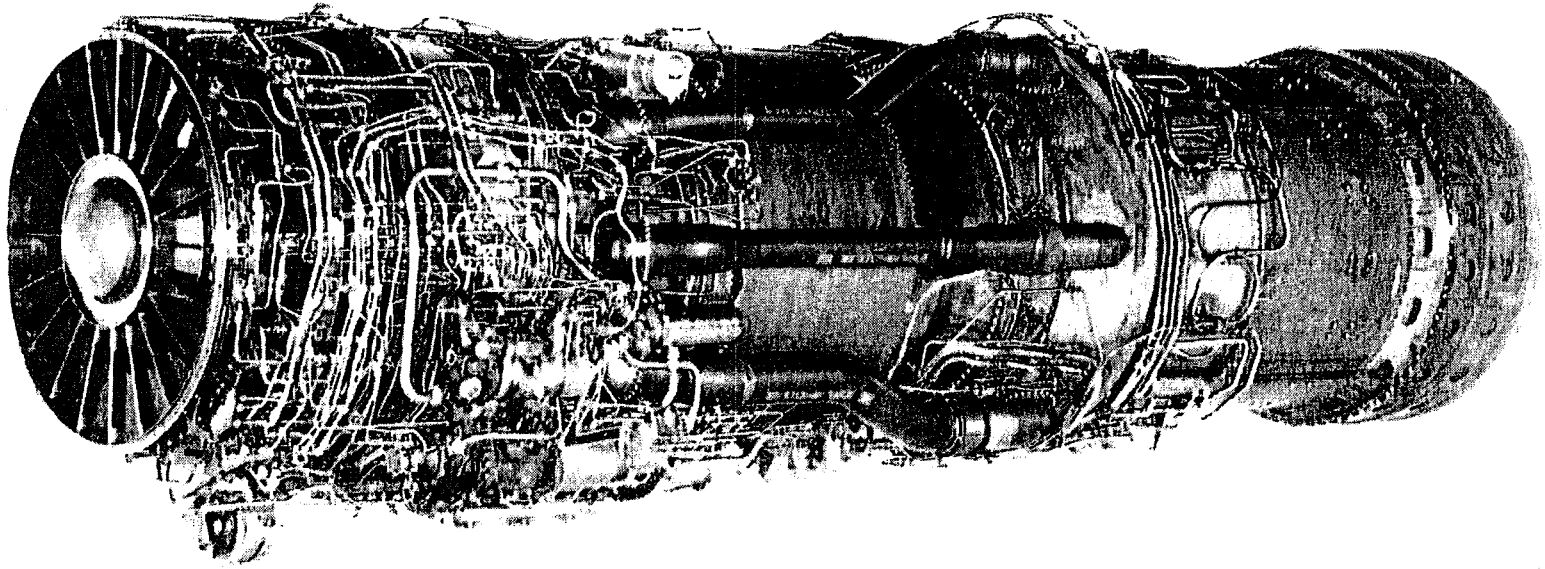
---

- HYDROMECHANICAL CONTROLS NOT ACCURATE ENOUGH
- ELECTRONIC CONTROLS ACCURATE AND RELIABLE
- TEMPERATURE GRADIENTS CAN GIVE CONTROL PROBLEMS
- MULTIVARIABLE CONTROLS ARE DESIRABLE
- REDUNDANT SENSORS AND FAIL-OPERATION LOGIC PAY OFF

6.13 Control lessons learned in the JT11D-20 engine, Figure 37, have been applied to control research and new generations of controls. In today's engines, hydromechanical controls have been replaced by full-authority electronic controls that are lighter weight, smaller size, more reliable and less expensive than their predecessors. Multi variable controls redundant sensors and fail-operational logic are the new standard. Electronic controls also interface with aircraft controls and engine diagnostics.

FIGURE 38

PLUMBING MUST BE LEAKPROOF AND RESIST FATIGUE



-60-

365

## 7. PLUMBING

Figure 38 shows the large number of pipes carrying fuel, oil and air that surround the engine. The high temperature environment precludes the use of rubber hoses. The plumbing is made from high temperature nickel base alloys and is routed and clipped to allow for thermal expansions and contractions. Line failures cannot be tolerated because of loss of control. Leaks cannot be tolerated because of fire hazard. Consequently fatigue failure is a primary concern. Fatigue can be caused by dimensional changes in the engine during Mach number excursions, by resonant vibration, by hydraulic pump pressure excitations, and by reduced materials properties at the elevated environmental temperatures.

The entire engine was mounted on a shaker table and subjected to the vibrations that had been measured on an operating engine in order to develop clip locations and clip types that prevent fatigue failures. As a result of this experience we are now able to develop plumbing by exciting individual lines instead of shaking the entire engine. Bosses and clips are riveted instead of being integral or welded in order to provide vibration damping. Typical clips that allow for thermal expansion are shown in Figure 39.

Early in the development program, difficulty was experienced making a mechanical joint between two fluid lines (or between a fluid line and a component) that would remain leak-tight during engine operation. The mechanical joint was superseded by a brazed joint that required special fixtures and tooling so that the joint could be brazed in-place on the engine. This turned out to be a completely non-maintainable arrangement, often requiring days to make relatively simple parts replacement on the engine. In addition, it proved impossible to maintain adequate quality control of contamination, and metal overheating could not be completely eliminated even with the most refined techniques. As a result, more leaks occurred than with the original joint.

A new mechanical joint was developed with integral ferrules, conical Voi-shan seals and threaded connections, Figure 40. The Voi-shan seal has a different contour than the mating ferrules. So it is elastically compressed when the joint is tightened. When cold fuel is introduced into a hot line, the inside of the fitting cools before the outer nut which causes a small gap between ferrules. The Voi-shan seal has enough resilience to seal under thermal shock conditions and prevents the fuel squirt that would otherwise occur. Integral ferrules are forged by heating and compacting about 2-1/2 feet of pipe at each end of a tube and then machining to the required geometry. We supplied this design to Lockheed for use in aircraft plumbing joints.

These joints have proved absolutely leak-proof, as well as maintainable by ordinary techniques. A special joint for the afterburner fuel connections was devised which will not leak even when cold fuel is initially introduced into 1200°F parts.

FIGURE 39  
TYPICAL PLUMBING CLAMPS

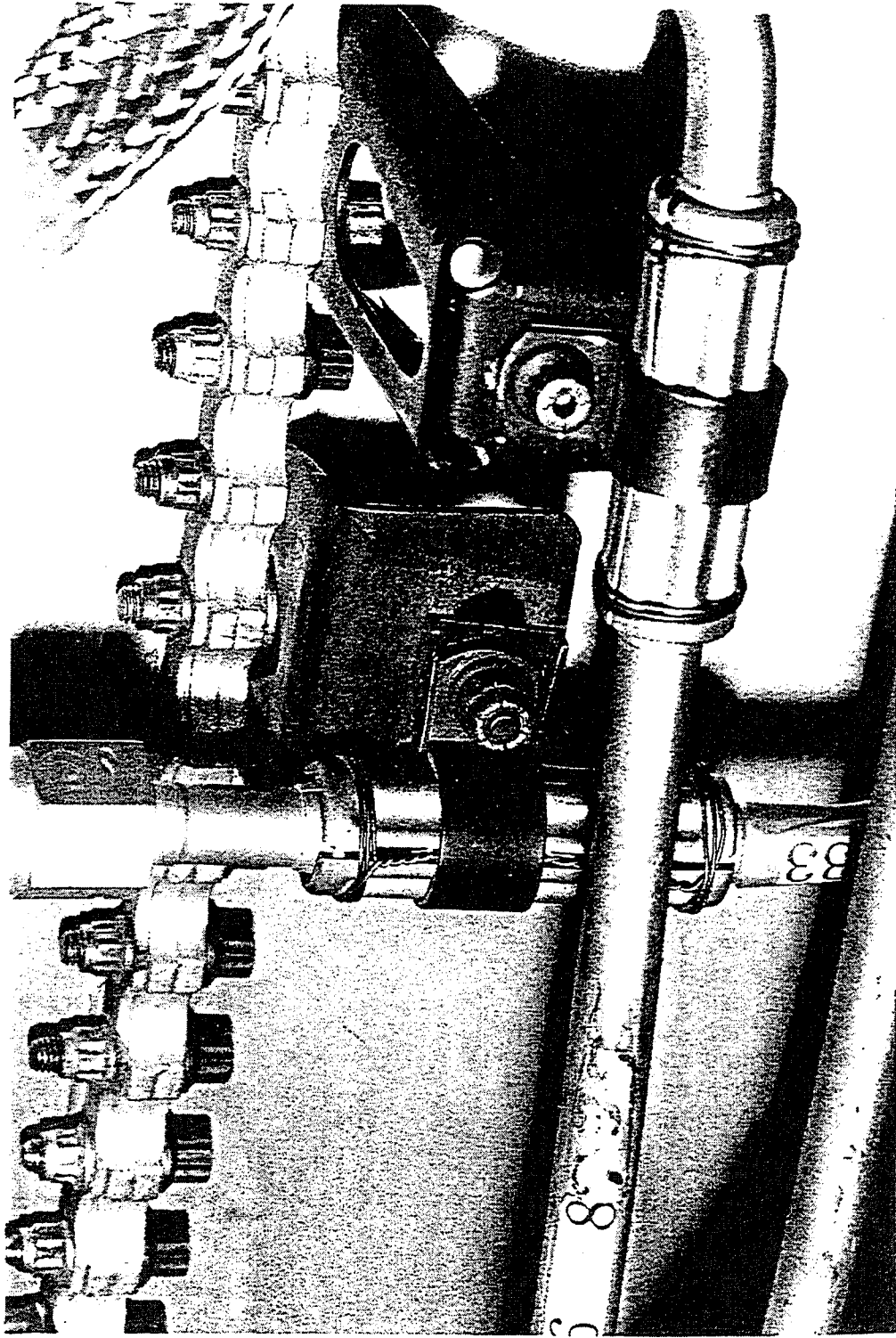
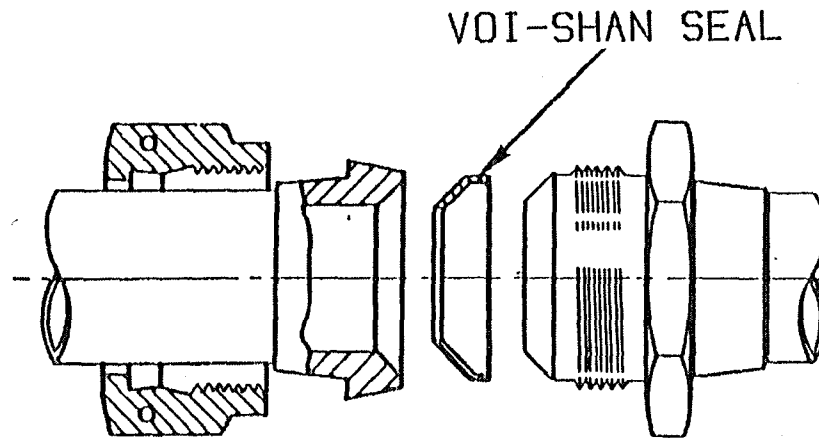


FIGURE 40

LEAKPROOF FLUID CONNECTOR

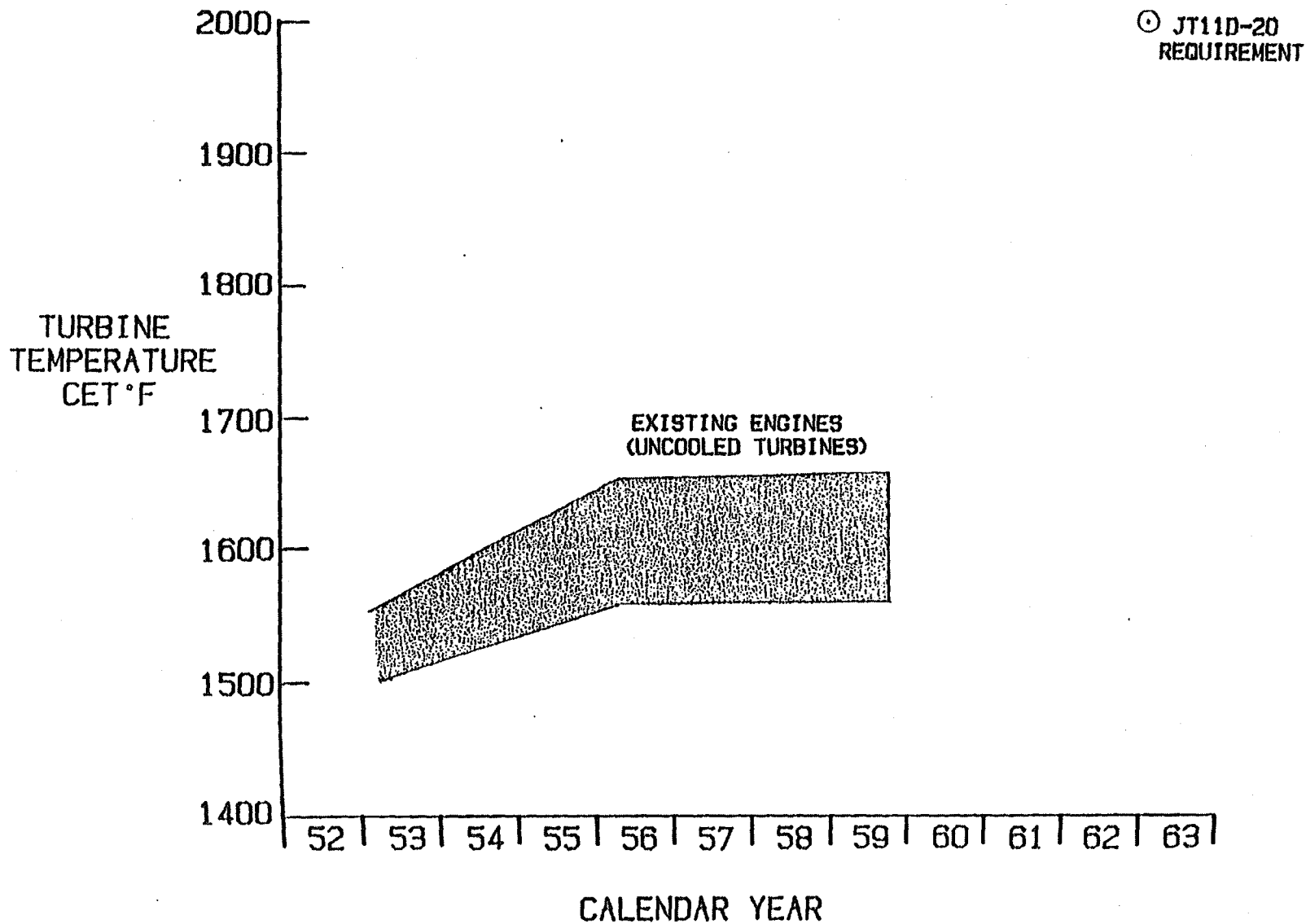
---





FIGURE

REQUIRED TURBINE TEMPERATURE WAS 350 °F HIGHER THAN EXPERIENCE



-75-

369

## 8. TURBINE

### 8.1 Turbine Temperature

In 1959 it was common practice to use Combustor Exit Temperature (CET) as the measure of turbine inlet temperature. All turbine inlet temperatures given in this report are combustor exit temperatures. At the present time several temperatures may be tracked in the turbine.

- Combustor exit temperature is the highest average total temperature in the engine and the temperature that the turbine vanes withstand.
- Rotor inlet temperature is the average total temperature that the rotor sees. It is lower than combustor exit temperature because of addition of turbine vane and disk cooling air and because turbine air is accelerated by the vanes to match the turbine rotating velocity.
- Temperatures of downstream blades and vanes may be important in some applications.
- Superimposed on average temperatures are radial profiles and pattern factors. Combustor design is tailored to produce radial temperature profiles that are cooler than average near the root where stress is highest. The pattern factor describes hot spots in the temperature profile. An important part of combustor development is to minimize the pattern factor because the turbine components have to be designed to withstand the maximum hot spot at the maximum average temperature.

The turbine temperature selected to give the required thrust for supersonic acceleration and cruise was 2000°F combustor exit temperature. In 1959 turbines on production engines were uncooled, with a maximum allowable gas temperature of 1650°F as shown in Figure 41. At the time 2000°F was an ambitious target that required a cooled turbine.

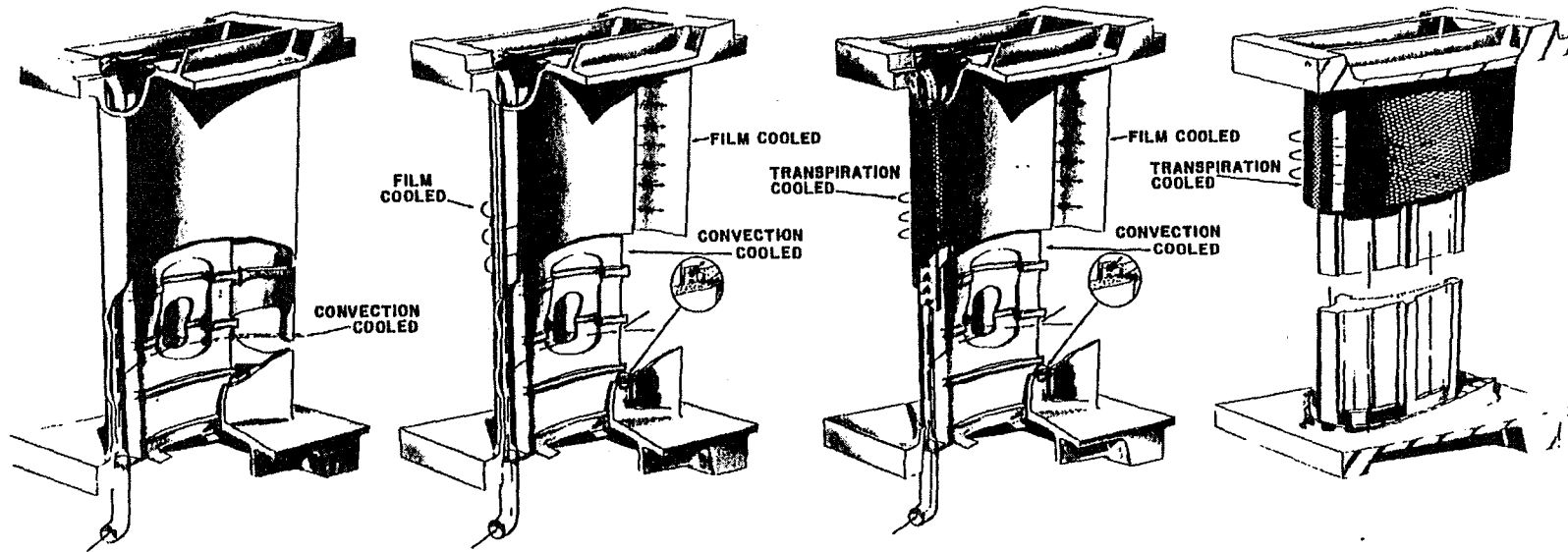
### 8.2 Turbine Design

Several cooling schemes were investigated including convection cooling, film cooling, transpiration cooling and mixtures of these cooling techniques.

Transpiration film cooling, while theoretically giving higher degrees of cooling, presents many practical problems. Transpiration cooling requires built-up structures on which prior experience was limited to use in non-rotating parts. The welded or brazed joints in such a built-up structure could not be inspected with sufficient confidence to use this type of construction in turbine blades and assure the required degree of reliability. In addition, with both film and transpiration cooling, the mixing losses of the low-energy cooling air discharged on the airfoil surface into the high-energy main gas stream cause turbine efficiency loss. Burnout, caused by local cooling failure from impact damage or pore plugging, is an additional hazard.

Figure 42 shows experimental designs of turbine vanes. The convection-cooled, one-piece vane with trailing edge discharge of cooling air shown in Figure 43 was selected for the JT11D-20 engine. Figures 44 and 45 show experimental designs of turbine blades. A convection-cooled,

FIGURE 42  
EXPERIMENTAL DESIGNS OF AIR-COOLED TURBINE VANES  
FOR RIG OR ENGINE TESTING



-99-

FE 5640

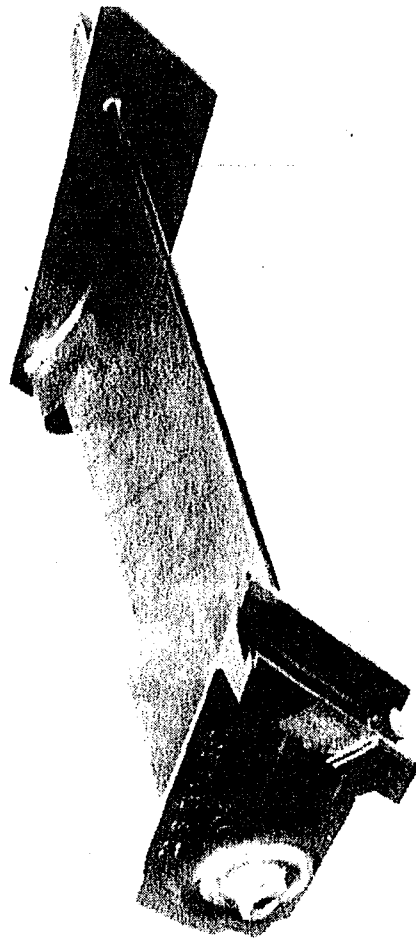
680608  
FD 24369

301

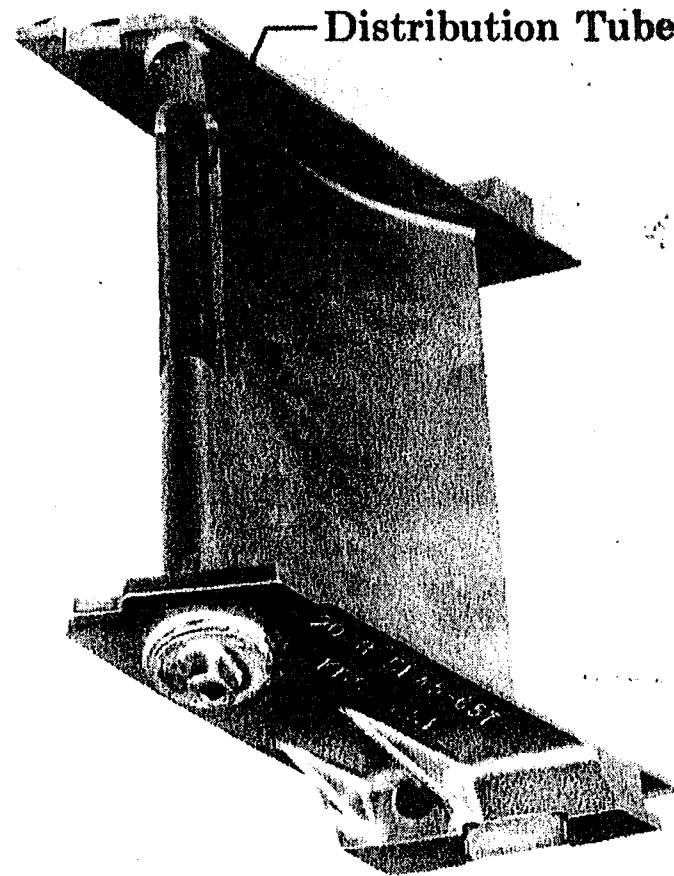
FIGURE 43

CURRENT JT11D-20 FIRST-STAGE TURBINE VANE  
CONVECTION COOLED-TRAILING EDGE DISCHARGE

---



FE 39598



Distribution Tube

FE 39599

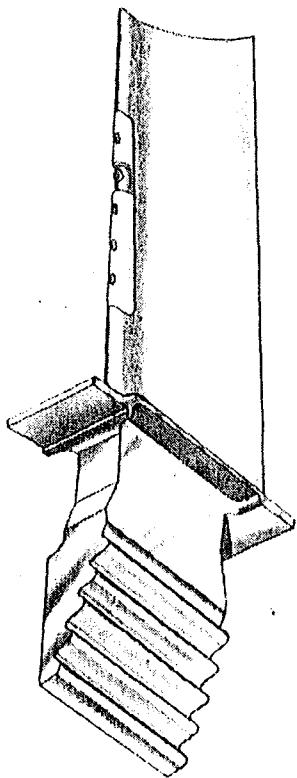
680608  
FD 24387

-67-

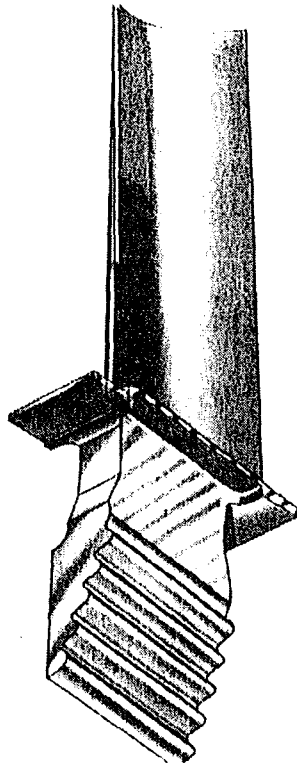
218

FIGURE 44

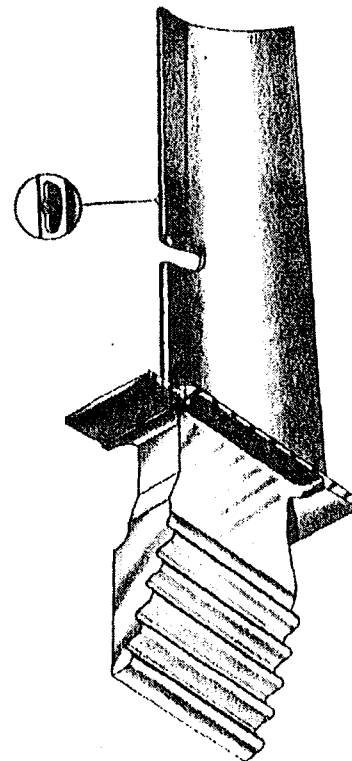
EXPERIMENTAL DESIGN OF AIR-COOLED TURBINE BLADES



Insulated  
Leading Edge



Tube & Slotted  
Leading Edge



Drilled Tube  
Leading Edge

-89-

313

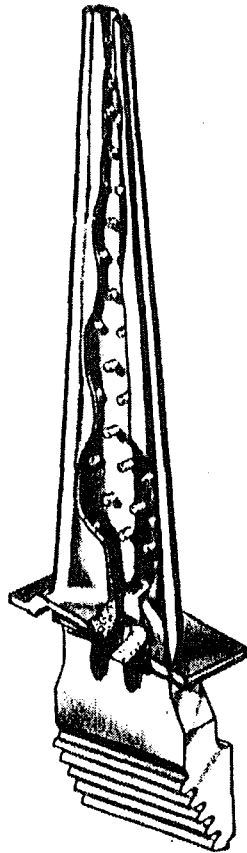
FE 5641

680608

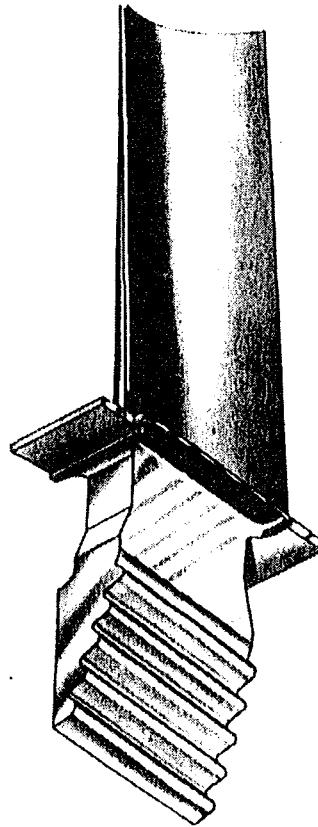
FD 24370

FIGURE 45

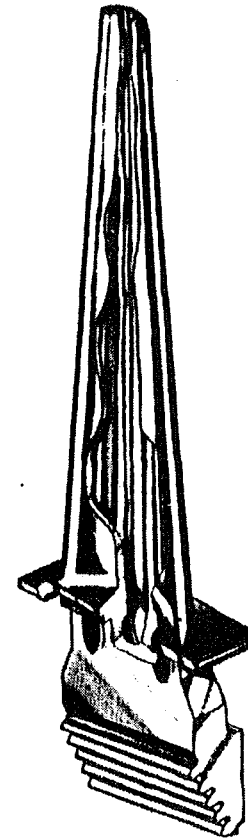
EXPERIMENTAL DESIGNS OF AIR-COOLED TURBINE BLADES



Cast



Slotted  
Leading  
Edge



Forged

-69-

314

FE 5642

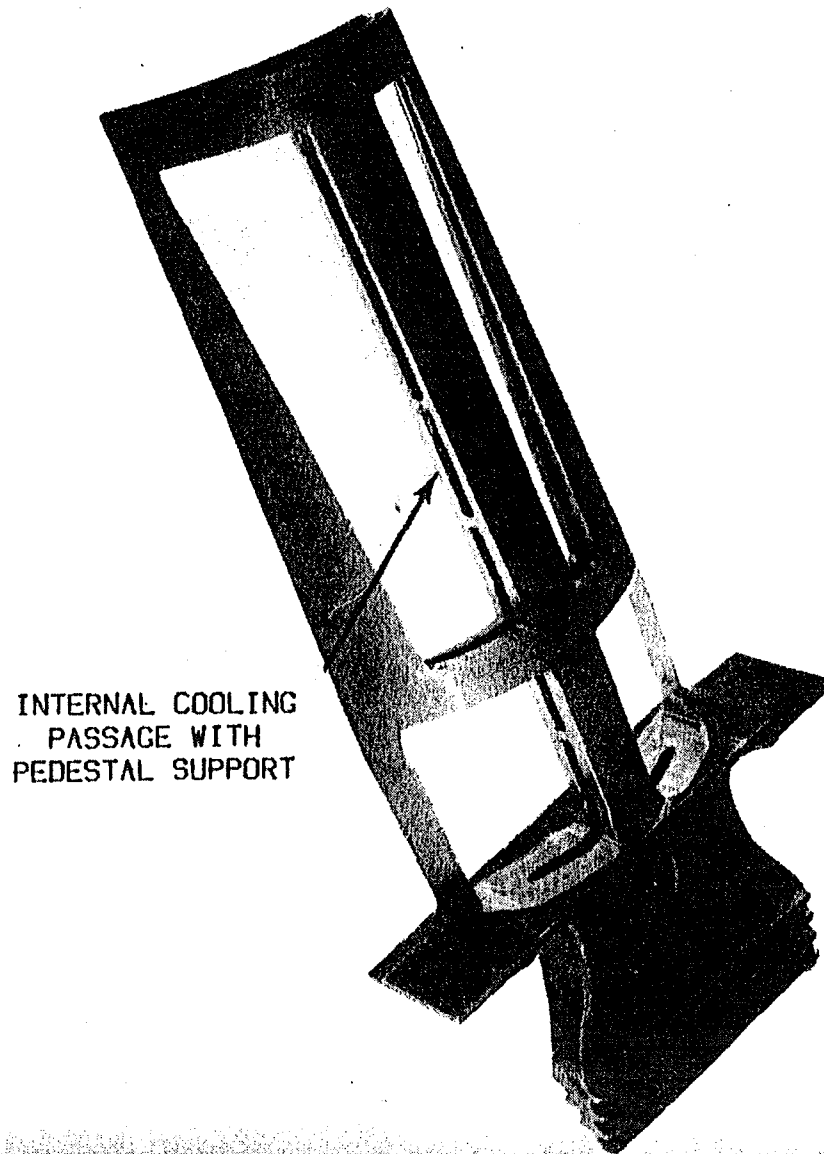
680608

FD 24383

FIGURE 46

CURRENT JT11D-20 FIRST-STAGE TURBINE BLADE  
CONVECTION COOLED TIP DISCHARGE

---



INTERNAL COOLING  
PASSAGE WITH  
PEDESTAL SUPPORT

one-piece, blade with tip discharge of cooling air, shown in Figure 46, was selected for the JT11D-20. Previous turbine designs had incorporated tip shrouds to improve efficiency and act as dampers. For this high temperature turbine, tip shrouds caused too much centrifugal load and were, therefore, eliminated. The JT11D-20 engine was the first engine to use root damping to prevent blade vibration.

### 8.3 Turbine Development

The design of the JT11D-20 turbine and its blade and vane cooling were proved in the engine development test program. More than 14,000 hours of test operation at turbine inlet temperatures at or above 1900°F, of which more than 7,300 hours have been at temperatures at or above 2000°F, were accumulated. A large part of this test operation has been under conditions simulating Mach 3+ flight, which results in high turbine cooling air temperatures. These high cooling air temperatures present a very large obstacle in the development of reliable high temperature turbines, because all high temperature turbine materials exhibit greatly reduced ductility at metal temperatures in the 1200-1400°F range. This loss in ductility prevents proper stress distribution and results in premature failures unless special precautions are taken. From the completion of the initial 50-hour endurance test in high Mach number environment at a turbine inlet temperature of 1850°F, the turbine inlet temperature has been increased to the 2000°F level employed for the current service engines.

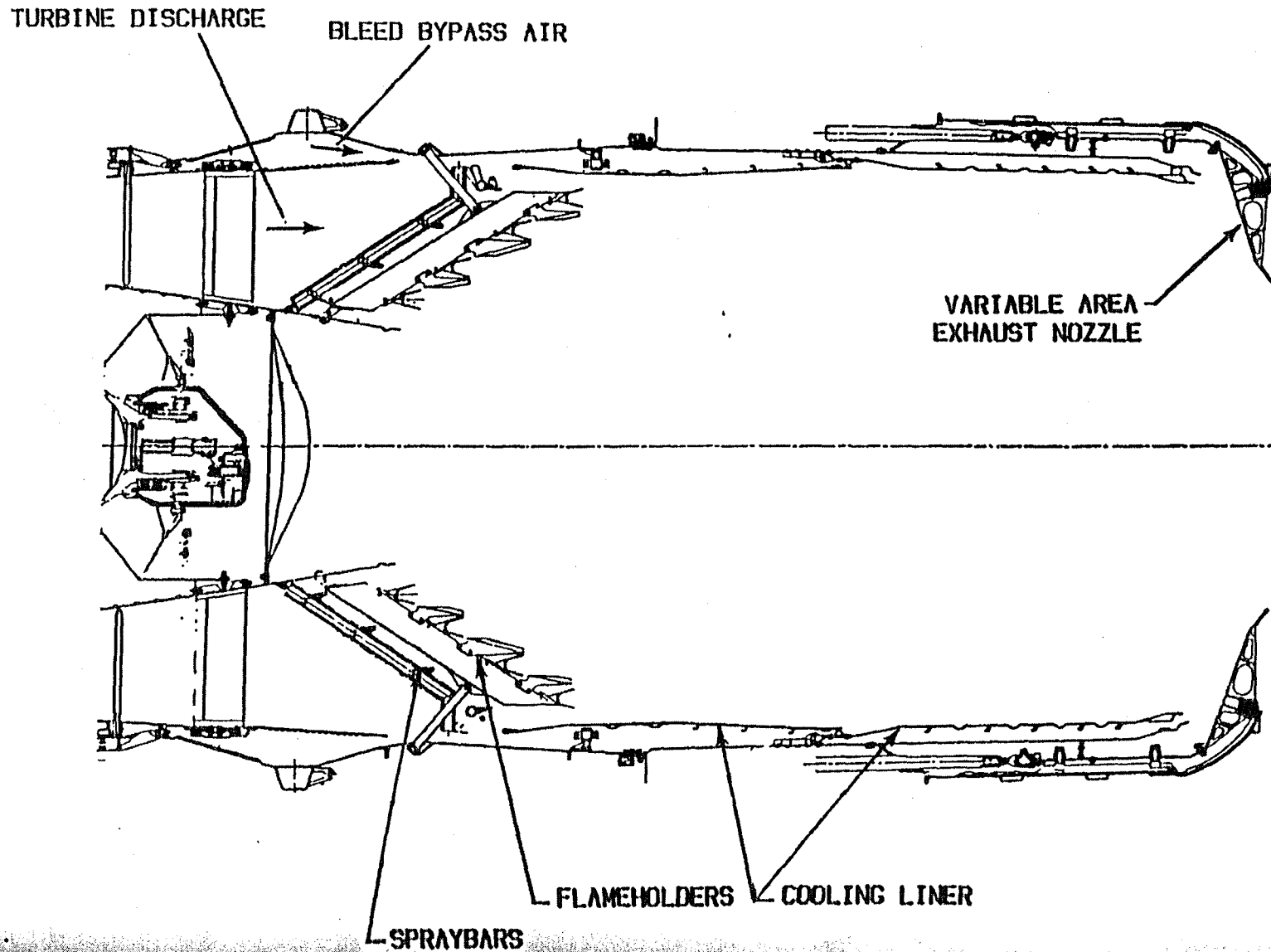
In any turbine operating continuously near the limits of its temperature capability, it is most important to maintain at all times an even turbine inlet temperature pattern. Otherwise, a 300°F hot spot that can be tolerated at lower temperature levels, will locally exceed the melting point of the best materials. In the JT11D-20 development program over 200 configurations of compressor blading, compressor diffuser, burner cans, and transition duct were tested before the required stable pattern could be achieved. The use of a burner can with a reasonably high pressure loss helps to maintain this pattern under conditions of compressor inlet pressure distortion. Flight experience on the JT11D-20 has substantiated the choice of this design.

In the JT11D-20 turbine development program, the principal problems were in the development of material processing techniques, parts quality control measures, and ductility of the turbine blade roots. It was necessary to develop adequate control of the grain size of the blade and vane castings of the new nickel base and cobalt base alloys in order to obtain consistent material characteristics in the engine parts. It was necessary to develop quality control tests to weed out defective parts. The most effective quality control test devised was to proof spin every turbine blade in a disk while heating the blade roots to their maximum operating temperature.



# JT11D-20 AFTERBURNER

FIGURE 47



## 9. AFTERBURNER

A cross section of the JT11D-20 afterburner is shown in Figure 47. For subsonic operation all the air entering the afterburner comes from turbine discharge. When the bleed bypass is opened above Mach 2.1 this bleed air enters in an annulus surrounding the turbine discharge. Part of this bleed air mixes with the turbine discharge air and is burned in the afterburner. Part of the cool bleed air passes behind the cooling liner and provides improved cooling at the high supersonic flight speed where the ambient temperature surrounding the afterburner is highest.

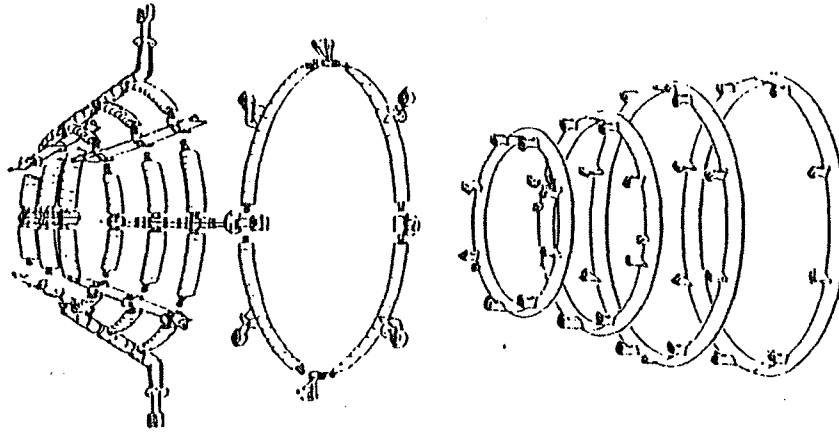
Gross thrust is proportional to the square root of the absolute temperature. The function of the afterburner is to increase gross thrust by increasing the temperature in the exhaust nozzle. Increased temperature reduces the density of the exhaust products and requires an increased jet area to pass the same airflow. Jet area is also proportional to the square root of the absolute temperature. Consequently the nozzle has continuously variable throat area which is controlled to maintain constant airflow.

Since the afterburner is used continuously for cruise, it must be efficient - fuel must be burned within the length of the afterburner, which is less than two diameters long. For best efficiency, the exit temperature must be as uniform as possible because a temperature profile gives lower thrust than uniform temperature. Liquid fuel does not burn. Fuel must be vaporized and mixed with air to a combustible mixture ratio before it can burn. The variable area spraybars, shown in Figure 30, give good fuel atomization over the large, 25 to 1, turndown ratio by keeping the fuel spray velocity high. The parasol pintle disperses the fuel into smaller droplets to further improve atomization and vaporization. The spraybars and pintles were located to give the desired local fuel-air ratio using downstream temperature and pressure traverses. Local cool spots when fuel is introduced show fuel concentration while baseline pressure and temperature traverses give the air distribution.

Flameholders cause turbulence that enables combustion before the fuel-air mixture leaves the exhaust nozzle. The blunt centerbody fairing also acts as a flameholder. The flameholders are placed close to the spraybars so that afterburner fuel does not have time to vaporize and auto-ignite ahead of the flameholder and burn the flameholders. Also, the upstream location of the flameholders gives more downstream volume for combustion.

FIGURE 48

# AFTERBURNER SPRAYRINGS AND FLAMEHOLDERS



SPRAYRINGS

FLAMEHOLDERS

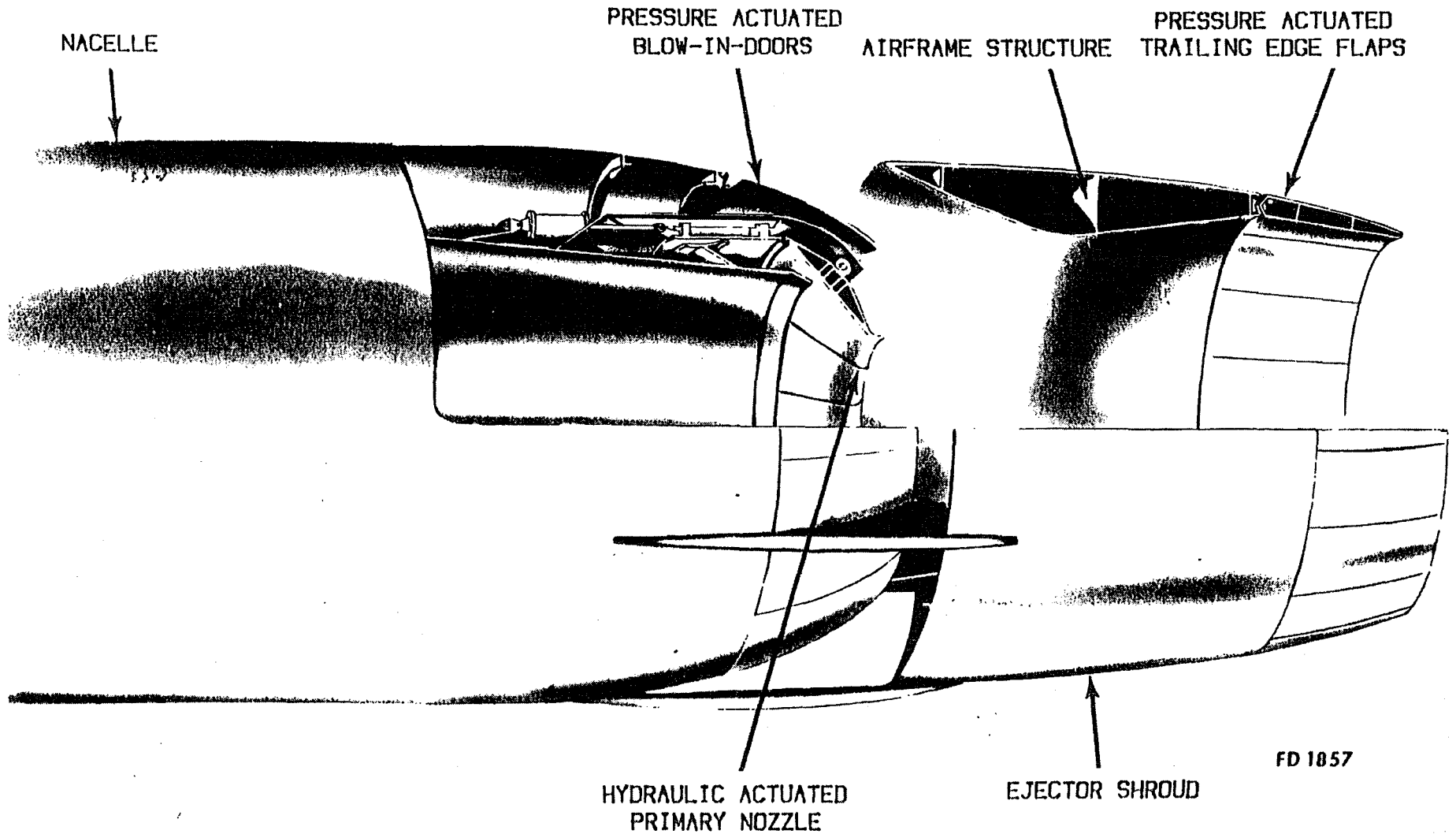
-74-

319

There are four annular sprayrings, manifolded together to a common fuel supply and four annular flameholders as shown in the exploded view on Figure 48.

FIGURE 49

BLOW-IN-DOOR EJECTOR NOZZLE



-76-

381

### BLOW-IN-DOOR EJECTOR NOZZLE

The term "ejector nozzle" was originally applied to nozzles that were used to induce secondary air into the nacelle for cooling. The secondary air was ejected through a cylindrical shroud. Ejector nozzles can operate in two ways (1) low flight speed pumping with an associated thrust loss compared to a convergent nozzle and (2) high flight speed thrust augmentation. At high flight speeds (high primary pressure ratio) the cylindrical shroud ejector restricts the flow of secondary air and produces thrust augmentation.

The JT11D-20 ejector nozzle, Figure 49, bears little resemblance to the earlier cylindrical shroud ejectors. It is closer in appearance to a convergent-divergent nozzle. The cylindrical shroud has been replaced by a divergent shroud to improve thrust augmentation and variable geometry has almost eliminated the low flight speed pumping characteristics of earlier ejectors.

Originally, the blow-in door ejector nozzle was to be part of the engine. It was subsequently decided jointly by Lockheed and Pratt & Whitney that it would save weight if it was built as part of the airframe structure. This was deemed appropriate particularly as the main wing spar structure had to go around the throat of the ejector. Pratt & Whitney, however, would still be responsible for the ejector nozzle performance in conjunction with the engine primary nozzle. In addition, we would perform all of the isolated wind tunnel testing. In exchange, Pratt & Whitney would develop the remote gearbox because Lockheed's gearbox vendor had no experience with gear materials or bearings and seals that would withstand the temperatures required. As a matter of fact neither did we, but we were already committed to learn.

FIGURE 50

## FEATURES OF THE JT11D-20/SR71 EJECTOR NOZZLE

- Airframe Mounted
  - Light weight
  - Easy engine removal
- Low drag exhaust of inlet bleed air
- Secondary air cushions expansion of primary stream
- Aerodynamic positioning of variable geometry
  - Blow-in-doors
  - Trailing edge flaps

## 10.1 Design Features

The JT11D-20/SR71 blow-in-door ejector nozzle has several features that have been tailored to the SR71 application, as shown in Figure 50.

10.1.1 Airframe Mounted - It is mounted on the airframe and is not mechanically coupled to the engine. This eliminates thermal expansion and structural deflection problems between engine and airframe at the exhaust nozzle location. The ejector shroud is part of the airframe structure: both wing and tail surfaces transmit loads through the ejector shroud. The blow-in-doors are attached to the nacelle as shown in Figure 49 and form a smooth aerodynamic contour with the nacelle. Isolation of the ejector nozzle from the engine facilitates engine removal.

10.1.2 Secondary Airflow - Inlet boundary layer bleed is necessary for stable and efficient operation of the inlet. When this low energy bleed air is discharged overboard through louvers, as in the forward bypass, it increases airplane drag. If, however, it is discharged through the exhaust nozzle shown in Figure 49 it cushions the expansion of the primary stream and produces thrust. At supersonic flight speeds the combination of the engine primary nozzle, the secondary airflow and the divergent portion of the ejector shroud produces an aerodynamic convergent-divergent nozzle that produces more thrust and less drag than an exhaust nozzle that terminates in the plane of the primary nozzle.

10.1.3 Aerodynamic Positioning of Variable Geometry - Engine exhaust leaving the primary nozzle will expand supersonically to fill the exit area at the high power conditions where engine performance is important. At low flight speed, the engine pressure ratio is relatively low and the primary stream expands to lower-than-ambient pressure causing installed thrust loss. This over-expansion of the primary stream causes blow-in-doors to open and trailing edge flaps to close. Both of these actions increase the thrust but also increase drag. The result is that both the blow-in-doors and trailing edge flaps float in a position that gives a compromise between thrust and drag. As flight speed increases, the exhaust pressure increases. The blow-in-doors close between Mach 0.9 and 1.4. The trailing edge flaps open up until they reach the full open position above Mach 2.4 when the external contour of the nozzle is cylindrical (apart from the cusps formed by the approaches to the blow-in-doors and trailing edge flaps which give very little pressure drag). The internal contour then approximates a convergent-divergent nozzle.



**FIGURE 51**

**EFFECT OF MODEL SCALE AND AIRCRAFT FLOW FIELD ON EJECTOR PERFORMANCE**

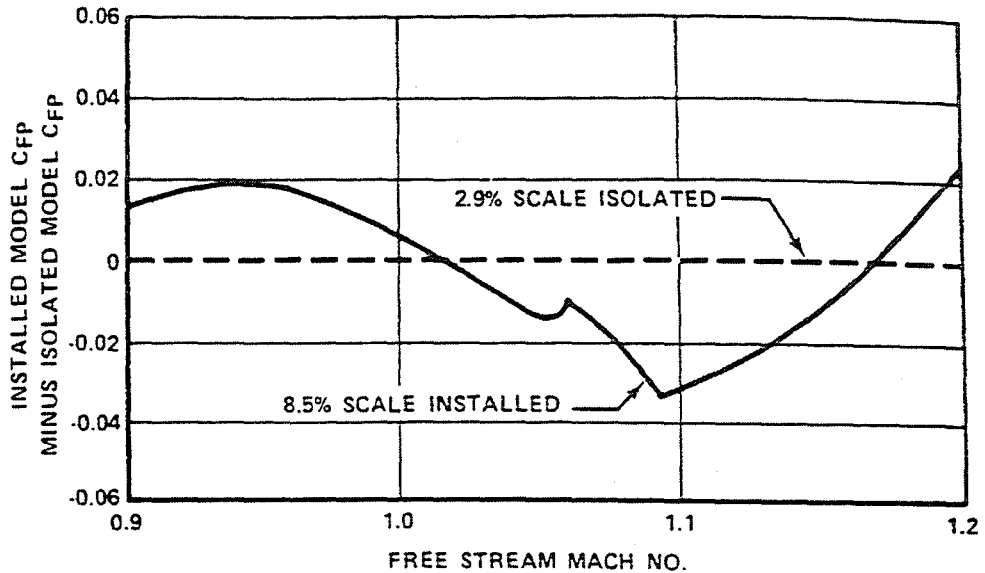


**FIGURE 52**

**EFFECT OF SCALE ON BOUNDARY LAYER THICKNESS**

	Isolated 2.9% Scale Model	Isolated 5.7% Scale Model	Installed Full Scale Aircraft
Boundary Layer Thickness to Blow-in-Door Height Ratio	4.2	2.1	0.65

Early scale model tests to define and optimize exhaust nozzle performance were made on 2.9% scale models. Later 5.7% scale models, with free floating blow-in-doors and trailing edge flaps, gave slightly improved performance when the blow-in-doors were open. Tests of an 8.5% scale model mounted in a scale model airplane showed about 2% better thrust coefficient below Mach 0.95 and above Mach 1.2 but up to 3-1/2% lower thrust coefficient in the transonic region, as shown in Figure 51. Improved performance with increased model scale is due to the relatively thinner boundary layer, shown in Figure 52. As the scale increases, more air and higher energy air passes through the blow-in-doors. The lower performance in the transonic region shown in Figure 51 by the installed model is due to the effect of the aircraft flow field on pressures outside the blow-in-doors. Figure 53 shows that Mach numbers at the blow-in-door location can be significantly different than the free stream Mach number. At a free stream Mach number of 1.0 the local Mach number at a top outboard location is 1.35. Increased local Mach number causes a local pressure reduction which can close the blow-in-doors in the vicinity of reduced pressure and partially close in blow-in-doors that remain open.

Flight data taken on the upper blow-in-doors shows different actuation of individual blow-in-doors, Figure 54. It is noted that blow-in-doors will move in response to changes in aircraft pitch and sideslip and also to changes in the position of the vertical tails.

FIGURE 53

LOCAL FLOW FIELD OF SR71 AIRCRAFT

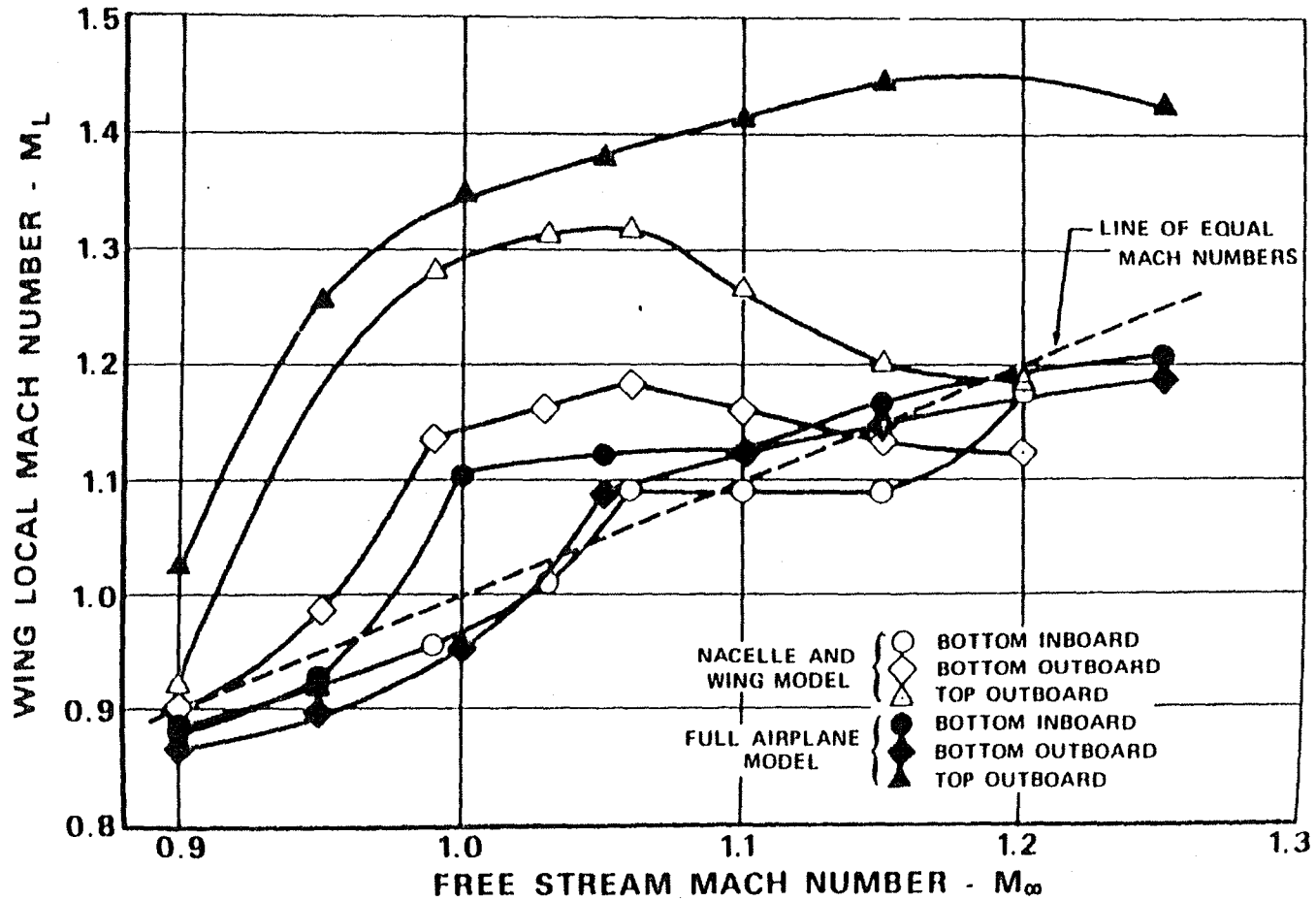
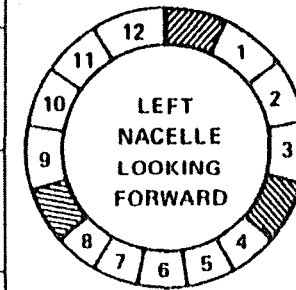
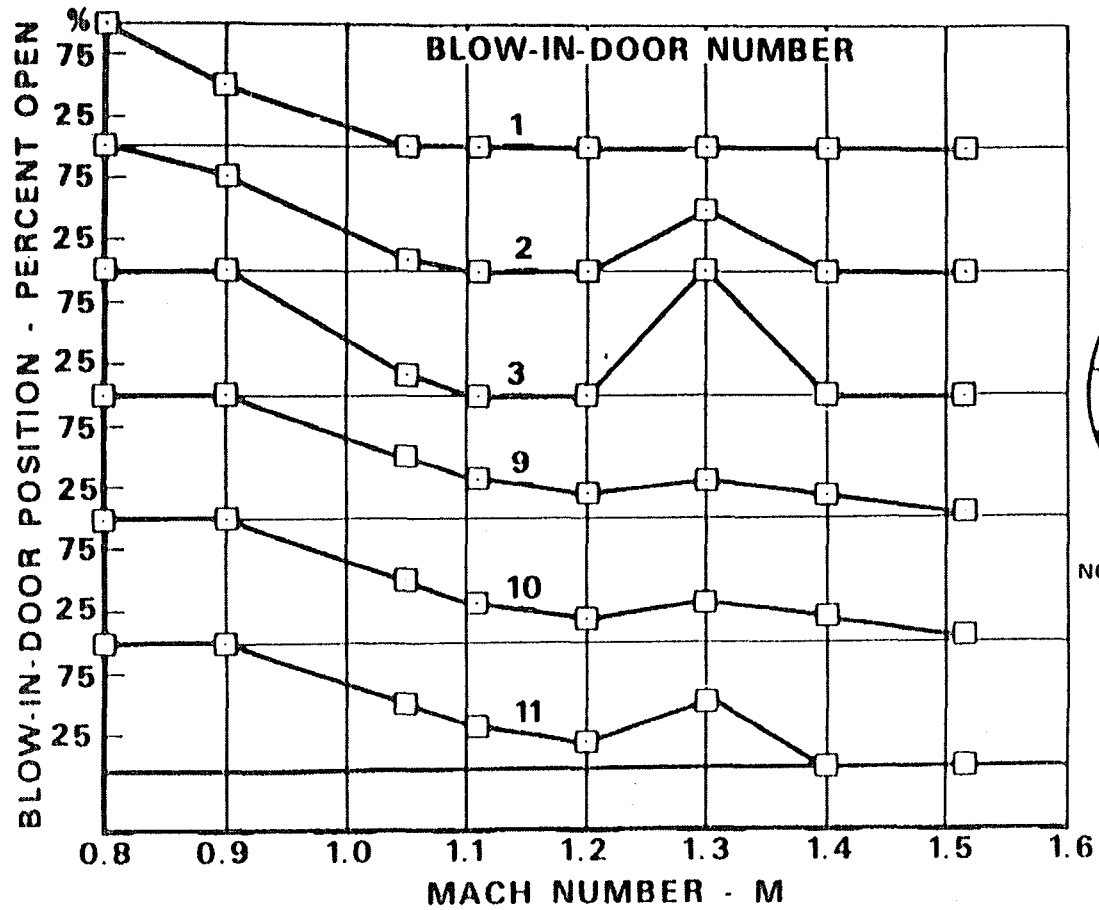


# FIGURE 54

## BLOW-IN-DOOR POSITION DEPENDS ON LOCAL FLOW FIELD



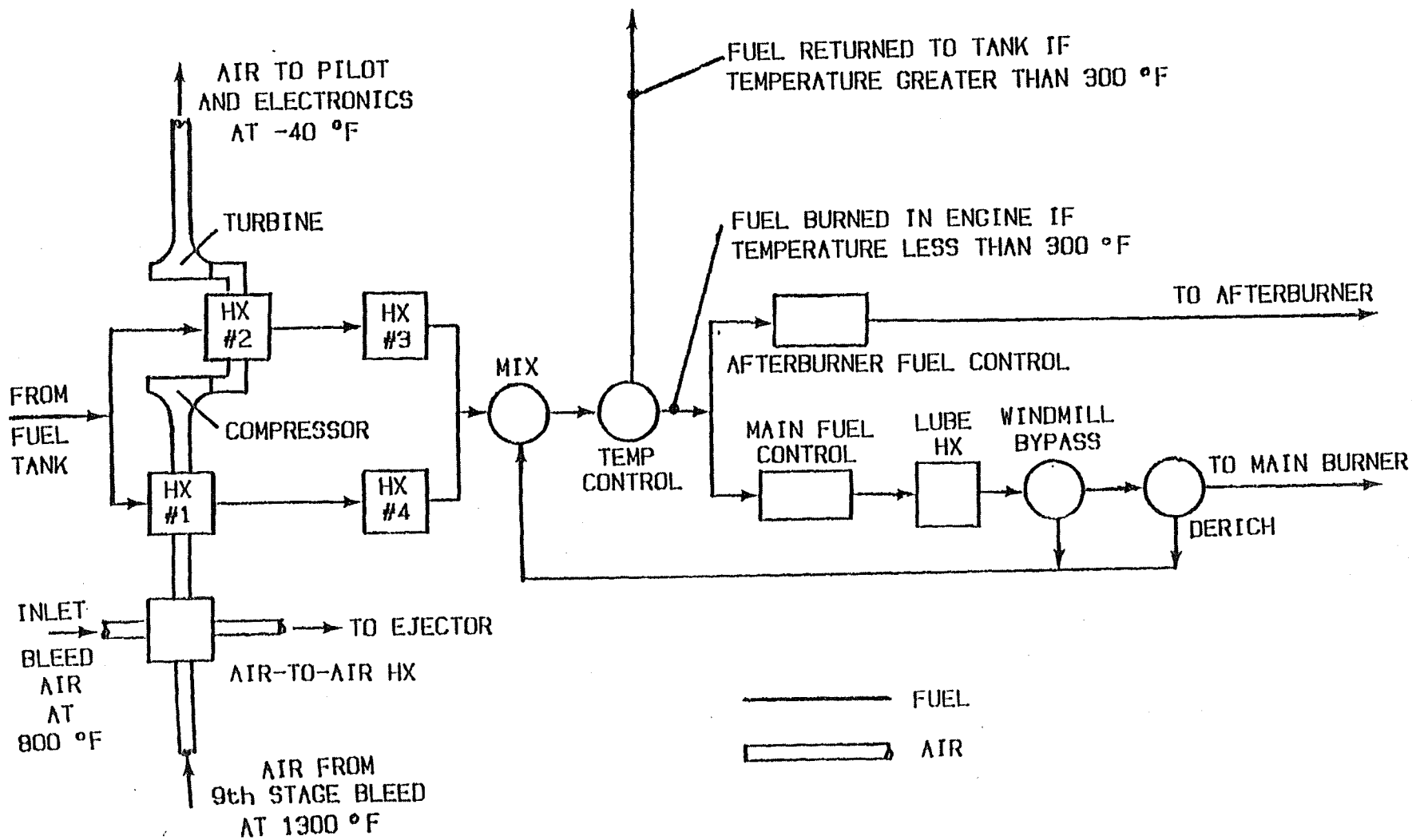
NOTE:

- 1 DATA RECORDED BY EXTERNAL CAMERAS
- 2 100% BLOW-IN DOORS FULLY OPEN
- 0% BLOW-IN DOORS FULLY CLOSED

FIGURE 55

SCHEMATIC DIAGRAM OF ENVIRONMENTAL CONTROL SYSTEM  
FUEL BURNED IN ENGINE IS MAJOR HEAT SINK

-84-



389

## 11. ENVIRONMENTAL CONTROL SYSTEM

The heat sink available to cool the pilot, electronics, lubricants and hydraulic fluid is the fuel that is burned in the engine.

It was necessary to develop a fuel with high thermal stability so that a higher maximum fuel temperature could be tolerated in the engine without coking and plugging of lines and nozzles. At the same time, to improve engine parts life at high turbine temperature, an increased luminometer number was desired to reduce heating by flame radiation, and a reduced sulfur content was required to prevent sulfidation attack on turbine blades. Lower vapor pressure, to reduce fuel boil-off from the aircraft tank at high altitude, was also required and this made obtaining adequate engine relight ability more difficult. A fuel (PWA 523) meeting these general characteristics has been produced in quantity by four petroleum refiners. This fuel specification is included in Appendix 1. As the result of further engine development, increased flame radiation became acceptable and a less stringent fuel specification (PWA 535 or JP-7) was adopted to reduce fuel cost.

Figure 55 shows a schematic diagram of the environmental control system. The pilot and the electronics require the coolest environment. This is accomplished by a conventional air-cycle air conditioning system. Air from compressor discharge at temperatures up to 1300°F is cooled by inlet bleed air (up to 800°F) and then further cooled by fuel in heat exchanger #1. This cooler air is compressed, cooled by fuel in heat exchanger #2 and then expanded by the turbine that drives the compressor. Air leaves the turbine at -40°F and is used for cockpit and electronics air conditioning.

Fuel leaving heat exchangers #1 and #2 is used as a heat sink for aircraft hydraulics, gearbox and the inlet spike and is then forwarded to the engine through a mixing valve and a temperature control valve.

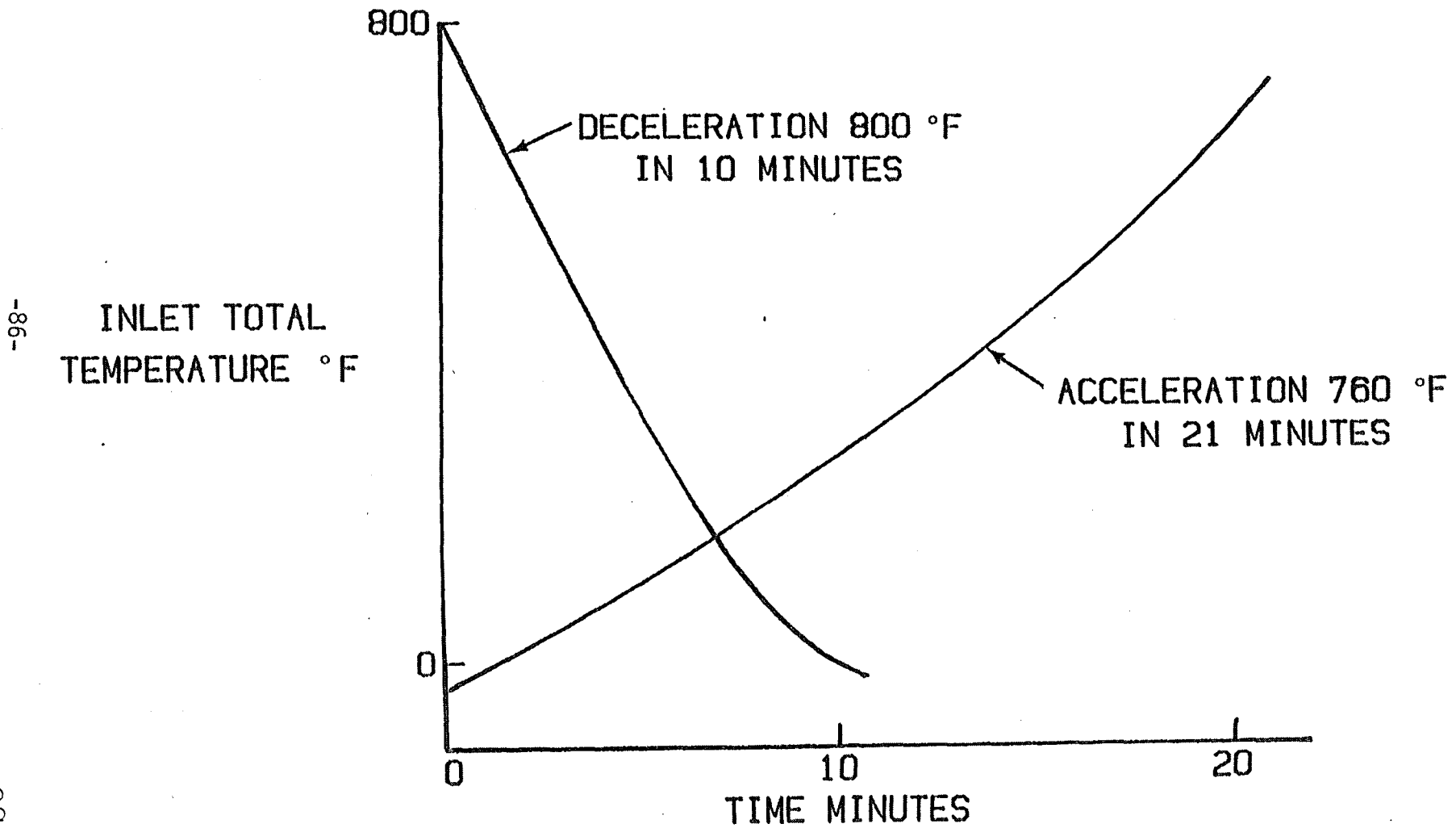
Fuel enters the engine system at temperatures less than 350°F. The main fuel flow is pumped to higher pressure, metered by the main fuel control and is then used to cool the engine lubricant. Heat exchange between lubricant and fuel must be high enough to cool the lubricant below the point where it breaks down chemically in the engine, yet low enough to prevent fuel coking and local, uncontrolled, fuel boiling in the engine. This requirement could not be met with conventional fuels and oils. A special lubricant was developed as well as a special fuel. The specification for this lubricant is included in Appendix 1.

The lubricant must be cooled even if the engine burner is not lit (windmilling engine). To accomplish this, fuel leaving the fuel control is diverted back to a mixing valve during windmilling and then is passed to the temperature control valve. If the fuel temperature is less than 300°F the fuel is recirculated to the engine. If it is greater than 300°F it is returned to the fuel tank. However, during transients the fuel temperature at the inlet to the engine can reach 350°F.

Fuel is continually circulated in all lines up to the afterburner control and up to the windmill bypass valve. Downstream lines are purged when fuel is not being delivered to the burner. This prevents stagnant fuel from decomposing into varnish or carbon and blocking lines and orifices.

FIGU. 56  
TEMPERATURE TRANSIENTS MORE SEVERE  
THAN PREVIOUS EXPERIENCE

---



391

## 12. THERMAL GRADIENTS

12.1 Temperature Transients - Not only were the high inlet temperatures a new challenge but both the rate of change of temperature and the temperature change were higher than previous experience. Typical rates of change of inlet temperature are shown in Figure 56. Deceleration from high Mach number and high altitude is the more severe transient. The deceleration shown in Figure 56 is  $1.3^{\circ}\text{F}/\text{sec}$ . The aircraft is capable of more rapid descent: descents higher than  $5^{\circ}\text{F}/\text{sec}$  have been experienced.

12.2 Compressor Tip Clearance - During rapid reductions in inlet temperature the outer cases of the engine cool faster than the compressor rotor. This has caused the rotor tips to rub against the shrouds. This does not damage the tip because the shrouds are abradable but it does lead to larger tip clearances and a stepped flow path after one flight. The size of the steps gives an accurate measurement of this differential contraction. The problem was solved by increasing clearances to accommodate a rate of change of  $1.5^{\circ}\text{F}/\text{second}$  and limiting the rate of descent to that value.

12.3 Rotor-Stator Clearance - Differential contraction between the rotor and the outer case during rapid descent also results in an apparent "growth" of the rotor relative to the stator of up to 1 inch, both forward and aft from the thrust bearing located near the middle of the engine. This produces a requirement for larger than usual clearance between the rotor and stator. Thermal growth of the rotor did not affect rotor dynamics. The JT11D-20 engine had low vibration without the benefit of viscous dampers that are used in later engines.

12.4 Design for Thermal Gradients - Cases were designed with relatively thin flanges and numerous small bolts to minimize the thermal shock resulting from thicker flanges and larger bolts. Likewise, the thick-thin ratio between various sections of rotating disks were minimized for the same reason. Heavy case bosses normally attached by welding were replaced with more forgiving riveted attachments.

12.5 Flubber Disks - Another differential expansion during high rates of descent occurred because the outer rim of a compressor disk cools before the bore. At rates of descent greater than  $3^{\circ}\text{F}/\text{sec}$  and  $5^{\circ}\text{F}/\text{sec}$  this caused plastic deformation of the 5th and 3rd compressor disks, respectively. When the engine was disassembled the disks were deformed and "oil canned". This phenomena was called a "flubber disk". A plasticity computer program was used to investigate this plastic deformation. The computer program showed that the deformed disk straightened out in use and consequently the problem was cosmetic not structural. This was confirmed by engine testing. However, the rate of descent was limited to  $1.5^{\circ}\text{F}/\text{sec}$  and "flubber" disks no longer occur.

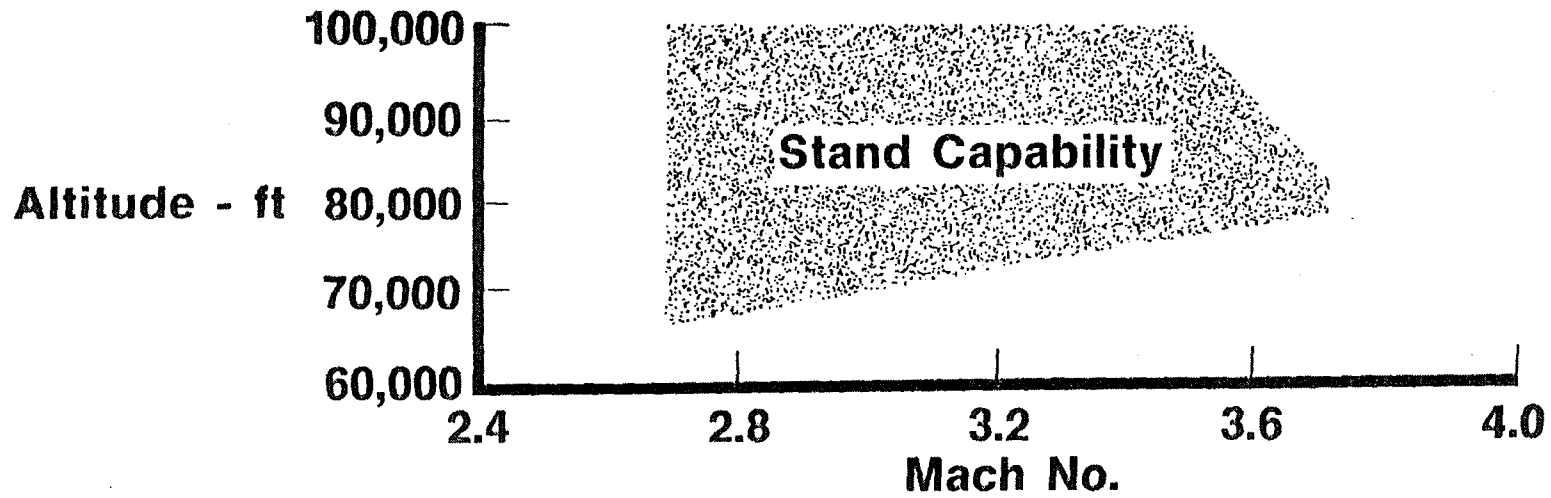
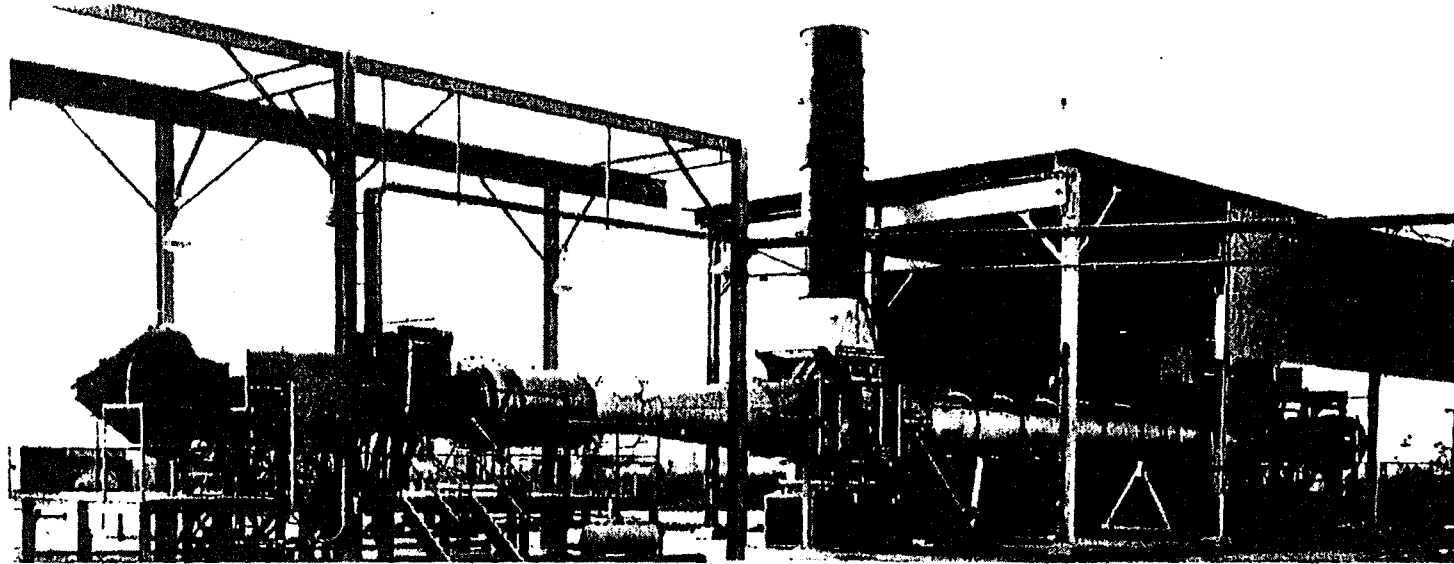
## 13. DEVELOPMENT

The purposes of an engine development program is first to ensure that the engine is safe to fly, then to ensure that it meets performance, weight, durability and cost commitments. Development is continued during the flight test phase to correct any problems that have surfaced during flight. Since the purpose of the engine is to fly, the key to development is rigorous simulation of the flight environment.



FIGURE 57

# HEATED ENVIRONMENT TEST STAND



-88-

AV 218314  
810604  
gn1-449

393

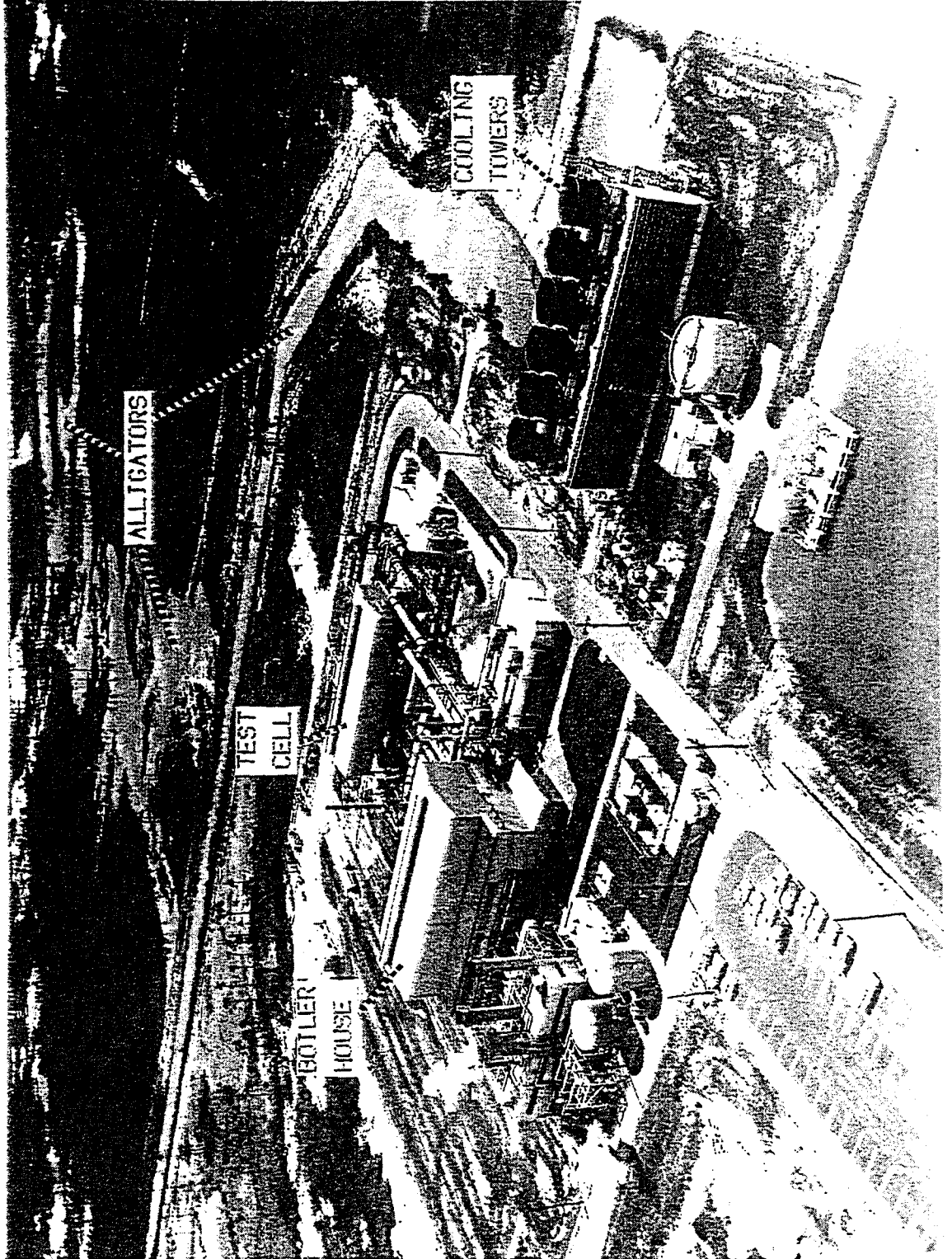
### 13.1 Test Facilities

At the start of the engine design program, the capabilities of the Arnold Engineering Development Center, Tullahoma, Tenn., were investigated to determine if the altitude test portion of the engine development program could be conducted at that facility. It was established that the facility was capable of handling the engine but, because of the severe restrictions on the amount of time during which the facility could be operated, it would have been possible to accumulate only some 16 hours per month of altitude test time, even if the highest priority was obtained for the JT11D-20 program. Consequently, the first problem we addressed was that we had no test facilities that had the capabilities to provide steady-state temperature and pressure conditions required for testing at maximum operating conditions nor for performing transients.

13.1.1 A Heated Environmental Test Stand, Figure 57 was a partial solution to simulated high Mach number testing. Heated air from a J75 jet engine is directed to the inlet of the JT11D-20 engine through an arrangement of control valves. An auxiliary, variable-area air intake downstream of the J75 exhaust is used for temperature control. Air at flows up to 250 pound per second and 900°F can be supplied to the inlet of the JT11D-20 engine.

When running simulated altitude conditions, the engine is shrouded in an enclosed container to provide high temperature air around the engine. The engine exhausts through an ejector to improve pressure recovery and, consequently, the capability to simulate higher altitude. A heated fuel system can supply fuel at temperatures up to 400°F. This test stand enables us to run temperature transients that simulate acceleration to and deceleration from the cruise Mach numbers.

FIGURE 56  
AERIAL VIEW OF THE ALTITUDE TEST FACILITY



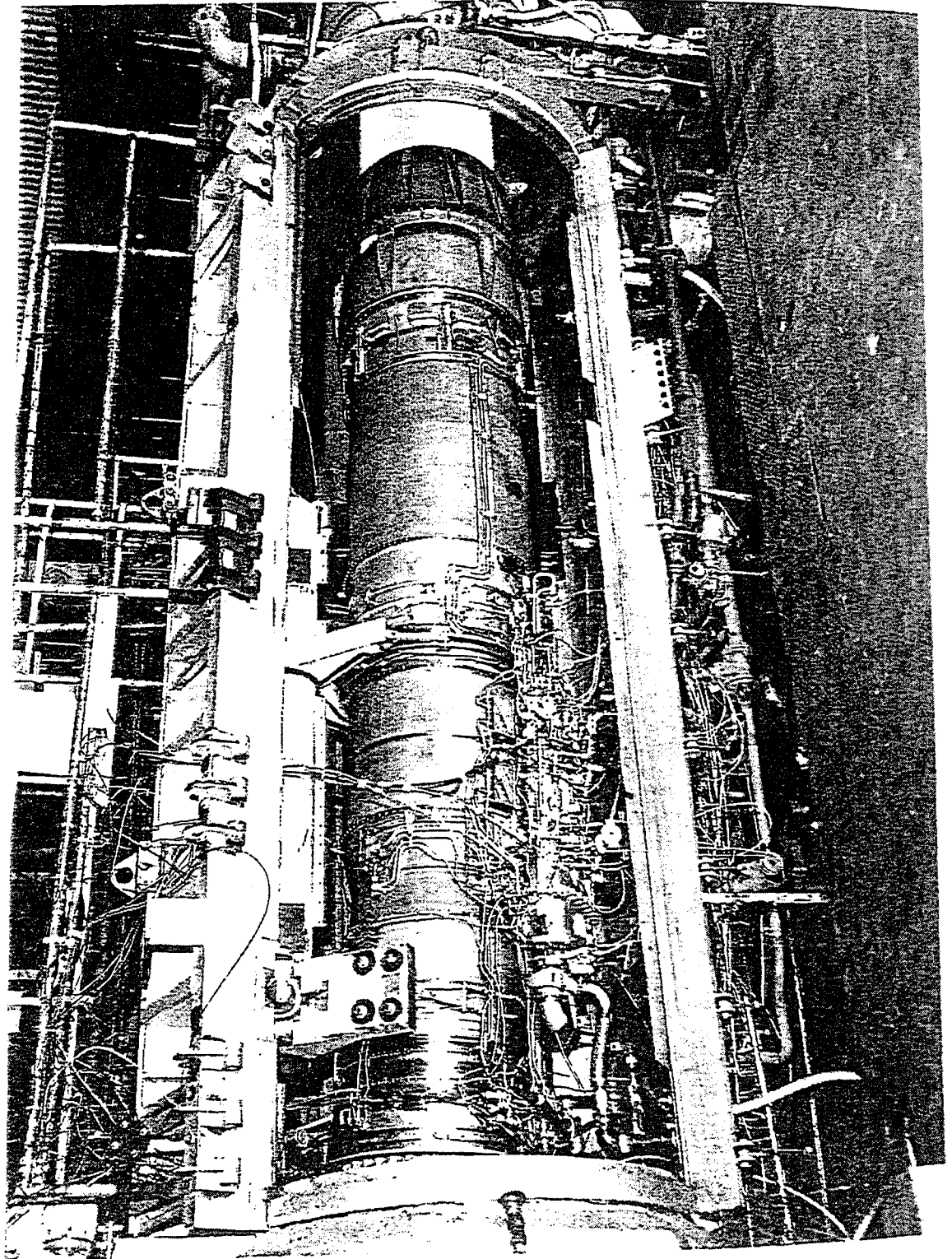
13.1.2 Other Test Stands - Test stands built for and dedicated to JT11D-20 development program included an altitude test facility capable of testing an engine under simulated flight conditions in excess of Mach 3.0 at more than 100,000 feet altitude. Figure 58 shows an aerial view of the altitude test facility. Power is supplied by six 13,500 horsepower steam-driven turbines. Pond water is used for cooling. Cooling towers cool the return flow to prevent harm to the fish, alligators and birds inhabiting the ponds and surrounding marshes. Figure 59 shows an F100 engine being tested in the altitude facility with the access door open and atmospheric exhaust. The normal test mode is with the access door closed and the exhaust sucked down to simulate operation at altitude. This altitude facility included two main burner component test stands, a compressor test stand, and two full-scale, high Mach number, engine test stands. It had a pebble bed heater and consequently supplied heated, unvitiated air to the engine inlet. It could operate over a larger altitude range than the heated environmental test stand discussed earlier. It was used for performance and endurance testing. Five additional stands operated at sea level atmospheric inlet and exhaust. For the engine components such as the fuel system parts and the controls, the hydraulic system parts, oil system parts, accessory drive gearbox, seals, and bearings, thirty-four component test stands and rigs were built that were capable of testing the components under a wide range of conditions including high temperature environment with high temperature oil and fuel. In addition, seven other major component environmental test stands were in continuous use at the plants of vendors of proprietary-design components.

13.1.3 Compressor Drive The compressor drive in the altitude facility required both high power and high rotational speed. Steam turbines were considered because the altitude facility contained a large steam plant. Commercial steam turbines were investigated, but existing designs with sufficient power operated at too low a speed and delivery times were excessive. Use of a low speed turbine with a step up gear box was considered, but delivery times were even longer and concerns existed for the reliability and durability of high power gear boxes with high output speed.

Another possibility considered was the use of a gas turbine engine such as the PT5, a shaft power derivative of the J57, but power turbines of such engines have large diameters and thus are below the speed range needed for this application unless step up gear boxes are provided.

The possibility of adapting a jet engine turbine to operate on the available steam was then considered. The JT4 "high" turbine was of particular interest because it was large enough to provide a power level of interest and had the mechanical speed capability required. Aerodynamic study showed that it would operate at nearly the same aerodynamic parameters on steam as on hot gas in the engine and would thus provide a high stage efficiency. The much lower temperature of the steam would compensate for the much lower molecular weight of steam (as compared to

FIGURE 9  
F100 ENGINE RUNNING IN THE ALTITUDE TEST FACILITY  
WITH AMBIENT EXHAUST PRESSURE



hot gas). However, the JT4 high turbine, having only one stage, could not expand the steam through much more than a pressure ratio of two, limiting power and causing excess steam consumption. This was solved by utilizing both the high and low turbines of the JT4, locked together. In an engine, each turned on its own shaft at independent but similar speeds, so this was acceptable.

In the compressor drive installation, the two turbines were mounted in their engine turbine cases, using their engine bearings. Thus the installation job was relatively simple and modest in cost and could be accomplished quickly.

The drive system performed well and was reasonably trouble free. The only significant problem was that some lubricating oil leaked into the steam, requiring seal modification to reduce contamination of the steam.

13.1.4 Installed Testing - An engine was tested with the inlet and nacelle on a sea level test stand, as shown in Figure 60. This testing substantiates inlet-engine flow stability at the critical takeoff operating condition. This type of sea level installed testing was new in the early 1960's. It is commonplace today.

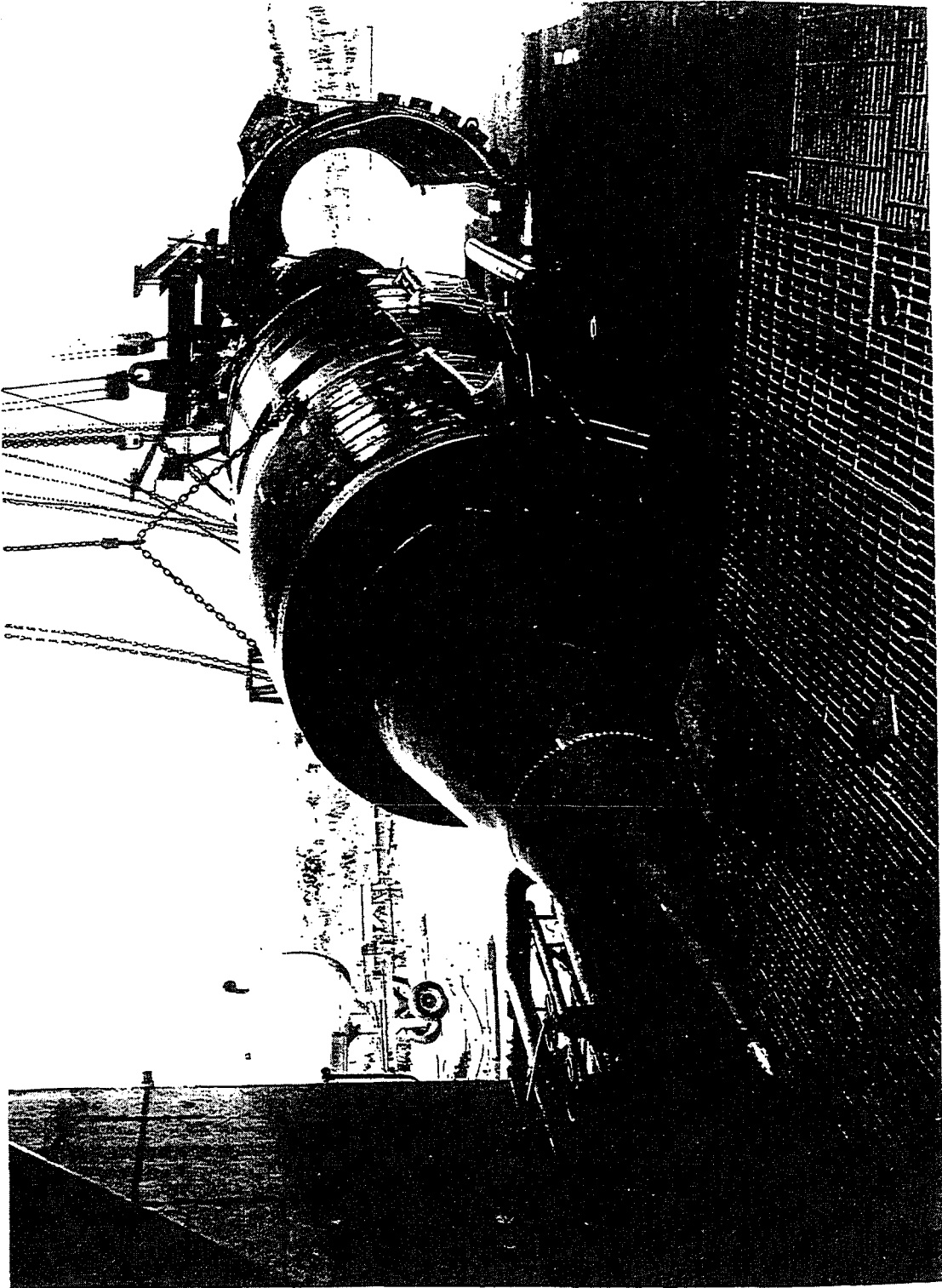
13.1.5 Instrumentation - There was essentially no instrumentation rugged enough to obtain accurate real-time measurements. Strain gages did not last as well as they do now during testing. You usually had to get your data within the first 5 minutes of run time on turbines and maybe a few hours, at most, on compressors. There was much slip ring noise and lead wire noise, and no isolation between channels, so one noisy strain gage would foul up all the channels. It was something of an art to be able to find the bad channel out of all the noisy channels, so that you could switch it out of the circuit and get data from the remaining good gages. There were no lead wire routing tubes through the engine from the turbine, as we have now, and the leadwires would always get damaged in assembly, to such a degree that gages were lost and skinned lead wires became noisy.

Slip rings were far inferior to what we have today, and would only last a little while during test. If the slip ring itself didn't fail, it would get fouled up from oil and water in the cooling air. All data was recorded on oscillograph, so data reduction was difficult and also data was missed during changes of magazines. High frequency data was almost unattainable because most galvanometer type oscillographs would not respond to it. There was a cathode ray tube recorder, but it was difficult to use and tended to run out of paper before you got any data.

A major task of the engineer evaluating engine or component performance is to validate the measurements made by the instrumentation by repeated calibration, by redundant measurements and by consistency checks with other measurements using the engine computer simulation as a reference.

One unusual instrumentation problem occurred in the altitude test facility. We had three methods of estimating engine airflow: pressure readings from a calibrated bellmouth, the speed-flow characteristics of the compressor and, the most accurate, an ASME calibrated orifice. The problem was that the accurate method intermittently disagreed with the

FIGURE 60  
INSTALLED TESTING ON A SEA LEVEL STAND



other two estimates. A leak in the ducting was suspected. A performance engineer and a test engineer were assigned to track down and fix the problem. They were told to crawl up the ductwork, if necessary - but don't come back until you have found the problem. The problem was not the suspected leak but swirling flow due to an upstream bend was giving false pressure readings at the calibrated orifice under high flow conditions. The orifice was relocated and the problem went away.

Another mystery that was harder to solve was the measured afterburner efficiency suddenly going over 100% while the engine was running. The initial suspect was afterburner fuel flow, however, two redundant fuel flow measurements agreed and a third measurement agreed intermittently. We could find no fault with any of the instrumentation that would explain the problem, so a performance engineer was assigned to solve the mystery. He reached a dead-end several times and asked for another assignment. He was told that we had perfect confidence in his ability as a detective and that he would get another assignment as soon as he finished the present one.

Persistence paid off and he solved the problem. Thrust in the altitude stand was estimated from gas generator performance, the measured nozzle area and the measured pressure profile at the exit of the nozzle. The larger the nozzle area or the larger the pressure - the higher the thrust. The nozzle was choked and the test stand operator knew that anything happening downstream of a choked nozzle could not affect engine data so he saved time by leaving off cover plates for instrumentation access ports that were just downstream of the nozzle exit. This was fine as long as the static pressure inside the stand ejector was substantially atmospheric. The apparent increase in afterburner efficiency occurred when the altitude simulated in the facility was increased. This dropped the pressure in the stand ejector so that flow through the access ports was both supersonic and at a higher Mach number than the primary flow. The result was that the aerodynamic exit area looked like a four leafed clover while the larger physical area on which performance is based is circular. The pressure rake extended across one of the clover leaves, so it looked, from pressure measurements, as if the nozzle was flowing full. A brave test engineer volunteered to cover and uncover these access ports while the engine was running at the simulated high altitude and lo and behold the estimated afterburner efficiency was as expected when the ports were closed and over 100% when the ports were open.

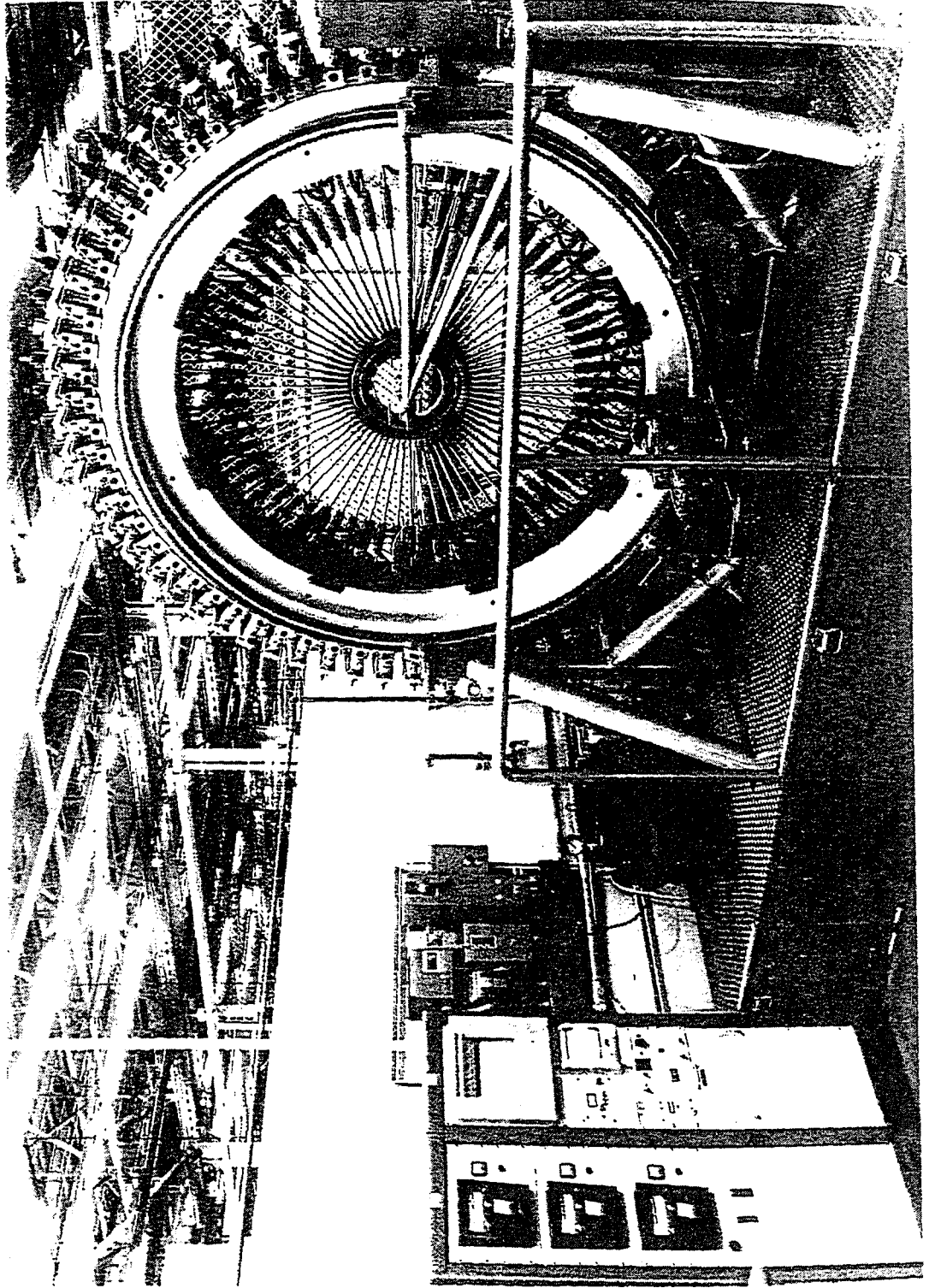
As Pratt & Whitney developed more rugged instrumentation and better calibration facilities, improved data were gradually obtained.

Lockheed, of course, was kept up-to-date as we obtained better data. A good part of the time Lockheed and Pratt & Whitney jointly ran fuel system rigs, inlet distortion rigs, etc., as well as some engine calibration tests and wind tunnel tests of the ejector.

13.2 Low-Cycle Fatigue - In April 1968, a Waspaloy compressor disk developed cracks in the rim area during thermal cycle testing on the heated environmental test stand. These cracks were attributed to low cycle fatigue. A "ferris wheel" type radial loading rig was built and experimental stress analyses and low cycle fatigue (LCF) tests were



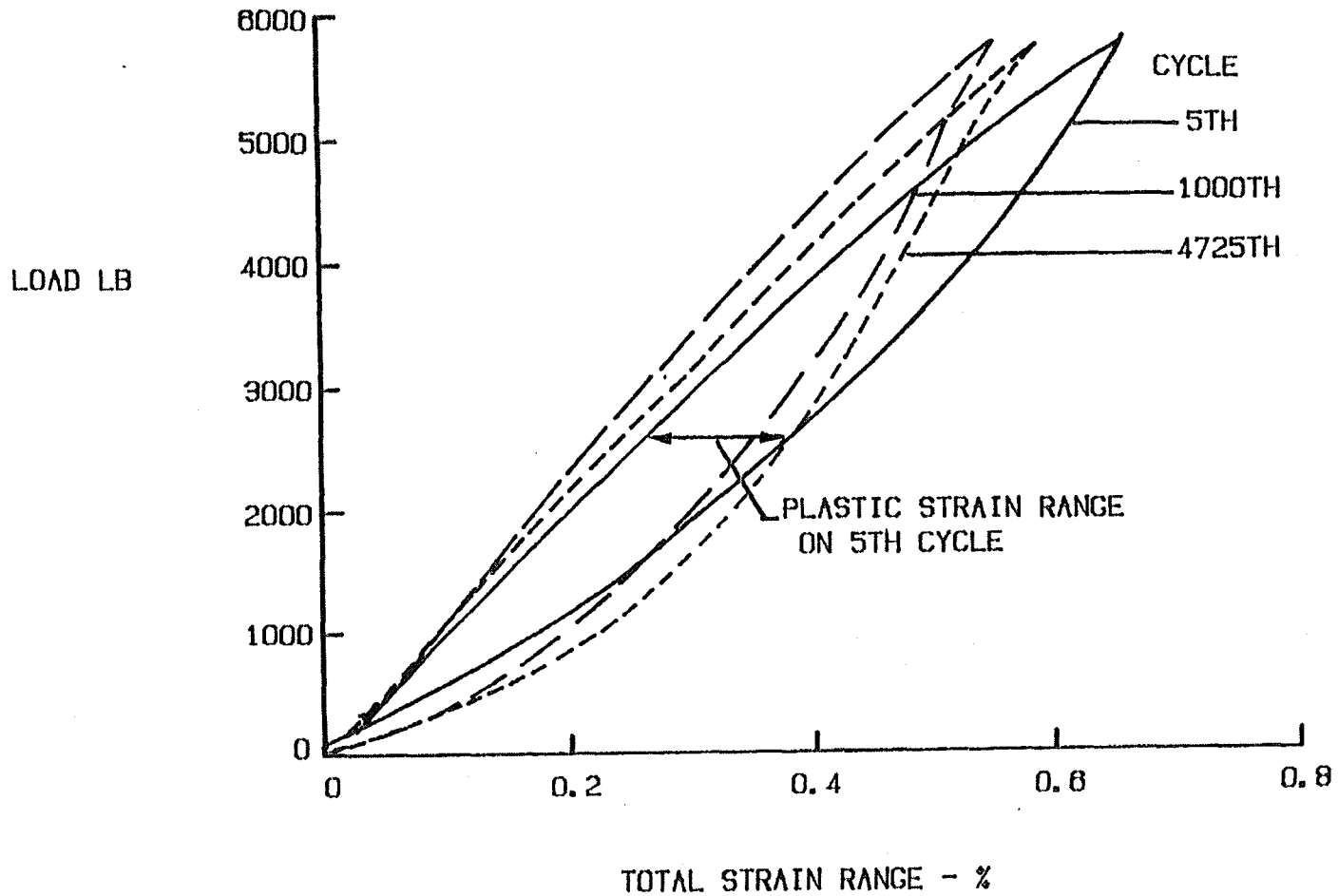
FIGURE 61  
STRUCTURAL TEST LABORATORY "FERRIS WHEEL" FACILITY



conducted on compressor disks (see Figure 61). Pan cake ovens, one on each side of the disk, are not shown on figure 61. The entire loading frame was rotated slowly past the ovens to maintain an even temperature on the disk. Each bar attached to the disk blade slots was loaded by a hydraulic cylinder attached to the outer rings. As the rig rotated, the cylinders extended and contracted. It is easy to see why the rig was name the "Ferris Wheel". The Ferris Wheel rotation is reversed after each 355° rotation. This enables flexible connections to the hydraulic cylinders and instrumentation and avoids sliding seals and slip rings.

FIGURE 62

TOTAL STRAIN RANGE CHANGES DURING CONSTANT LOAD CYCLIC TESTING



-86-

1507

All previous materials data for fatigue life analyses was based upon load controlled (sontagg) data. The wide variation between the predicted (290) disk LCF cycles and the actual (5000) disk ferris wheel cycles to crack initiation underscored the inadequacy of existing disk material LCF data and the methods of predicting disk LCF life.

Ferris Wheel tests are carried out at constant load. This produces constant strain in the critical areas of a disk. However, constant load does not produce constant strain during tests of material specimens. Figure 62 shows the results of specimen tests. For a constant load, the total strain range does not change very much after repeated cycles. But it does change. Plastic strain range also changes. Since load controlled specimen tests were not satisfactory for predicting LCF life, strain controlled testing was investigated. Plastic strain range may be a better parameter, however, total strain was selected because it is easier to control.

**FIGURE 63**  
**CONSTANT STRAIN LOW CYCLE FATIGUE RIG**

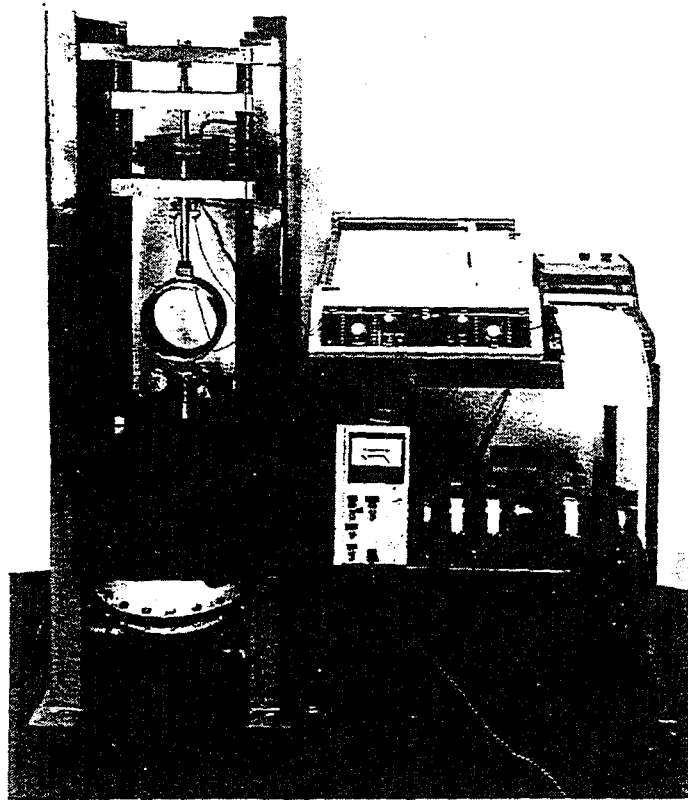
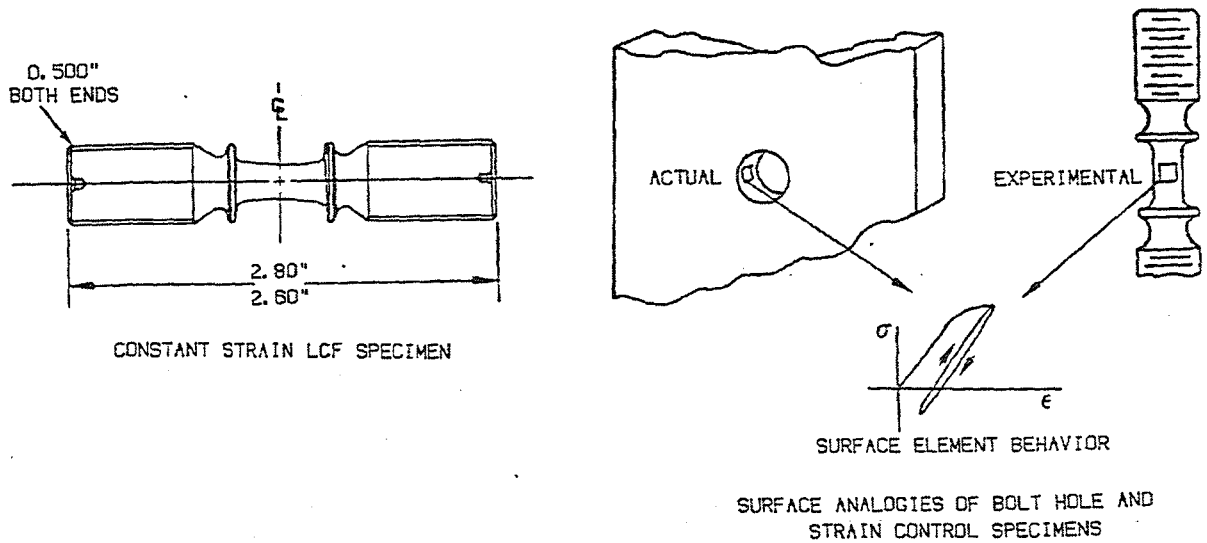


**FIGURE 64**  
**CONSTANT STRAIN LCF SPECIMEN**



A closed loop test rig was built with the capability of conducting specimen tests at selected values of constant total strain range (Figure 63) and a special test specimen was developed (Figure 64). This basic specimen design is still in use today. Four specimens, like Figure 64, were made from a new disk and four specimens were made from an engine failed disk. Different values of total strain range were applied to each specimen. These tests on the specimen rig agreed well with the test of an entire disk on the Ferris Wheel facility, as shown in Figure 65.

Subsequent analyses and testing of other J58, TF30 and F100 materials and disks, at both room and elevated temperatures have also correlated well.

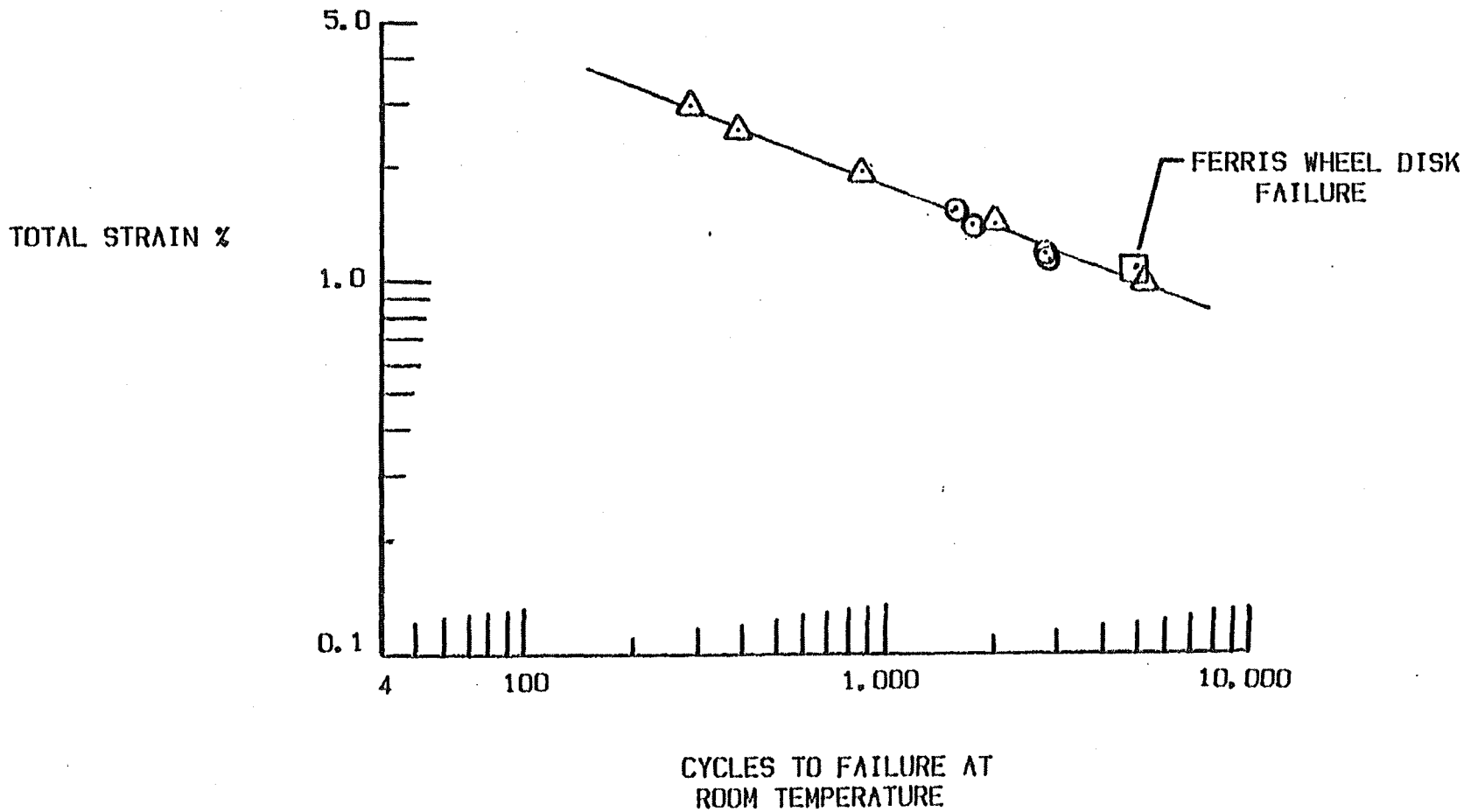
This early strain controlled testing was done under purely cyclic loading as shown in the sawtooth cycle in Figure 66. Engines do not operate totally under cyclic conditions, but include periods of cruise or relatively stable conditions. During these periods - dwell at a steady state condition - creep can occur. Creep-fatigue interaction can result in significantly different disk life than either LCF or creep considered separately. Test data for an LCF cycle with a creep-dwell is shown in Figure 67 for a Waspaloy specimen tested at 1200°F. A dwell time of 30 minutes per cycle halves life compared to sawtooth cycles (zero dwell time).

This combination of cyclic and dwell testing was used to predict disk life with greater accuracy than ever before and was a major step in improving life prediction systems. Subsequent application of cumulative damage concepts, with the appropriate material characterizations lead to improved life prediction capability for complex mission cycles. This system was used in later analyses of the JT11D-20 disks. It has evolved into the life prediction system now used by P&W for engine components.

FIGURE 65

# TOTAL STRAIN VS CYCLES CORRELATES TEST DATA

- △ SPECIMENS MANUFACTURED FROM A NEW DISC
- SPECIMENS MANUFACTURED FROM AN ENGINE FAILED DISC

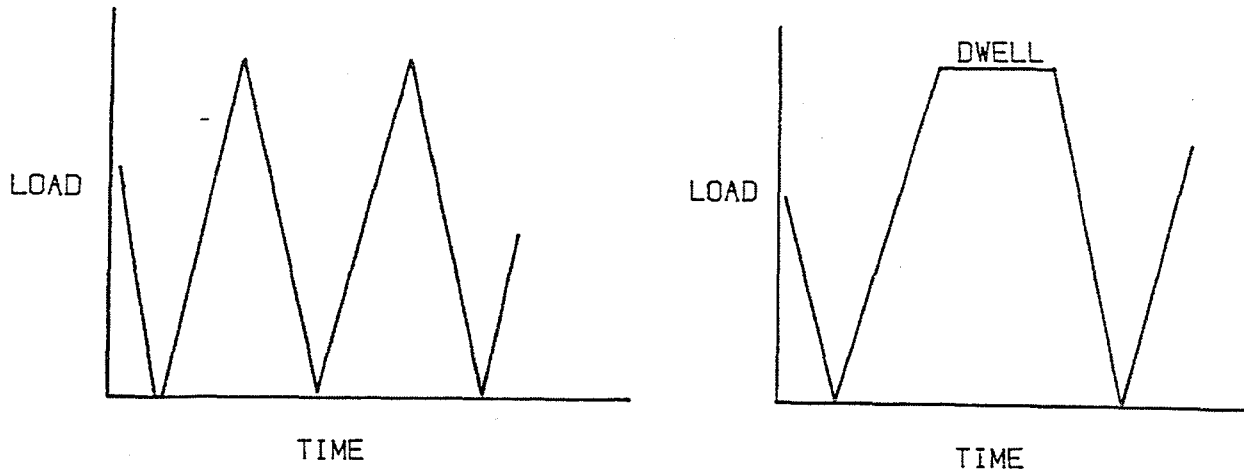


-102-

481

FIGURE 66

LCF CYCLES



TYPICAL "SAWTOOTH" LCF CYCLE

TYPICAL DWELL-LCF CYCLE. DWELL AT MAX LOAD SHOWN. DWELLS MAY BE INSERTED AT ANY POINT IN CYCLE.

FIGURE 67

EFFECT OF DWELL ON SPECIMEN CYCLIC LIFE

WASPALOY SPECIMEN TESTED AT 1200 °F

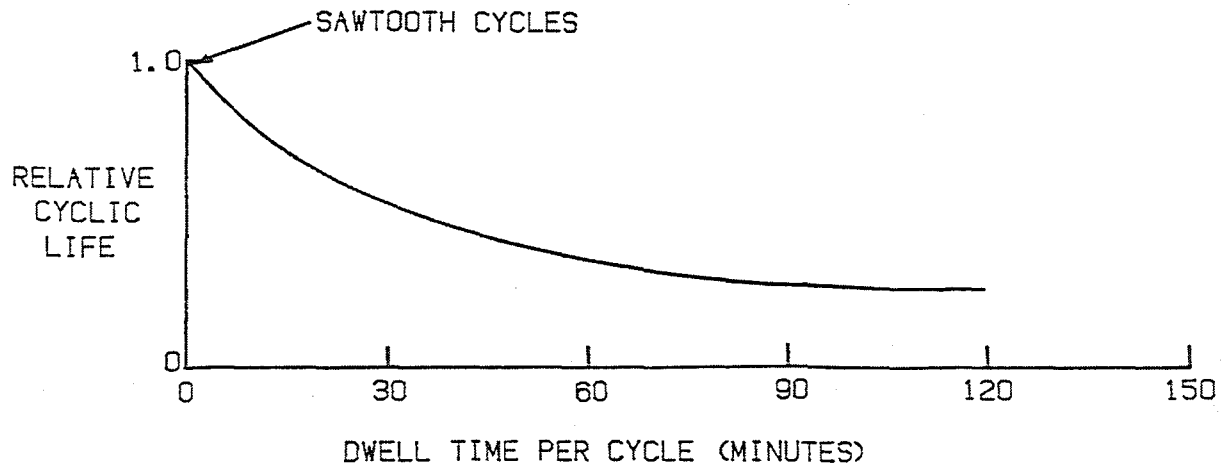
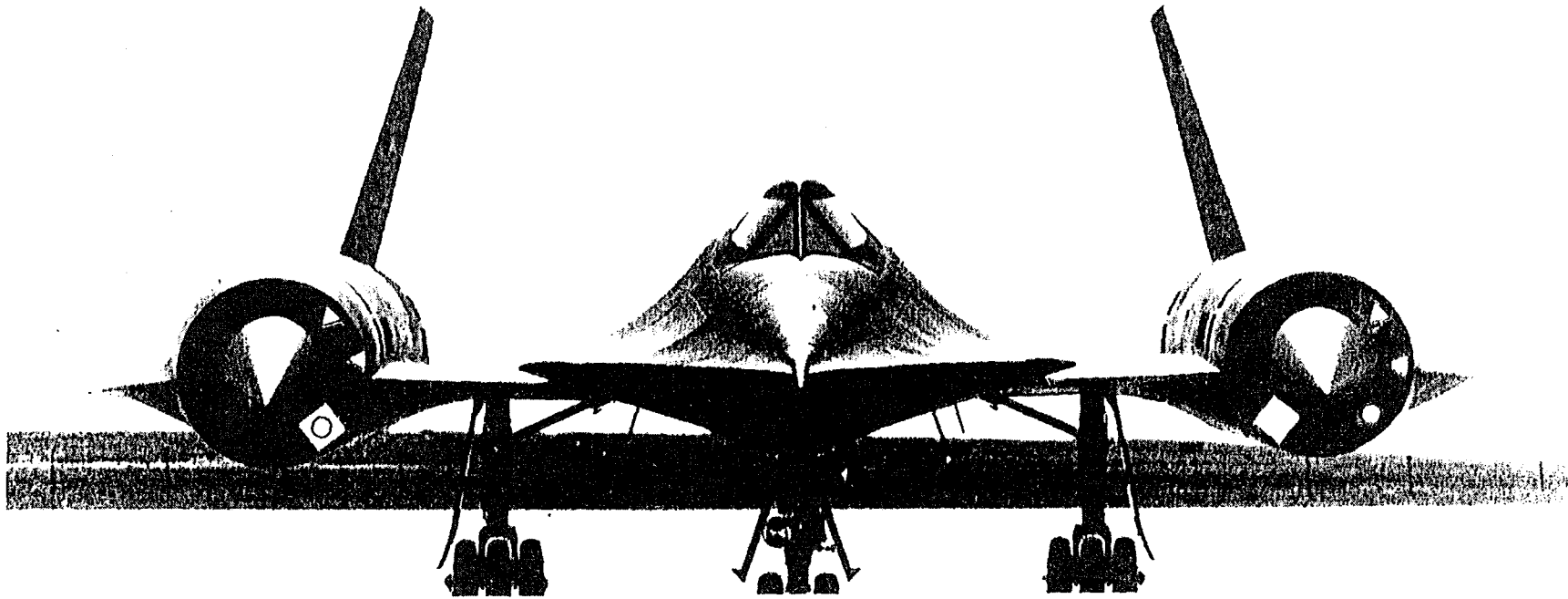




FIGURE 68

DUCT LINES UP WITH ENGINE TEMPERATURE SENSOR



○ ▽ COMPRESSOR INLET TEMPERATURE SENSOR LOCATIONS

◇ ENVIRONMENTAL CONTROL SYSTEM DUCT

-104-

409

## FLIGHT TESTING

The learning experience continued as the SR-71 airplane entered flight test. The first "Blackbird" took to the air approximately nine months before Pratt & Whitney finished the Pre Flight Rating Test 3 years and 4 months after go-ahead (the Engine Model Qualification Test was completed 14 months later). At first the 'Blackbird' was powered by two afterburning J75 turbojet engines to check out the aircraft in subsonic flight. As soon as Lockheed felt comfortable with the aircraft, a JT11D-20 was installed in one side. After several months of subsonic flight tests, JT11D-20 engines were installed in both sides, and we started flight testing for real.

Naturally there were problems. Here are a few notable ones and the solutions.

### 14.1 Starting Problem

The first problem happened very early--the engine wouldn't start! The small inlet wind tunnel model did not show the inlet being so depressed at the starting airflow. In fact, instead of air flowing out of the compressor 4th-stage through the bleed ducts into the afterburner, it flowed the other way! As a temporary fix, Lockheed removed an inlet access panel for ground starts. They later added two suck-in doors (see Figure 26) and Pratt & Whitney added an engine bleed from the bleed bypass ducts to the nacelle. These two changes eliminated the ground starting problem.

### 14.2 Engines Differ

Lockheed and Pratt & Whitney spent many hours coordinating the inlet and engine arrangement so that doors and-bleeds would not affect any of the engine control sensors in the engine inlet. Ram air, used to cool the pre-compressor heat exchanger in the environmental control system (ECS), is taken from a duct in the inlet located 45° from the engine centerline and discharged into the secondary air passage leading to the ejector. The early engines had a single temperature sensor for the hydromechanical control located 45° on the opposite side from the ECS duct on the port engine. Lockheed built one inlet as a mirror image of the other while both engines were identical. The location of this engine temperature sensor is shown by the circles in Figure 68, while the squares show the location of the ECS duct. The duct entry lines up with the temperature sensor on the starboard engine.

For a while the fact that one engine always ran faster than the other was a big mystery! During takeoff the low inlet pressure at the engine face caused reverse flow of hot air through this duct. The starboard engine then sensed a higher temperature than the port engine. Engine airflow is scheduled by regulating engine speed as a function of inlet temperature according to the schedule shown in Figure 24. Consequently the starboard engine operated at higher speed during takeoff. The problem was fixed by preventing reverse flow in this duct. The sensor locations were moved to the positions shown by triangles in Figure 68 when the hydromechanical control was upgraded from a single temperature sensor to redundant sensors. This removes the sensors governing speed from the vicinity of the ECS duct. The sensor locations indicated by circles in Figure 68 are now used for the inlet temperature input into the electronic trim control of turbine exhaust gas temperature.

### 14.3 Transonic Acceleration

A problem partially related to the ejector was that the airplane burned too much fuel going transonic. To help solve the problem, thrust measurements were taken in flight and movies were made of ejector operation in flight. Local Mach numbers were also measured. Two fundamental causes were uncovered. The back end of the nacelle (the ejector) went supersonic long before the airplane did, and the fairing of the aircraft transonic wind tunnel drag data was not accurate. From this we learned not to run nacelle wind tunnel tests unless the model contains at least a simulation of the adjacent aircraft surfaces.

More transonic thrust was required. The conventional solution (increasing turbine temperature) did not work because the resulting increase in net thrust was offset by increased nozzle drag that resulted from smaller primary jet area. The solution was to increase airflow. To increase airflow at transonic speeds, while maintaining the high compressor efficiency required for supersonic speeds, required a variable inlet guide vane.

Transonic fuel usage was high on the original climb procedure. Two solutions were proposed (1) partial afterburning to achieve the best climb fuel consumption on the original flight path (2) the pilots found another approach, climb at maximum afterburning above the original flight path and then dive through the transonic region. Both used less fuel than the original climb procedure but the pilots' solution reached cruise faster and was more fun! So it was adopted.

#### 14.4 Thrust and Drag

Airplane performance was initially below expectations. Suspects were low thrust or high drag. A task force of Lockheed and P&W engineers covered everything from how engine performance was measured to a review of wind tunnel test data. The problem was in airflow accounting. Estimates of airflow supplied by the inlet agreed with the airflow used by the engine. However, the inlet estimate was based on the cold capture area of the inlet. When thermal expansion of the inlet at the elevated cruise temperature was accounted for, it became obvious that there was a leak from the nacelle. Ground pressure checks confirmed the leak. The leak was fixed and then performance matched predictions.

#### 14.5 Remote Gearbox

As flight testing increased to the higher Mach numbers, new problems arose. One, which today may be considered simple with our modern computer techniques, concerned the remote gearbox. The gearbox mounts started to exhibit heavy wear and cracks, and the long drive shaft between the engine and the gearbox started to show twisting and heavy spline wear. After much slide-ruling, we finally decided that the location of the gearbox relative to the engine was unknown during high Mach number transients. We resorted to the simple test of putting styluses on the engine and mounting a scratch plate on the gearbox. We found, to our astonishment, that the gearbox moved about 4 inches relative to the engine. This was much more than the shaft between the engine and the gearbox could take. The problem was solved by providing a new shaft containing a double universal joint.

FIGURE 69

LARGER CROSS SECTIONAL AREA OF HEAD END OF NOZZLE ACTUATOR

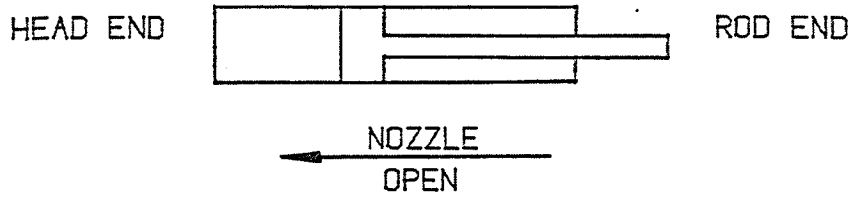
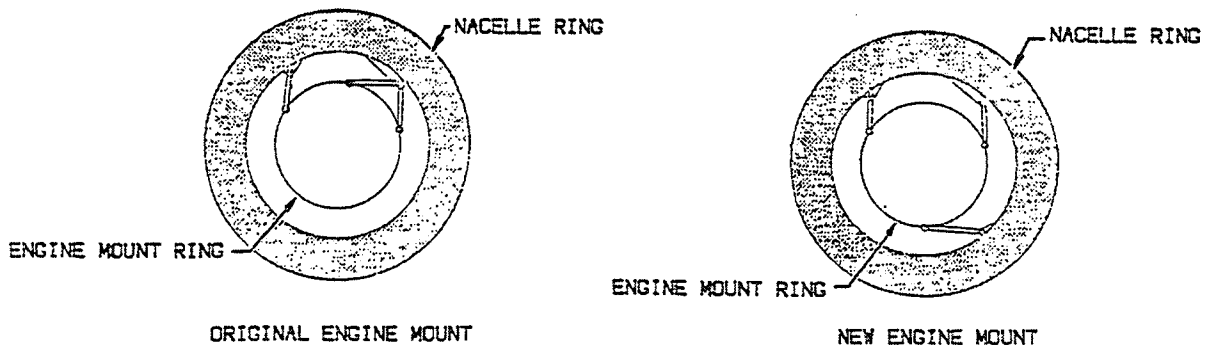


FIGURE 70

ENGINE MOUNT REVISION



#### 14.6 Plumbing Fatigue

Another problem arose when the aircraft fuel system plumbing immediately ahead of the engine started to show fatigue and distortion. Measurements with a fast recorder showed that pressure spikes at the engine fuel inlet were going off-scale. This overpressuring was found to be caused by feedback from the engine hydraulic system. The cross sectional area of a nozzle actuator is larger at the head end than the rod end, as illustrated in Figure 69. On engine shutdown the nozzle opens to relieve back pressure on a subsequent start. When the nozzle opened fuel was "added" to the aircraft and engine lines. With the small volume in the lines this led to unacceptable pressure spikes.

This phenomenon did not surface either during Lockheed's or Pratt & Whitney Aircraft's rig testing or during the engine ground testing because of the large fluid volumes involved. To solve the problem Lockheed invented a "high-temperature sponge" (promptly named "the football") which they installed in an accumulator ahead of the engine. This reduced the pressure spikes to a tolerable level.

#### 14.7 Engine Mount

A mounting-related problem occurred under certain conditions of down load on the wing. At these conditions, the outer half of the nacelle would rotate into the engine and crush the engine plumbing and anything else in the way.

Originally, the engine was mounted on a stiff rail structure at the top of the nacelle with a stabilizing link from the top of the engine rear mount ring to the aircraft structure as shown in Figure 70. At Lockheed's request P&W undertook a task to solve the problem by redesigning the rear mount ring so that a tangential link could be installed between the engine and the outboard side of the nacelle. This maintained a finite distance between the nacelle and engine under all conditions.

#### 14.8 Throttle "Creep"

During the first flight testing of the JT11D-20 engine, we experienced a problem not uncovered in the development testing. The phenomenon was when engine power was set to that required for landing, engine power would sometimes increase and other times decrease. The pilot could reset the desired power but when he released the throttle it would move again. The cause was found to be due to the torque required to move the fuel control power lever. This change in torque could only be "felt" when the engine was operating without a stand throttle cable setup. Pratt & Whitney safety rules prevented anyone being near the engine when it was operating above idle so the solution was to have the leader of the control group join the flight test group, on the west coast, to "feel" the problem. The "creepy" throttle was stabilized by incorporating an anti-torque device to hold torque change to no more than 5 in-lb/degree of movement.

#### 14.9 It's Always a Hot Day

The aircraft specification was based on the 1959 standard atmosphere which

umed a constant ambient temperature from 36,089 feet to 82,021 feet. The problem was that the isotherm really ended at 65,000 feet and it started to get warmer above that. All the cruise data at 80,000 feet seemed to "always" be on a hot day. Worldwide U-2 data and balloon measurements confirmed what was finally published as the 1962 standard atmosphere. The aircraft really performed well at 80,000 feet. It was just that it was expected to perform even better, since all the assumptions were that it would be cooler at that altitude.

#### 14.10 Flow Stability

The most sensational and most confusing problem was inlet unstarts in supersonic flight. These occurred without warning and were seemingly inconsistent. To add to the confusion, the pilots consistently reported the unstart occurring on the wrong side of the airplane. This anomaly was solved rather quickly when Lockheed found that the Stability Augmentation System (SAS) slightly overcompensated for the sudden one-sided drag. This led the pilot to believe that the wrong side had unstarted, and consequently, his corrective action usually resulted in worsening the problem. Oddly enough, the engine did not blow out. It just sat there and overheated because the inlet airflow was so reduced that the engine minimum fuel flow was approximately twice that required. Worst of all, the inlet would not restart until the pilot came down to a much lower altitude and Mach number.

Engine surge causes inlet unstart and an inlet unstart causes engine surge. The instrumentation response was not fast enough to detect which event occurred first. Consequently we called the event an aerodynamic disturbance and Lockheed and Pratt & Whitney engineers worked together to isolate the cause and define a solution.

The total pressure recovery produced by an inlet is not uniform. The area weighted average total pressure is the pressure used to evaluate engine performance. The total pressure distribution is called inlet distortion, which is described by both the pattern and intensity of total pressure deviations from the average pressure. Severe inlet distortion can cause engine surge.

Lockheed had measured inlet pressure distortion in the wind tunnel. New flight measurements of inlet distortions were made and found to be in agreement with scale model tests: The engine was tested in the altitude facility with inlet distortion simulated using wire mesh screens that were tailored to reproduce the inlet pattern and intensity. The engine was surged both with and without inlet distortion by closing down the exhaust nozzle using manual control. The compressor pressure ratio was measured at surge. The difference in compressor surge line with inlet distortion was defined. The effect of the flight measured distortion on the engine was not sufficient to explain the aerodynamic disturbances.

The aft bypass which ducts surplus inlet air to the ejector, was added to improve engine-inlet airflow matching. It consists of a series of slots around the periphery of the inlet duct just forward of the engine face. The aft bypass was simulated in the altitude test facility and tests were made for several flow levels, both with and without inlet distortion. One

surprise that we could not explain at the time occurred during tests with the aft bypass open but a downstream valve closed so that there was no flow through the bypass. We found that the surge line was a band not a line. Within this band it was possible to run an engine at steady state conditions. Sometimes the engine would surge quickly but on other occasions it would operate stably for several minutes before surging. With 20-20 hindsight we believe that we were observing the results of time variant distortion which was discovered by Plourde & Brimelow in 1969 (reference 1,2). They found that pressure fluctuations as rapid as 200 Hz could cause engine surge. Such fluctuations are caused by shock-boundary layer interaction and could be caused by turbulence or resonance from the open forward bypass doors. It is now standard practice to measure inlet distortion with high response pressure probes but in the 1960's we did not have suitable high response instrumentation and did not see the need for it.

During the engine tests in the altitude facility we calibrated the effects of variable geometry on flow stability and found that the engine would tolerate more inlet distortion at Mach numbers higher than 2.1 if the bleed bypass is open. Consequently, the bypass opening was moved from Mach 3.0 down to Mach 2.1. Similarly cambering the inlet guide vanes improved distortion tolerance so the inlet guide vane actuation was moved to Mach 1.9.

Three major causes of the aerodynamic disturbances were finally isolated:

- 1) Manual trimming of the engine turbine temperature was not sufficiently fast or accurate to maintain the scheduled turbine temperature. If the turbine temperature dropped sufficiently, limits on engine jet area and inlet bleed caused mismatch between the inlet airflow supply and the engine airflow demand that resulted in an unstart.

- 2) High, inconsistent nacelle leakage at the approximately 40:1 pressure ratio.
- 3) Alpha signal (angle of attack from nose boom) to inlet control  
\* subject to G-loading.

The following improvements were incorporated by Lockheed and Pratt & Whitney essentially as a package:

- 1) Improved sealing of the inlet and bypass doors.
- 2) Auto-trimmer of engine turbine temperature was installed.
- 3) Increased area inlet bypass doors and addition of an aft inlet bypass door which bypassed inlet air direct to ejector.
- 4) Added "G" bias on inlet control.
- 5) Bleed bypass open and inlet guide vanes cambered at a lower Mach number.

In addition to the above preventative measures the following changes were made to minimize the impact of an unstart:

- 6) Automated inlet restart procedure on both inlets regardless of which unstated.
- 7) A solenoid valve was added to the engine fuel system that diverts fuel from the main burner if the exhaust gas temperature reading reaches a level that indicates unstart. This valve, called a de-richment valve, prevents turbine over-temperature during an unstart.



The foregoing seven items essentially eliminated inlet unstart as a problem. An additional benefit was also realized by the ability to use the aft inlet bypass door in normal flight instead of dumping all inlet bypass air overboard. This air becomes heated as it passes over the engine to the ejector and produces thrust instead of going overboard and creating drag. Better sealing of the nacelle also reduced drag.

#### 14.11 In-Flight Performance Measurement

In-flight engine performance was estimated using an engine and instrumentation that were calibrated in a simulated flight environment. These performance estimates were made during high Mach number cruise operation where the ejector blow-in-doors are closed. Instrumentation readings were cross-checked, using the engine digital performance simulation, to provide redundant information on performance parameters. This cross check validates both instrumentation and performance estimates.

##### 14.11.1 Flight test instrumentation used for flight performance estimates consisted of:

- An inlet rake to measure inlet total pressure distribution
- Inlet total temperature
- Total fuel flow
- Afterburner fuel flow
- Engine rotor speed
- Pressure and temperature rakes at turbine discharge
- Exhaust nozzle position indicator
- Temperature in the nacelle at the exhaust nozzle position indicator.

##### 14.11.2 Performance Estimation Procedure

- Engine airflow was estimated from inlet total pressure, rotor speed, inlet temperature and the speed-flow characteristics of the calibrated engine.
- The exhaust pressure was estimated from the measured pressure at turbine discharge and the afterburner pressure loss vs. afterburner fuel flow characteristic of the calibrated engine.
- The jet area was estimated from the nozzle position indicator, the nacelle temperature in the vicinity of the nozzle and the jet area vs. nozzle position indicator characteristics of the calibrated engine.
- Gross thrust of a convergent nozzle was estimated from jet area and exhaust pressure.
- Net thrust with a convergent nozzle was estimated from gross thrust flight Mach number and estimated engine airflow.
- The thrust specific fuel consumption is the measured total fuel flow divided by the estimated net thrust.

This estimated net thrust and specific fuel consumptions are compared with the thrust and fuel consumption calculated by the engine performance simulation at the same operating conditions. i.e. Inlet recovery, flight Mach number inlet temperature, engine speed, exhaust gas temperature and a convergent nozzle.

The following cross checks were made to assure data consistency:

- Measured turbine discharge temperature compared to the value calculated from measured inlet temperature, measured fuel flow and estimated airflow.
- Measured exhaust nozzle area compared to the area calculated from measured turbine discharge pressure, measured turbine discharge temperature, measured afterburner fuel flow, estimated airflow and the engine calibration.

The "measured" engine performance was generally within  $\pm 2\%$  of the calculated value (reference 3).

Ejector performance is measured in flight by pressure taps on the inner ejector surfaces. The gross thrust of the ejector nozzle is equal to the gross thrust of a convergent nozzle plus the impulse of the secondary air and the integral of the ejector surface pressures over the projected area in the thrust direction. Measured ejector performance agreed within  $\pm 2\%$  of predictions when the blow-in-doors are closed, (reference 3, 4).

#### 14.11.3 Performance Validation

Performance validation consists of two phases:

- 1) Validation of altitude performance measurements by calibration of a performance instrumented engine on both a sea level stand with a thrust bed and the altitude facility.
- 2) Calibration of the flight performance engine in the altitude facility with both the flight performance instrumentation and the instrumentation which is used to measure thrust in the altitude facility.

On a sea level stand thrust and fuel flow are measured directly. Airflow is measured by static pressure taps in the bellmouth entry to the engine, and total temperature measured at many locations on a screen at the entry to the bellmouth. This airflow measurement uses venturi formulae. The bellmouth was calibrated against the ASME calibrated orifice in the altitude facility so these two methods of airflow measurement agree. Performance instrumentation also includes pressures and temperatures throughout the engine and rotor speed so that component performance can be checked against rig results and the engine simulation. These cross checks are a valuable part of performance validation as shown by the examples given in section 13.1.5 where facility problems were detected as a result of cross checks.

On the altitude stand there is no direct thrust measurement so gross thrust is estimated from pressure measurements taken with a rake at the engine exhaust and jet area measured by a "pucker string" that measures the circumference of the nozzle. Thermal expansion is taken into account by temperature correction to the pucker string reading. This thrust estimating procedure has been validated by pressure, temperature and combustion products traverses across the exhaust and also by using the same procedure on a sea level test stand and comparing the estimated thrust with the thrust measured by the thrust bed load cell. Airflow on the altitude stand is measured by a calibrated ASME orifice ahead of the engine and another ASME calibrated orifice measuring the flow going around the engine. Cross checks of airflow are given by pressure measurements on the bellmouth attached to the engine inlet and by the speed-flow

characteristics of the compressor. Instrumentation is provided to measure component efficiencies, as on the sea level stand, so cross checks on performance can be made. A detailed description of performance calibration in the altitude facility is given in Appendix 2.

The flight performance engine does not have all the instrumentation used in the altitude facility: engine airflow is measured from speed-flow, jet area is measured by actuator position and exhaust pressure is estimated from turbine exit pressure readings. Therefore, the flight engine was calibrated to provide a method of correcting from the flight instrumentation readings to the parameters normally measured in the altitude facility. This calibration covered the range of inlet temperature, nacelle temperature, rotor speed, turbine discharge temperature and afterburner fuel flow expected during flight test. This procedure was only valid for, and consequently, only used for, the calibrated engine.

#### 15. CONTRACTOR-CUSTOMER RELATIONSHIP

The successful completion of this complex, difficult program is largely attributable to the management philosophy adopted by the Government people in charge. Their approach was that both the engine and airframe contractors must be free to take the actions which in their judgment were required to solve the problems. The Government management of the program was handled by no more than a dozen highly qualified and capable individuals who were oriented toward understanding the problems and approaches to solutions, rather than substituting their judgment for that of the contractors. Requirements were minimal for Government approval as a prerequisite to action and were limited to those changes involving significant cost or operational impact. As a result, reactions to problems were exceptionally quick. In this manner, the time from formal release of engineering paperwork to the conversion to hardware was drastically shortened. This not only accelerated the progress of the program but saved many dollars by incorporating the changes while the number of units were still relatively small.

On this program, the Government fully recognized that many of the problems involving either the engine or airframe manufacturer, or both, could be solved most effectively by a joint engineering effort and the contracts were written to allow this activity without penalties. As a result, an extremely close working relationship between the engineering groups was developed and flourished until the SR-71 became fully operational. The engineering teams worked well together in an open relationship. There was difficulty in differentiating between "we" Pratt & Whitney and "we" Lockheed. But that is the kind of program it was. This method of operation led to prompt solutions of many problems which, under a more cumbersome management system, could have severely impeded the program by introducing very costly delays or forcing inappropriate compromises because of contractual interpretations.

The method of managing this program by the Government resulted in shorter development time, faster reaction to field problems, reduced retrofit costs, and earlier availability of production systems incorporating corrections for problems uncovered by operations in the field. The result

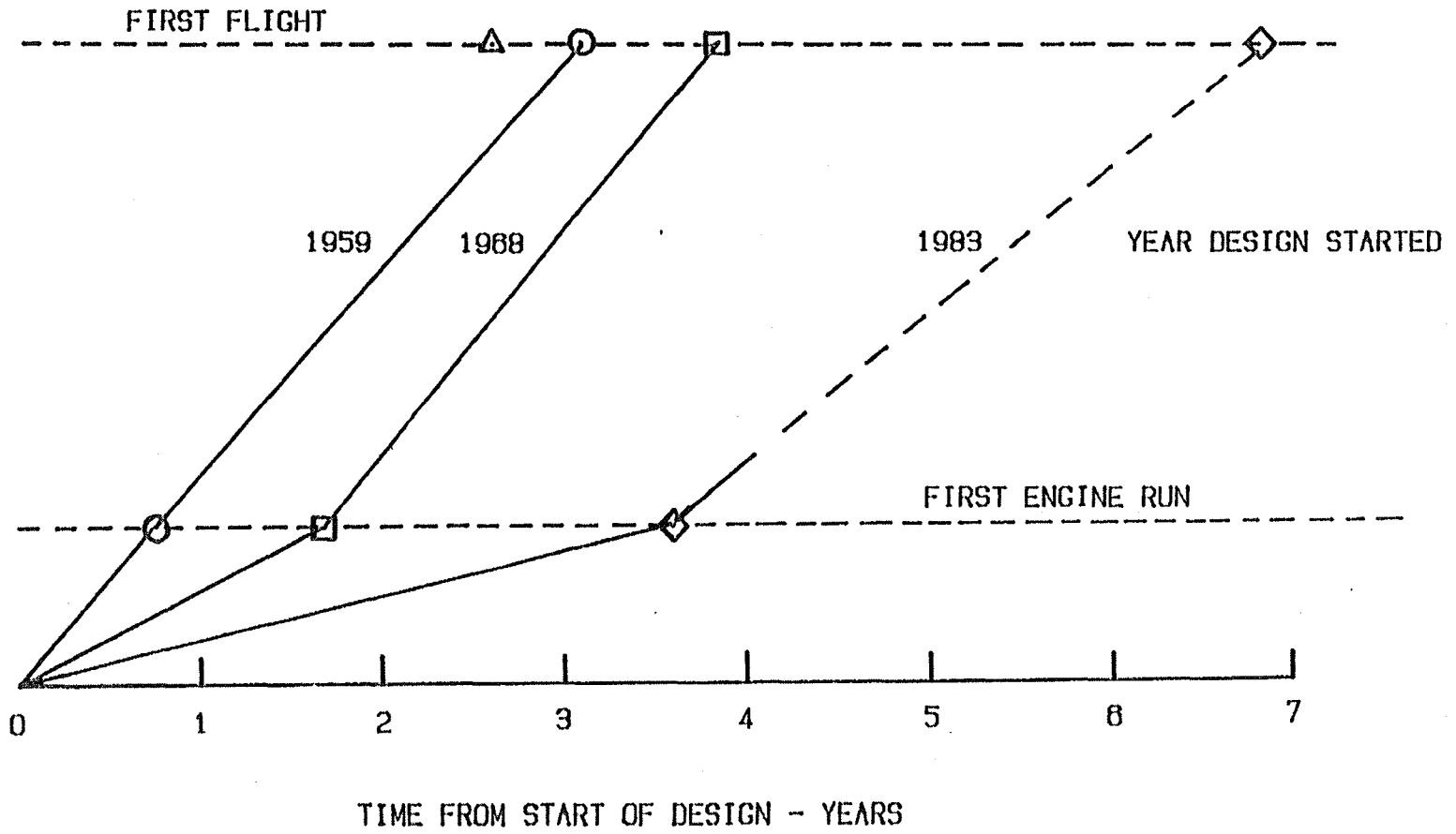
was an operating system incorporating a quantum step in the state-of-the-art at an earlier time and at less cost to the Government than would otherwise have been possible.

FIG 111

THE MORE DESIGN, THE MORE DEVELOPMENT  
RESULT IS LONGER TIME TO FLIGHT

- △ SR 71 WITH J75 ENGINE
- SR 71 WITH JT11D-20 ENGINE
- F15 WITH F100 ENGINE
- ◇ ATF WITH YF119 ENGINE

-116-



127


Programs subsequent to the SR71 aircraft/JT11D-20 engine have longer design and development phases; moreover, this stretchout appears to continue to increase with time, as shown in Figure 71. As a result, later engines are better designed, have been operated through more simulated mission cycles and are more durable at first flight than earlier engines. However, this improved quality at first flight may not be cost effective because the real design requirements may not be identified before squadron service.

## 16. References

1. Plourde, G. A. and Brimelow, B. "Pressure Fluctuations Cause Compressor Instability" Airframe/Propulsion Compatibility Symposium, June 1969, sponsored by the Air Force Aero Propulsion Laboratory, Air Force Flight Dynamics Laboratory, Wright-Patterson AFB, Ohio.
2. Campbell, J. L. and Ellis, S. H. "Engine/Inlet Compatibility Analysis Procedure", Journal of Aircraft, Vol. 8, No. 5, May 1971, pp 301-307, American Institute of Aeronautics and Astronautics.
3. Campbell, D. H. "F12 Series Aircraft Propulsion System Performance and Development", Journal of Aircraft, Vol. 11, No. 11, November 1974, pp. 670-676, American Institute of Aeronautics and Astronautics.
4. Herrick, P. W. "J58/YF-12 Ejector Nozzle Performance", Paper No. 740832, SAE National Aerospace Engineering and Manufacturing Meeting, October 1974.

APPENDIX 1 SPECIFICATIONS

1 Fuel Specifications

<b>Pratt &amp; Whitney Aircraft</b> <small>DIVISION OF UNITED AIRCRAFT CORPORATION</small>		<b>P&amp;WA</b> <b>SPECIFICATION</b>	PWA 523
			REVISION E
			ISSUED 1/5/60
			REVISED 8/25/66

FUEL, AIRCRAFT TURBINE ENGINE

- ACKNOWLEDGMENT:** Vendor shall mention this specification number and its revision letter in all quotations and when acknowledging purchase orders.
- PURPOSE:** To establish requirements for low volatility fuel for use in Pratt & Whitney Aircraft turbine engines.
- TECHNICAL REQUIREMENTS:** Tests shall be performed, insofar as practicable, in accordance with the test methods listed. P&WA-MCL refers to Pratt & Whitney Aircraft Materials Control Laboratory Manual Sections.

Gravity, deg API	47 - 53	ASTM D287-64
Distillation Temperature, F		ASTM D86-62
Initial Boiling Point	375 min	
10% Evaporated	400 min	
20% Evaporated	To be reported	
50% Evaporated	420 min	
90% Evaporated	max 500	
End Point	max 550	
Loss, %	max 1.5	
Residue, %	max 1.5	
Sulfur, %	max 0.1	ASTM D1266-64T
Mercaptan Sulfur, % by wt	max 0.005	ASTM D1323-62 or D1219-61 (Note 1)
Existent Gum, mg per 100 ml	max 7.0	ASTM D381-64
Freezing Point, F	max -40	ASTM D2386-65T
Net Heat of Combustion, Btu per lb	18,900 min	ASTM D2382-65
Luminometer Number	160 min	ASTM D1740-60T
Aromatic Content, % by volume	max 5	ASTM D1319-65T
Copper Strip Corrosion	Slight discoloration permitted	ASTM D130-65
Viscosity, Cs at -30F	max 15	ASTM D445-65
Water Tolerance, ml	max 2	ASTM D1094-57
Flash Point, F	150 min	ASTM D93-62
Vapor Pressure, psia at 300 F	max 2.7	P&WA-MCL Q-50 (Note 2)
Vapor Pressure, psia at 500 F	max 45	P&WA-MCL Q-50 (Note 2)
Specific Heat, Btu per lb per deg F at 300 F	0.6 min	P&WA-MCL Q-51
§ Thermal Precipitation Test	Equal to or cleaner than PWA 523 color standard	P&WA-MCL Q-67

Thermal Stability

P&amp;WA-MCL Q-62

Pressure Change, in. Hg max 5

Preheater Deposit Code max 2

Note 1. Mercaptan sulfur determination may be omitted provided Doctor Test in accordance with ASTM D484-52 is conducted and results are negative.

Note 2. Right is reserved by purchaser to determine conformance to the 300 F vapor pressure requirement by using a reflux method as outlined in P&WA-MCL Q-50.

### 3.2 Additives:

3.2.1 One or a combination of the following inhibitors may be added to the basic fuel in total concentration not greater than 1.0 lb of inhibitor, not including weight of solvent, per 5000 gal of fuel, to prevent formation of gum:

- N, N'-di-secondary-butyl-para-phenylenediamine
- 2, 4-dimethyl-6-tertiary-butyl phenol
- 2, 6-ditertiary-butyl-4-methyl phenol
- 2, 6-ditertiary-butyl phenol
- 75% 2, 6-ditertiary butyl phenol 10-15% 2, 4, 6-tritertiary butyl phenol
- 10-15% ortho-tertiary butyl phenol

3.2.2 The use of Pratt & Whitney Aircraft approved additives to inhibit corrosion and to extend the high temperature stability is permitted.

### 4. QUALITY:

4.1 Fuel shall consist solely of hydrocarbon compounds except as otherwise specified herein. It shall be free from water, sediment, and suspended matter, and shall be suitable for use in aircraft turbine engines.

The odor of the fuel shall not be nauseating or irritating. No substances of known dangerous toxicity under usual conditions of handling and use shall be present.

5. CONTROL: Control of quality and control of shipments shall be in accordance with the latest issue of PWA Specification 300.

6. REJECTIONS: Fuel not conforming to this specification or to authorized modifications will be subject to rejection.

Note. Section 1 and 5 apply only to Pratt & Whitney Aircraft operation.



TABLE 11  
**U.S. MILITARY SPECIFICATIONS**  
 Special and Referee Test Fuels

Specification:	MIL-T-38219	MIL-T-25524B (Amendment 1)	<del>USAF</del>	<del>MIL-T-5624H, Amend. 1</del>
Latest Revision Date:	Dec. 17, '70	July 1970		July 30, 1971
Grade Designation:	JP-7	Thermally Stable	JP-4	JP-5
Fuel Type:	Low Vol.		Wide-Cut	High Flash Kerosene

<b>COMPOSITION</b>	Acidity, Total (mg KOH/g)	Max. 5	5-20	0.015	0.015	
	Aromatics (vol %)	Max. 5	3	25	25	
	Olefins (vol %)	Max. .001	.001	5	5	
	Sulfur, Mercaptan (wt.%) or Doctor Test N = Neg.	Max. N	N	.001	.001	
	Sulfur, Total (wt.%)	Max. 0.1	0.3	N	N	
<b>VOLATILITY</b>	Distillation Init. BP F	Min. 360	315	Report	Report	
	Temp. 10% Rec F	Max. 385	380	Report	400	
	20% Rec F	403 Max.		290	Report	
	50% Rec F	Report	400 Max.	370	Report	
	90% Rec F	500 Max.	450 Max.	470	Report	
	95% Rec					
	Final BP F	Max. 550		Report	550	
	Residue (%)	Max. 1.5	1.5	1.5	1.5	
	Loss (%)	Max. 1.5	1.5	1.5	1.5	
	Recovery @ 400 F (%)					
	Explosiveness (vol %)				50	
	Flash Point (F)	Min. 140	110		140	
Gravity, API (60 F)	44-50	46-53	45-57	36-48		
Gravity, Specific (60/60 F)	.806-.779	.7972-.7669	.802-.751	.845-.788		
Vapor Pressure psia @300F	Max. 3(1)		2-3			
Vapor Pressure psia @500F	Max. 48(1)					
<b>FLUIDITY</b>	Freezing Point (F)	Max. -46	-64	-72	-51	
	Viscosity @ -30 F (cSt)	15 Max.			16.5	
	Viscosity @ -40 F	Max.	12			
<b>COMBUSTION</b>	Aniline-Gravity Product	Min. 7380	5250	5250	4500	
	or Net Heat of Comb. (Btu/lb)	18700 Min.	18400 Min.	18400	18300	
	Luminometer No.	Min. 75		60	50	
	Smoke Point		25 Min.		19	
	Naphthalenes (vol %)	Max.				
<b>CORROSION</b>	Smoke-Volatility Index	Min.		52(4)		
	Net Heat of Comb. MBTU/G	Min. 124(2)				
	Copper Strip (2 h @ 212 F)	Max. 1b	No. 1	1	1	
Silver Strip						
<b>STABILITY</b>	Coker AP (in. Hg)	Max. 3.0(3)	3(5)	3	3	
	Coker Tube Color Code	Max. <3(3)	<3(5)	<3	<3	
	Pot. Gum mg/100ml	Max. 10	10			
<b>CONTAMINANTS</b>	Copper Content (ug/kg)	Max. 5	5	7	7	
	Existent Gum (mg/100 ml)	Max. 1.0	0.25	1.0(6)	1.0	
	Particulates (mg/liter)	Max. 1b	1b	1b	1b	
	Water Reaction Vol Ch. (ml)	Max. 85	Report	70	85	
	Water Reaction Ratings	Min. 85				
<b>ADDITIONS</b>	WSIM					
	Anti-Icing (Vol.%)	0.10-0.15	0.10-0.15	0.10-0.15	0.10-0.15	
	Antioxidant	Option	Option	Option	Option	
	Corrosion Inhib.			Required	Required	
	Metal Deactivator	Option	Option	Option	Option	
Thermal Stability		Required				
Lubricity, ppm	200-250					
<b>OTHER</b>	Conductivity (CU)			15		
	Thermal Precipitation Rating	Pass(4)				

Service  
Intended Use

USAF                      USAF  
High Performance Spec. A/C

All                      Navy  
F-40                      Aircraft Turbine Engines.  
F-44

Fuel Lubricity Additive

Pratt &  
Whitney  
Aircraft



P&WA  
SPECIFICATION

PWA 536

REVISION

ISSUED - 8/25/67

REVISED

FUEL ADDITIVE, AIRCRAFT TURBINE ENGINE

1. ACKNOWLEDGMENT: Vendor shall mention this specification number in all quotations and when acknowledging purchase orders.
2. PURPOSE: To establish requirements for fuel lubricity additive for use in Pratt & Whitney Aircraft turbine engines.
3. TECHNICAL REQUIREMENTS:
  - 3.1 Composition: Blend of fluorocarbon chemicals, technical grade toluene, and technical grade methyl isobutyl ketone.
  - 3.2 Properties: Tests shall be performed, insofar as practicable, in accordance with the test method listed. P&WA-MCL refers to Pratt & Whitney Aircraft Materials Control Laboratory Manual Sections.

Specific Gravity, 60 F/60 F	0.912 - 0.925	ASTM D1298-55
Concentration, % by wt		
Fluorocarbon	24 - 26	P&WA-MCL Q-48
Toluene	max 40	P&WA-MCL Q-69
Methyl isobutylketone	max 40	P&WA-MCL Q-69
Mercaptan Sulfur, % by wt (Note 1)	max 0.005	ASTM D1323-62 or D1219-61
Freezing Point, F (Note 2)	max -76	ASTM D2386-65T or D1477-65T
Fuel Insolubility, ml	max 0.010	P&WA-MCL Q-49
Thermal Stability (Note 3)	Deposit code and filter pressure drop shall be no greater than base fuel rating.	P&WA-MCL Q-62
Thermal Precipitation Test (Note 3)	Equal to or cleaner than PWA 523 color standard	P&WA-MCL Q-67
Hydraulic Pump Lubricity, 48 hr Endurance (Notes 3 & 4)	Pass	P&WA-MCL Q-66

- Note 1. Mercaptan sulfur determination may be omitted provided Doctor Test in accordance with ASTM D484-52 and Note 2 is conducted and results are negative.
- Note 2. Shall be tested using a 0.020% by wt mixture of additive in normal heptane conforming to ASTM D2268-64T.
- Note 3. Shall be tested using 0.020% by wt additive in PWA 535 fuel.
- Note 4. Test required only for initial qualification and when changes have been made in formulation or processing of the fuel additive.

A 536

- 2 -

REVISION

4. QUALITY: Additive shall be free from water, sediment, and suspended matter.
5. CONTROL: Control of quality and control of shipments shall be in accordance with the latest issue of PWA Specification 300.
6. PACKAGING: Unless otherwise specified, additive shall be supplied in 1 gal containers containing 7.60 - 7.70 lb of additive. Container must be permanently marked with PWA 536 and batch or lot number.
7. APPROVAL:
  - 7.1 Fuel additive shall be procured only from sources approved by Pratt & Whitney Aircraft Engineering Department.
  - 7.2 Vendor shall use the same ingredients and manufacturing processes for production material as for approved sample. If necessary to make any change in ingredients or processing, vendor shall obtain written permission from purchaser prior to incorporating such change.
8. REJECTIONS: Fuel additive not conforming to this specification or to authorized modifications will be subject to rejection.

Note. Sections 1 & 5 apply only to Pratt & Whitney Aircraft operation. I & WA-MCL Q Sections and PWA 523 color standard available upon request from Pratt & Whitney Aircraft Purchasing Department.

Lubricant

**Pratt &  
Whitney  
Aircraft**



**P&WA  
SPECIFICATION**

PWA	524
REVISION	C
ISSUED	4/25/60
REVISED	6/6/69

**LUBRICANT, AIRCRAFT TURBINE ENGINE**

- 1. ACKNOWLEDGMENT:** Vendor shall mention this specification number and its revision letter in all quotations and when acknowledging purchase orders.
- 2. TYPE:** Blend of synthetic and/or mineral oils capable of meeting certain performance requirements as measured by special tests.

**3. TECHNICAL REQUIREMENTS:**

- 3.1** Composition of lubricant is not limited; formulations composed substantially or entirely of non-petroleum materials are permitted provided the following requirements are met.
- 3.2 Properties:** Tests shall be performed, insofar as practicable; in accordance with the latest issue of the test methods listed. P&WA - MCL refers to Pratt & Whitney Aircraft Materials Control Laboratory Manual Sections.

Specific Gravity at 100/60 F	1.18 - 1.20*	ASTM D1298 (See Note 1)
Viscosity, Kinematic, cSt.		
at -40 F (diluted)	max 7000	P&WA-MCL Q-58 (See Note 2 & 4)
at 100 F	330 - 375	ASTM D445
at 210 F	12 - 14	ASTM D445
at 500 F	min 1.0	P&WA-MCL Q-57 (See Note 4)
Pour Point, F	max 40	ASTM D97
Flash Point, F	min 525	ASTM D92
Evaporation Loss at 500 F, %	max 35	P&WA-MCL Q-55
Specific Heat, Btu/lb/F		P&WA MCL Q-51 (See Note 4)
at 300 F	min 0.40	
at 500 F	min 0.45	
Vapor Pressure at 500 F, mm Hg	max 3.0	P&WA-MCL Q-53
∅ Foaming, ml,		ASTM D892
Sequence 1, Tendency/Stability	max 625/550	
Sequence 2, Tendency/Stability	max 250/0	
Sequence 3, Tendency/Stability	max 625/550	
∅ Gear Scuffing Load, lb/in., avg	min 2000	ASTM D1947 (See Note 3)
∅ Autogenous Ignition Temp., F	min 1130	ASTM D2155 (See Note 4)

## Corrosion - Oxidation Stability

PWA -MCL Q-52

Weight change after 48 hr at 600 F, mg/sq cm

Silver	± 0.10
Inconel X-750	± 0.10
M 50 Steel	± 0.10
Titanium	± 0.10
Waspaloy	± 0.10
L 605 Cobalt Alloy	± 0.10
Aluminum	± 0.10

Viscosity at 100 F,

% change from original max 20

Ø Refractive Index at 77 F.	1.628 - 1.633	ASTM D1218 (See Note 4)
Bearing Test, Type 3	to be reported	P&WA-MCL Q-61 (See Note 4)

Note 1. Use ASTM 114H-62 hydrometer (Ref. ASTM E100-62).

Note 2. Diluent shall be 29% by wt reagent grade trichloroethylene.

Note 3. ASTM standard reference oil shall have a range of 2500 - 3300 lb per in. when evaluated with Ryder Gear Machine. Permissible to conduct up to two additional tests and to calculate an average based on any 4 of the 6 sides.

Note 4. This test required only for original qualification and when changes have been made in formulation or processing of the lubricant.

**QUALITY:** Lubricant shall be free from suspended matter, grit, water, and objectionable odor.

After packaging for shipment, the lubricant shall be subject to inspection in accordance with Pratt & Whitney Aircraft Materials Control Laboratory Manual Section Q-59. Maximum total contamination shall not exceed 10 mg per gal of particles greater than 1.2 microns; this 10 mg total shall include not more than 2.5 mg per gal of particles greater than 10 microns.

5. **CONTROL:** Control of quality and control of shipments shall be in accordance with the latest issue of PWA Specification 300.

6. **APPROVAL:**

6.1 Vendor shall not supply lubricant to this specification until samples have been approved by purchaser. After approval, compounds and method of manufacture shall not be changed without notification to purchaser prior to first shipment of lubricant embodying such change. To qualify for batch acceptance, results of tests on subsequent lubricant lots shall be essentially equal to those on approved samples.

6.2 Right is reserved to submit oils of new or unusual composition to such additional tests as are considered necessary to assure serviceability of the material.

7. **REJECTIONS:** Lubricant not conforming to this specification or to authorized modifications will be subject to rejection.

Note. Sections 1 and 5 apply only to Pratt & Whitney Aircraft operation.

Code Ident No. 77445  
Furnished Under Contract

SPECIFICATION  
EXHAUST GAS TEMPERATURE VERNIER CONTROL SYSTEM  
FOR  
JT11D-20 ENGINES  
PRATT & WHITNEY AIRCRAFT .

1. SCOPE

1.1 Scope - This specification covers the requirements for the exhaust gas temperature (EGT) vernier control system for the Pratt & Whitney Aircraft JT11D-20 engine.

1.2 Classification - The EGT vernier control system is an automatic closed loop system which adjusts the main fuel control to provide vernier control of EGT. The component parts of the system are as follows.

1.2.1 Airframe Mounted Units - The following units are airframe mounted:

- a. EGT vernier control
- b. EGT error gage
- c. Interconnecting wiring necessary to operate the EGT vernier control system.

1.2.2 Engine Mounted Units - The following units are engine mounted:

- \*a. Compressor inlet temperature (CIT) probe consisting of a temperature sensing probe and an integral lead assembly.
- \*b. Permission switch cable with associated mounting brackets.

- \*c. Trim permission switch consisting of a power lever angle sensing switch which is an integral part of the afterburner fuel control.
- \*\*d. Exhaust gas temperature (EGT) sense system consisting of temperature sensing probes and lead assemblies.
- \*\*e. Main fuel control trim motor consisting of an electrical motor which is an integral part of the main fuel control.

\*Becomes part of engine part list upon incorporation of the system defined in this specification.

\*\*Part of existing engine parts list.

## 2. APPLICABLE DOCUMENTS

2.1 The specifications listed below are applicable to the EGT vernier control system only to the extent specified herein:

MIL-E-5400H Notice-1	Electronic Equipment, Aircraft, General Specification for
MIL-E-6181D Notice-3	Interference Control Requirements, Aircraft Equipment
MIL-I-27209C	Indicator, Temperature, Thermocouple, Self-Balancing, Potentiometer Type
MIL-STD-704A	Electrical Power, Aircraft, Characteristics and Utilization of
MIL-STD-794A	Parts and Equipment, Procedures for Packaging and Packing of
MIL-STD-810A	Environmental Test Methods for Aerospace and Ground Equipment

2.2 Drawings - The following Pratt & Whitney Aircraft drawings form a part of this specification. Changes to these drawings, when required, shall be accomplished through the drawing change procedure in effect for the JT11D-20 engine.

2137700 Control - Exhaust Gas Temperature Vernier (Installation Drawing)

2137500 Error Gage - Exhaust Gas Temperature (Installation Drawing)

2078003 Diagram, Electrical Installation Connection (JT11D-20)

DF58679 Diagram, Suggested Airframe Wiring, EGT Vernier  
Control System

### 3. REQUIREMENTS

3.1 Mockup - Engineering mockups of the EGT vernier control and the EGT error gage will be used as necessary by the contractor to coordinate changes which affect the airplane installation and will be available to the using service. The mockups will be kept current with approved changes through the first production contract.

3.1.1 EGT Vernier Control System Installation Requirements (Airframe) - The details of the electrical installation are shown on the EGT Vernier Control System Suggested Airframe Wiring Diagram.

Electrical power requirements for the system are in accordance with applicable requirements of MIL-STD-704. The required aircraft wiring terminates at the engine-airframe interface.

The details of the mechanical installation of the EGT vernier control are shown on the Exhaust Gas Temperature Vernier Control Drawing. The details of the mechanical installation of the EGT error gage are shown on the Exhaust Gas Temperature Error Gage Drawing.

3.1.1.1 Weights - The estimated weight of the EGT vernier control is 6.5 pounds. The estimated weight of the EGT error gage is 1.0 pound.

3.1.1.2 Engine - Airframe Interface - The connector details of engine mounted components of the system are shown on the Electrical Installation Connection Diagram (JT11D-20). The fuel control trim motor, EGT sense system, and trim permission switch terminate electrically at the engine disconnect station located at the bottom of the engine near the compressor inlet. The engine mounted CIT probe terminates electrically at the compressor inlet case on the lower left hand side of the engine when viewed from the aft end.

3.1.1.3 Ground Check - Ground check of the EGT vernier control system on installed engines requires the availability of the P&WA Tool Kit No. PWA 18928. This kit includes output simulation of CIT and EGT and indicates the EGT vernier control output trim direction and trim rate. EGT simulation is also used to check the EGT error gage for accuracy and operation.



### 3.2 Performance

3.2.1 General - Automatic vernier control to scheduled exhaust gas temperature limits as a function of compressor inlet temperature is provided by the EGT vernier control system. The EGT vernier control system is a limited authority electrical system which adjusts the main fuel control fuel flow to minimize the difference between scheduled EGT and measured EGT.

The EGT vernier control system functions in accordance with a programmed schedule in response to: (1) electrical input of CIT; (2) electrical input of EGT; (3) an electrical input of power lever position; and (4) airframe mounted manually operated switches. The system accomplishes main fuel control trimming by energizing an electric motor which adjusts the "mean" level of the main fuel control flow schedule. The system includes a visual indication of EGT and EGT error. Interconnecting airframe wiring which electrically connects the engine mounted and airframe mounted components includes the following:

- a. "Auto-manual" mode select switch. This switch allows selection of either automatic or manual EGT control.
- b. Manual trim switch. Actuation of this switch trims the "mean" level of the main fuel control flow schedule when the manual mode has been selected.
- c. Trim permission relay. This relay opens the trim motor circuit, thereby preventing any trimming if the power lever angle is below the military position or if EGT as measured by the EGT error gage is above the emergency over-temperature level.

3.2.2 Demonstrated Systems Performance - Indicated engine EGT when using the prototype EGT vernier control system has been demonstrated to be within the limits of figure 1 except for short duration transients outside the limits caused by power lever angle changes, rapid CIT changes, or rapid inlet pressure transients.

3.2.3 System Performance Goal - The performance goal for the production model EGT vernier control is to maintain indicated EGT within the closer limits of figure 2 except during the transients described in 3.2.2.

#### 3.2.4 EGT Vernier Control Component Performance

3.2.4.1 Schedule - The scheduled "no-trim" band of EGT at military power and above is shown on figure 3. The EGT vernier

control is programmed to adjust the main fuel control to effect a return to the scheduled "no-trim" band.

3.2.4.2 Accuracy of Schedule - The tolerance goal of the EGT vernier control in scheduling the "no-trim" band is as follows:

<u>Condition</u>		
Ambient Temperature, °C	CIT, °C	Tolerance, °C
11 to 39	-55 to 450	±3.5
-54 to 11	-55 to 5	±8.0
39 to 71	-55 to 5	±8.0
-54 to 11	5 to 450	±4.5
39 to 71	5 to 450	±4.5

3.2.4.3 Response - The EGT vernier control is programmed to make adjustments at rates dependent upon magnitude of deviation (error) from the scheduled "no-trim" band. Nominal trim rates are designed to be as follows based upon a 400 Hz power supply:

<u>Deviation (error) from "No-Trim" Band</u>	<u>EGT Trim Direction and Rate</u>
Zero to 10°C high	Down trim, 20°C per minute
More than 10°C high	Down trim, 480°C per minute
Zero to 10°C low	Up trim, 20°C per minute
More than 10°C low	Up trim, 60°C per minute

The EGT trim rate tolerance goal is ± 20%. Tolerance of the various error levels at which trim rates change are the same as those shown in 3.2.4.2 for the schedule tolerances.

3.2.4.4 Error Gage Signal - The EGT vernier control provides signals for the EGT error gage to drive the "hot" and "cold" flags specified in 3.2.5 when the nominal deviation from the "no-trim" band is more than ± 10°C. Design tolerance of the signals is the same as those defined in 3.2.4.2.

3.2.5 EGT Error Gage Component Performance - The EGT error gage serves as a visual monitoring device for the EGT vernier control system by providing the following displays:

- a. Visual (digital) display of EGT.
- b. A visual (flag) indication that deviation from the scheduled "no-trim" band, as computed by the EGT vernier control as specified in section 3.2.4, is more than  $\pm 10^{\circ}\text{C}$ . High temperatures are indicated by a red flag and the word "hot" and low temperatures are indicated by a yellow flag and the word "cold."
- c. A visual (light) indication and an external electrical signal to indicate an emergency over-temperature condition. The external signal can be utilized in an engine fuel derichment type emergency correction system.
- d. A visual (flag) indication that aircraft operating electrical power (approximately 110v, 400Hz) to the EGT error gage is "on" or "off." Loss of power is indicated by a red flag and the word "off." The various operating modes of the EGT error gage are shown on figure 33. The EGT error gage tolerance goal is as shown below exclusive of EGT sensing and transmission tolerances:

Function	Ambient Temperature, $^{\circ}\text{C}$	Tolerance, $^{\circ}\text{C}$
Visual (digital) display of EGT	20 to 30	$\pm 2$
	-55 to 20	$\pm 8$
	30 to 70	$\pm 8$
Visual (light) display and signal of Emergency Over-Temperature	20 to 30	$\pm 4$
	-55 to 20	$\pm 10$
	30 to 70	$\pm 10$

3.3 EGT Vernier Control Programmability - The EGT vernier control is designed to be reprogrammable within certain limits. The "no-trim" band width and nominal CIT-EGT relationship can be changed within the limits of figure 5 with minimum rework, and recalibration by the manufacturer. Minimum separation of "break" points as a function of CIT is  $8^{\circ}\text{C}$  for CIT from  $-55^{\circ}$  to  $100^{\circ}\text{C}$  and  $24^{\circ}\text{C}$  for CIT from  $100^{\circ}$  to  $450^{\circ}\text{C}$ . Maximum slope of nominal CIT-EGT schedule is  $5^{\circ}\text{C}$  (EGT) per  $1^{\circ}\text{C}$  (CIT).

Appendix 2: ESTIMATING JT11D-20 ENGINE PERFORMANCE FROM MEASUREMENTS  
TAKEN IN THE ALTITUDE TEST FACILITY

This appendix contains a description of the methods used in the acquisition and analysis of data obtained from the JT11D-20 engine running in an altitude test stand. The test procedure is discussed in section 1. Section 2 describes engine parameters and the procedure used to measure or calculate each parameter.

1. Test Procedure

The altitude facility is regulated to maintain a predetermined inlet Mach number and altitude. This is done by controlling pressure to  $\pm 0.1$  psia and temperature to  $\pm 2^\circ\text{F}$ . The nozzle pressure ratio is maintained between 2.0 and 2.17 to ensure choked nozzle flow without an excessive exit Mach number. The secondary air flow is set at 6%  $\pm 5\%$  of engine air flow rate.

The main engine controls are trimmed to maintain a turbine temperature within  $\pm 10^\circ\text{F}$  and engine rotational speed, N, within  $\pm 7$  RPM. Since turbine inlet total temperature is not measured directly, the turbine discharge temperature, Tt5, is measured and controlled to a schedule that is a function of compressor inlet temperature.

The engine is required to stabilize for 5 minutes at each setting before a data point is taken. A data point consists of the average of the data collected during two consecutive, twenty second, data scan periods. During each scan period each parameter is sampled approximately ten times. (This varies slightly with the number of items recorded). To ensure that the engine has reached equilibrium prior to recording data, the variation within scan and scan to scan is noted. If the variation is outside of acceptable limits the data is not considered valid.

2. Engine Parameters

The engine stations used to describe parameters are shown in the schematic diagram of the engine mounted in the altitude facility, Figure 2.1.

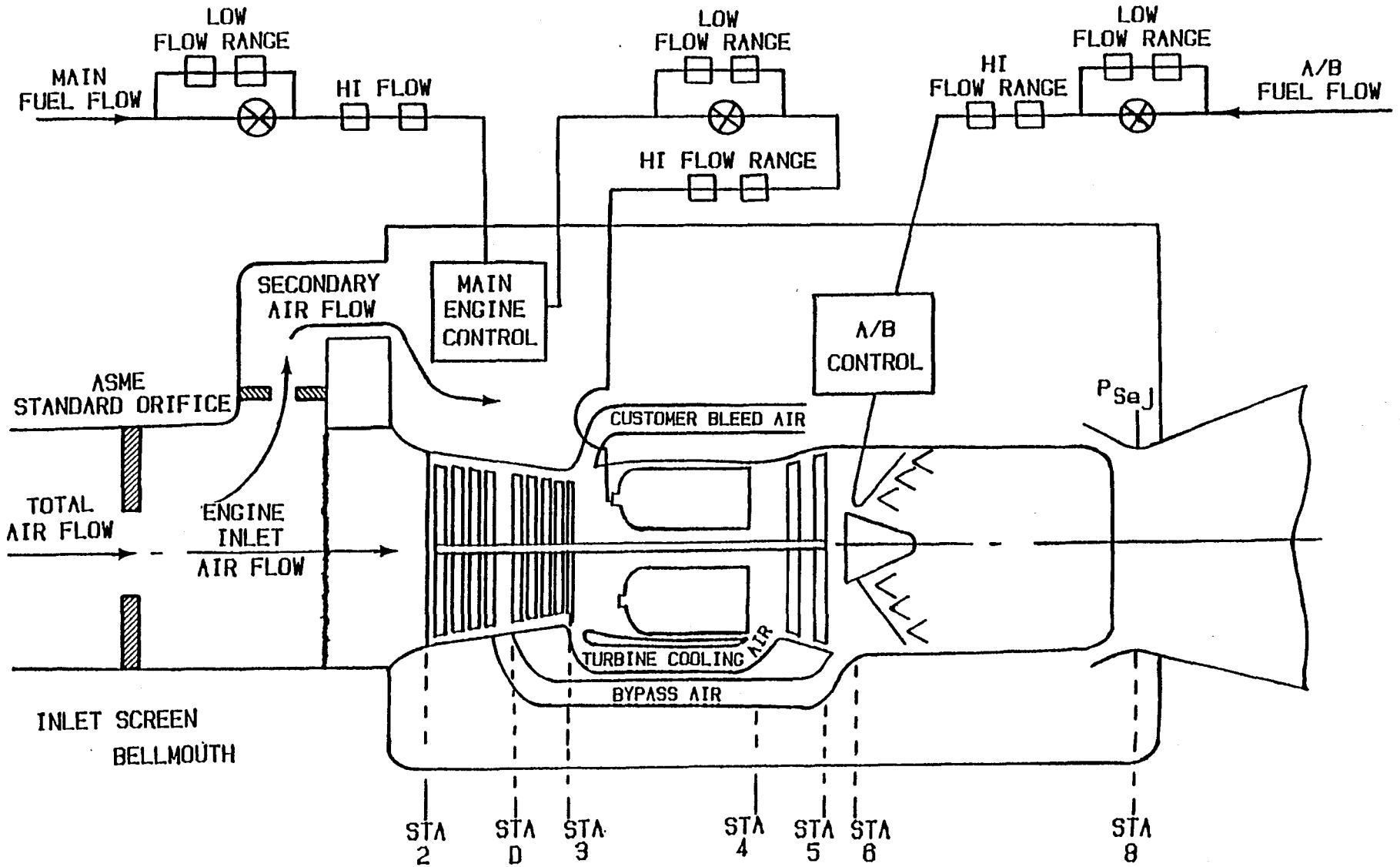
2.1 Engine Inlet Conditions The Mach number, altitude, ram recovery and ambient temperature are required operating conditions. These are translated into compressor inlet total pressure (Pt2) which is measured by six pitot probes and total temperature (Tt2) which is measured by twenty-four thermocouples mounted on the inlet screen.

2.2 Total Air Flow is measured by an ASME standard orifice located upstream of the engine. Three orifice sizes are available to cover the complete flow range. Specific humidity and orifice expansion factor corrections are applied to the flow rate.

2.3 Secondary Air Flow A controlled secondary air flow (approximately 6% of engine inlet air flow) is introduced to the engine exterior to simulate the installed environment. This flow is measured by an ASME standard orifice and corrected for specific humidity.

FIGURE 2.1

SCHEMATIC DIAGRAM OF THE JT11D-20 ENGINE MOUNTED IN THE ALTITUDE TEST FACILITY



-132-

439

2.4 Engine Inlet Air Flow,  $W_a$ , is obtained by subtracting the secondary air flow from the total air flow. As a check on the accuracy of this flow, it is compared to inlet air flow estimated from Bellmouth instrumentation and nominal compressor speed-flow-pressure ratio characteristics. The upstream duct is also checked for leakage by running a speed-flow calibration with the duct pressure maintained at ambient pressure.

2.5 Bypass Air Flow is measured by instrumentation placed in each of the six bypass ducts. Each duct has a total pressure rake, a total temperature rake and a static pressure tap.

2.6 Turbine Cooling Air Flow cannot be measured directly but is estimated as a function of engine internal conditions. Pressures, temperatures, and areas have been measured in specially instrumented engines to establish turbine cooling air flow.

2.7 Compressor Bleed Flow is used to drive the afterburner pump. The flow is not measured but is estimated from pump rig calibrations as a function of engine and altitude conditions.

2.8 Compressor Work The work done by the compressor and therefore, by the turbine, is calculated using engine air flow, air specific humidity, the total pressure ( $P_{t2}$ ) and total temperature ( $T_{t2}$ ) at the compressor inlet and the pressure and temperature at compressor discharge (i.e. fourth stage discharge for the bypass air and ninth stage discharge for the air entering the burner). The bypass duct instrumentation, described in section 2.5, is used as fourth stage discharge instrumentation. The ninth stage discharge total pressure ( $P_{t3}$ ) and total temperature ( $T_{t3}$ ) are each measured by two rakes containing a total of five probes.

2.9 Compressor Efficiency is a ratio of ideal to actual compressor work. The ideal work is obtained by assuming isentropic compression of air with the same specific humidity as the incoming air.

2.10 Main Burner Air Flow is obtained by subtracting bypass air flow, turbine cooling air flow, and compressor bleed air flow from engine inlet air flow.

2.11 Main Engine Fuel Flow The main engine fuel flow is measured by liquid turbine meters placed in the stand lines upstream of the main engine control and between the main engine control discharge and the main burner inlet. Both high and low range turbines are available at each location with redundant meters covering each range. The redundant meters at each location must agree within 0.5% for the flow to be considered valid. The meters at the main burner inlet are used as the primary measuring system (except for certain heated fuel runs discussed later) and are compared to the meters at the main engine control inlet for further verification of accuracy. When the fuel has been heated to a temperature above that considered within the range of acceptable specific gravity correction, the control inlet meter system flow is used. The measured flow is corrected for fuel specific gravity and meter growth due to the fuel temperature and pressure encountered. A sample fuel specific gravity is measured every hour.

2.12 Ideal Main Burner Temperature Rise is computed as a function of the main burner air flow, main engine fuel flow, air specific humidity and burner inlet total temperature ( $Tt3$ ).

2.13 Turbine Discharge Total Temperature,  $Tt5m$ , is measured by thirty-six thermocouples arranged in nine averaging rakes with four ports each.

Turbine discharge total temperature,  $Tt5c$ , temperature is also estimated by adding the ideal main burner temperature rise to compressor inlet total temperature ( $Tt2$ ) and subtracting a correction which accounts for the flow through the turbine being less than the flow through the compressor. The assumptions used here are that (a) combustion is complete by the time the burning gases have passed through the turbine and (b) the heat added in the compressor (work) is equal to the heat withdrawn by the turbine with appropriate adjustments for flow differences through each unit.

2.14 Turbine Inlet Total Temperature,  $Tt4$ , is estimated by adding the main burner temperature rise to the measured main burner inlet total temperature,  $Tt3$ . The main burner efficiency is 98%. This has been verified by rig testing.

Turbine inlet total temperature is also estimated by adding the temperature drop across the turbine, which corresponds to turbine work, to the measured turbine discharge total temperature,  $Tt5$ . An adjustment to this temperature is then made to compensate for the fact that combustion is not complete at the turbine inlet while it probably is at the turbine discharge measurement location. This is accomplished by assuming that two percent of the available combustion temperature takes place in the turbine.

2.15 Calculated Main Burner Efficiency The main burner efficiency is a ratio of the actual to the ideal burner temperature rise. The actual temperature rise is determined from a measured burner inlet total temperature ( $Tt3$ ) and a main burner discharge total temperature ( $Tt4$ ) based on measured  $Tt5$ .

2.16 Main Burner Pressure Loss is calculated using the measured main burner inlet total pressure ( $Pt3$ ), and the burner discharge total pressure, ( $Pt4$ ), which is not measured directly but is assumed to be equal to a measured burner static pressure ( $Pb$ ). This relationship was established during previous testing with measured  $Pt4$ .

2.17 Turbine Efficiency is calculated from actual and ideal turbine work. The actual work per lb. of turbine flow is calculated from total compressor work (see section 2.8) and turbine flow. The turbine flow is calculated by adding together the main burner air flow and the main engine fuel flow. The ideal turbine work per lb. of flow rate is calculated assuming isentropic expansion from the turbine inlet conditions,  $Pt4$  and  $Tt4$ , to turbine discharge total pressure,  $Pt5$ . The ideal work is corrected for specific humidity. Turbine discharge total pressure is measured by three total pressure averaging rakes or, on special tests, by thirty-six individual total pressure readings.

2.18 Bypass Duct Pressure Loss was determined as a function of bypass air flow by tests on a specially instrumented engine. Measured values of: bypass duct total pressure (section 2.5), turbine discharge total pressure, Pt5, (section 2.17) and a pressure traverse at station 6 were used to estimate bypass duct pressure loss. The bypass duct pressure loss is defined as that pressure loss which will make the mass weighted average of bypass total pressure and turbine discharge total pressure agree with the measured average total pressure at station 6. This pressure loss definition includes friction and bend loss in the bypass ducts, entry loss into the afterburner and mixing loss.

2.19 Afterburner Air Flow is calculated by subtracting the customer bleed air flow from the engine inlet air flow. All other air flows, previously removed from the main gas stream, have been returned to the main stream by the time the afterburner is reached.

2.20 Afterburner Inlet Total Temperature, Tt6, is calculated by assuming that combustion of the main engine fuel is complete by the afterburner inlet using the afterburner airflow determined in 2.19.

2.21 The Afterburner Fuel Flow is measured by liquid turbine meters placed in the stand line upstream of the afterburner pump. Both high and low range turbine meters are available with redundant meters covering each range. The redundant meters must agree within 0.5% for the flow to be considered valid. The measured flow is corrected for fuel specific gravity and meter growth due to fuel temperature and pressure. A fuel sample specific gravity is measured every hour.

2.22 Total Engine Fuel Flow is calculated by adding the main fuel flow rate to the afterburner fuel flow.

2.23 Ideal Afterburner Temperature Rise is obtained by calculating the ideal temperature rise available from the afterburner fuel flow and air flow with adjustments for vitiation (afterburner inlet gas is partially burned).

2.24 Nozzle Total Pressure, Pt8, is measured by a water cooled total pressure rake containing 42 total pressure probes. The rake is located one to five inches down stream of the nozzle exit. An effort is made to hold the nozzle exit Mach number close to one, by controlling the nozzle exit pressure, so that errors in total pressure reading caused by shocks, and expansion of the exhaust stream are kept to a minimum. The pressures, within the confines of the nozzle area are averaged to give "one dimensional" exhaust nozzle total pressure.

2.25 Afterburner Pressure Loss; is obtained by subtracting the measured value of nozzle total pressure, Pt8, (section 2.24) from the estimated mixed value of afterburner inlet total pressure, Pt6, that is determined from the mass weighted average of measured turbine discharge pressure, Pt5, (section 2.17), and the effective bypass duct discharge pressure (section 2.18).



## APPENDIX 3

### PROPULSIVE FORCE ACCOUNTING PROCEDURE

#### 1. SUMMARY

The propulsive force on a nacelle is broken down into inlet, engine and nozzle components. In this breakdown it is current practice to reference engine thrust to free stream inlet conditions. The engine is credited with increasing momentum from free stream conditions to the exhaust whereas it only increases momentum from the engine inlet to the exhaust. This procedure gives the correct installed performance when combined with inlet performance as it is currently defined.

Engines are tested with a bellmouth and inlet screen. Performance is required at free stream inlet conditions. A method of correcting thrust from test inlet conditions to free stream inlet conditions is derived in this Appendix.

#### 2. SYMBOLS FOR APPENDIX 3

A	Projected area normal to the thrust axis - sq ft
Fb	Thrust obtained from a bellmouth - screen combination on a sea level test stand - lb
Fe	Thrust obtained from an engine on a sea level test stand. - lb
Fg	Gross thrust - lb
Fn	Engine net thrust - lb
Fp	Propulsive force from nacelle - lb
g	Gravitational constant 32.2 ft/sec <sup>2</sup>
Pam	Ambient pressure - lb/ft <sup>2</sup>
P	Static pressure - lb/ft <sup>2</sup>
Pt	Total pressure - lb/ft <sup>2</sup>
W	Flow lb/sec
Ws1	Air spilled before cowl lip - lb/sec
Ws2	Inlet bleed air discharged after the cowl lip and before the engine face -lb/sec
Ws3	Air bypassing the engine that is discharged in the ejector in the JT11D-20 installation -lb/sec
V	Axial component of velocity along thrust axis - ft/sec

#### Suffixes

o	Entry to the control surface
c	Capture, cowl lip.
max	Maximum cross-sectional area of the nacelle.
2	Engine inlet.
8	Primary nozzle exhaust
9	Ejector exit.

#### 3. NACELLE PROPULSIVE FORCE

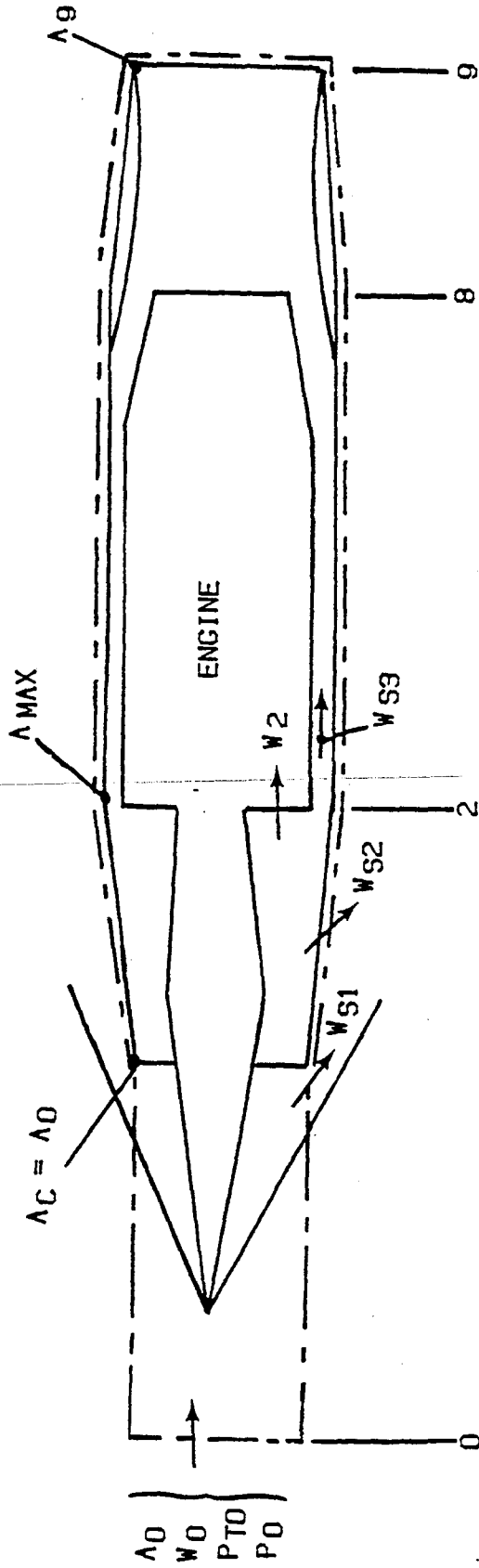
The propulsive force of a nacelle can be determined by integrating the impulse around any closed control surface that surrounds the nacelle. The control surface, shown by chain dotted lines on Figure 3.1, starts at free stream conditions where it has the same area as the inlet capture area, maintains the same area to the cowl lip, follows the nacelle contour to the nacelle exit (A<sub>9</sub>) and then closes across the jet plume.

The propulsive force is the integral of the axial component of impulse around the control surface.

$$F_p = \oint \left( \frac{WV}{g} + PA \right) \quad -(1)$$

FIGURE 3.1

NACELLE CONTROL SURFACE



Expanding equation (1)

$$F_p = -\frac{W_o V_o}{g} - P_{am} A_o + \frac{W_{s1} V_{s1}}{g} + \frac{W_{s2} V_{s2}}{g} - \int_{A_c}^{A_{max}} P dA + \int_{A_2}^{A_{max}} P dA + \frac{W_9 V_9}{g} + P_9 A_9 \quad (2)$$

The integral of a fixed pressure such as ambient pressure around any closed contour is zero.

Therefore:

$$0 = -P_{am} A_o - P_{am} (A_{max} - A_c) + P_{am} (A_{max} - A_2) + P_{am} A_2 \quad (3)$$

For flow balance:

$$W_o = W_2 + W_{s1} + W_{s2} + W_{s3} \quad (4)$$

$$\text{and } W_9 = W_2 + W_{s3} + \text{Fuel flow} \quad (5)$$

Using equation (4) to substitute for  $W_o$  in equation (2), subtracting equation (3) from equation (2) and rearranging gives

$$F_p = \underbrace{\frac{W_9 V_9}{g} + (P_9 - P_{am}) A_2}_{\text{gross thrust of primary and secondary streams}} - \underbrace{\frac{(W_2 + W_{s3}) V_o}{g}}_{\text{Ram drag of primary and secondary streams}}$$

Net thrust of primary and secondary streams

$$- \underbrace{\frac{W_{s1} (V_o - V_{s1})}{g}}_{\text{Additive drag}} - \underbrace{\int_{A_c}^{A_{max}} (P - P_{am}) dA}_{\text{Inlet pressure drag}} - \underbrace{\frac{W_{s2} (V_o - V_{s2})}{g}}_{\text{Bleed drag}}$$

Inlet Drag

$$- \underbrace{\int_{A_2}^{A_{max}} (P_{am} - P) dA}_{\text{Afterbody pressure drag}}$$

(6)

Equation (6) shows the conventional accounting system for propulsive thrust. The gross thrust of primary and secondary streams is the sum of momentum and pressure-area terms at the nacelle exit (station 9). The net thrust of primary and secondary streams is equal to the gross thrust minus the ram drag of the primary and secondary streams which is evaluated at free stream momentum. Consequently, the engine is credited with raising momentum from free stream condition (station 0) to nacelle exit (station 9); whereas the engine only increases momentum from station 2 to station 9. The difference in propulsive force between stations 0 and 2 is charged to inlet drag.

The difference in propulsive force between stations 0 and c is called additive drag. It is equal to the loss in momentum of the air spilled before the cowl lip. An alternative description of additive drag, which has the same numerical value, is the pressure-area term along the boundary streamline of the air entering the inlet. Since  $W_{s1}$  can change the inlet pressure drag, the change in inlet pressure drag due to  $W_{s1}$  is included in additive drag. For a subsonic inlet, loss of momentum due to increasing  $W_{s1}$  is approximately cancelled by lip suction caused by  $W_{s1}$ . Consequently, subsonic inlets with rounded lips have little or no additive drag.

Loss of total pressure from station 0 to station 2 is charged to inlet ram recovery. The bleed that is used to stabilize the inlet boundary layer ( $W_{s2}$ ) gives inlet bleed drag. There are two components of bleed drag: the loss of momentum due to bleed and the increase in inlet pressure drag due to discharging the bleed.

Inlet drag therefore consists of three terms: pressure drag defined with no spillage and no bleed, additive drag which includes the effect of spillage forward of the cowl lip and bleed drag which includes the effect of bleed discharged overboard before the compressor face.

#### 4. SEA LEVEL THRUST MEASUREMENT

Sea level static thrust is measured with a bellmouth to provide smooth flow to the engine inlet and with a screen in front of the bellmouth to prevent foreign object damage.

The thrust we would like to measure on a sea level stand, is the thrust at free stream inlet conditions to be consistent with nacelle thrust. At sea level static, these conditions are an engine inlet total pressure equal to ambient pressure i.e., no inlet screen and zero forward velocity, i.e., no ram drag.

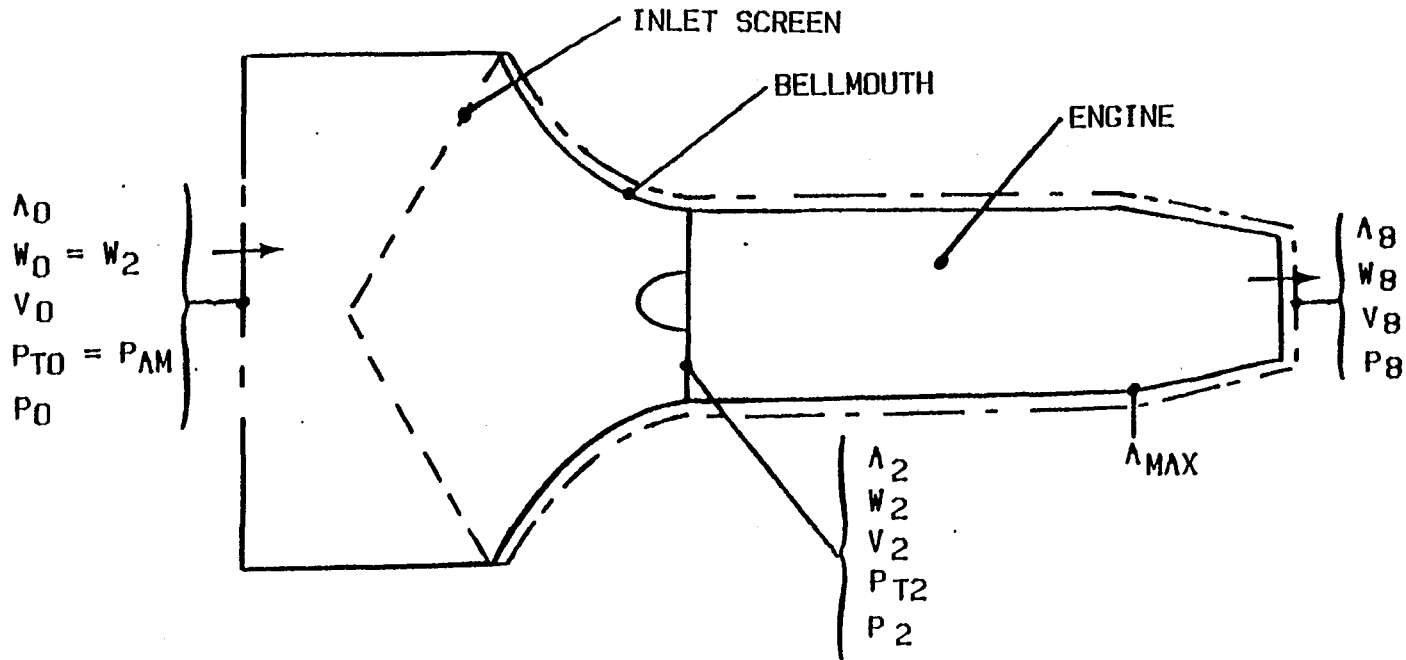
Because of the inlet screen the engine inlet total pressure is less than ambient pressure. An alternative procedure to having inlet total pressure equal ambient pressure is to evaluate performance at an ambient pressure that is equal to the inlet total pressure, i.e., the exhaust back pressure equal to inlet total pressure.

The required sea level static thrust at an inlet total pressure of  $P_{t2}$  and an exhaust static pressure equal to  $P_{t2}$  is:

$$F_n = F_g = \frac{W_8 V_8}{g} + (P_8 - P_{t2}) A_8 \quad -(7)$$

FIGURE 3.2

CONTROL SURFACE FOR A SEA LEVEL STATIC THRUST BED



-142-

445

Consider a bellmouth, inlet screen, engine combination as shown in Figure 3:2. The control surface, shown by chain dotted lines, has the same maximum diameter as the bellmouth, follows the external contour of the bellmouth and engine and cuts across the flowpath ahead of the bellmouth and behind the engine. It is assumed in this analysis that the bellmouth has a cylindrical extension following the control surface so that all the air entering the bellmouth passes through area  $A_0$  with uniform axial velocity  $V_0$ , whereas a real bellmouth has radially inwards flow through the cylindrical portion of the control surface ahead of the bellmouth.

The action of the bellmouth, inlet screen, and nose cone changes the impulse function of the air passing through the bellmouth:

$$\begin{aligned}
 \frac{W_2 V_2}{g} + P_2 A_2 &= \frac{W_0 V_0}{g} + P_0 A_0 - \underbrace{\int_{A_{max}}^{A_0} PdA}_{\text{Bellmouth}} \\
 - \underbrace{\int_{A_2}^{A_{max}} PdA}_{\text{Nose cone}} &- \underbrace{(P_{am} - P_{t2}) A_0}_{\text{Screen loss}} \qquad \qquad \qquad - (8)
 \end{aligned}$$

The thrust produced by the inlet air on the bellmouth and screen is the axial component of the pressure times area terms acting on the hardware:

$$F_b = -(P_{am} - P_{t2}) A_0 - \int_{A_{max}}^{A_0} PdA + P_{am} (A_0 - A_{max}) \qquad \qquad \qquad - (9)$$

From equations (8) and (9):

$$\frac{W_2 V_2}{g} + P_2 A_2 = \frac{W_0 V_0}{g} + P_0 A_0 + F_b - P_{am} (A_0 - A_{max}) - \int_{A_2}^{A_{max}} PdA \qquad \qquad \qquad - (10)$$

The thrust force produced by the engine is:

$$\begin{aligned}
 F_e = & \underbrace{\frac{W_8 V_8}{g} + P_8 A_8}_{\text{Exit impulse}} - \underbrace{\frac{W_2 V_2}{g} - P_2 A_2}_{\text{Inlet impulse}} \\
 & - \underbrace{\int_{A_2}^{A_{max}} P dA}_{\text{Nose cone}} + \underbrace{\int_{A_8}^{A_{max}} P dA}_{\text{Boattail}}
 \end{aligned} \tag{11}$$

Combining equations (10) and (11), using  $W_0 = W_2$

$$\begin{aligned}
 F_e + F_b = & \frac{W_8 V_8}{g} + P_8 A_8 - \frac{W_2 V_0}{g} - P_0 A_0 \\
 & + P_{am} (A_0 - A_{max}) + \int_{A_8}^{A_{max}} P dA
 \end{aligned} \tag{12}$$

The integral of ambient pressure around the control volume is zero:

$$0 = - P_{am} A_0 + P_{am} (A_0 - A_{max}) + P_{am} (A_{max} - A_8) + P_{am} A_8 \tag{13}$$

Subtracting equation (13) from equation (12) and rearranging:

$$\begin{aligned}
 \frac{W_8 V_8}{g} + (P_8 - P_{am}) A_8 = & F_e + F_b + \frac{W_2 V_0}{g} + (P_0 - P_{am}) A_0 \\
 & - \int_{A_8}^{A_{max}} (P - P_{am}) dA
 \end{aligned} \tag{14}$$

From equations (7) and (14) the required thrust at an engine inlet pressure  $P_{t2}$  is:

$$\begin{aligned}
 \underbrace{F_n = F_g}_{\text{Required Thrust}} = & \underbrace{F_e + F_b}_{\text{Measured thrust with the bellmouth mounted on the thrust bed}} + \underbrace{(P_{am} - P_{t2}) A_8}_{\text{Screen pressure loss correction}} + \underbrace{\frac{W_2 V_0}{g} + (P_0 - P_{am}) A_0}_{\text{Bellmouth}} \\
 & - \underbrace{\int_{A_8}^{A_{max}} (P - P_{am}) dA}_{\text{Boattail}}
 \end{aligned} \tag{15}$$

JT11D-20 practice is to mount a bellmouth and inlet screen on open air thrust bed, apply the screen pressure loss correction shown in equation (15) and then correct the data to standard inlet pressure standard inlet temperature and nominal turbine temperature. The bellmouth and boattail corrections of equation (15) are ignored: the resultant thrust is usually a fraction of 1% lower than the value that would be obtained using all these corrections.

Figure 3.3 shows the magnitude of the bellmouth correction calculated from one-dimensional equations for the bellmouth with a cylindrical extension shown in Figure 3.2. It is noted that the radially inward flow at the entry of a real bellmouth will reduce the magnitude of the bellmouth correction shown in Figure 3.3. It can be seen that bellmouth areas greater than 10 times the inlet area contribute little to measured thrust.

The boattail correction is only significant if there is a substantial boattail area, as with a convergent nozzle. If a convergent nozzle has a pressure ratio less than 2, the aspiration of the jet reduces pressures on the boattail causing a drag force on the thrust bed and a positive boattail thrust correction. If a convergent nozzle has a pressure ratio significantly higher than ambient, then pressures on the boattail may be higher than ambient resulting in a thrust force and a negative boattail thrust correction. For an open air, sea level, stand, the boattail corrections are usually small and ignored. However, if the test stand configuration may give rise to boattail pressures significantly different than ambient, then pressures should be measured on the boattail and, possibly, the external surfaces of the bellmouth and the resultant, experimentally - determined, correction applied. Pressures different from ambient may be caused by an ejector, baffles or secondary flow in the test stand.

It is noted that although the inlet screen has a projected area  $A_o$  in Figure 3.2 the screen pressure loss correction in equation (15) uses a much smaller projected area,  $A_8$ . This is because although the screen produces a drag force acting on Area  $A_8$  the resulting lower pressures throughout the bellmouth and engine produce compensating thrust forces, so the net area giving a drag force is  $A_8$ . The measured thrust is also reduced by the pressure loss, but this is accounted for by applying a pressure recovery correction from  $P_{t2}$  to  $P_{am}$ .

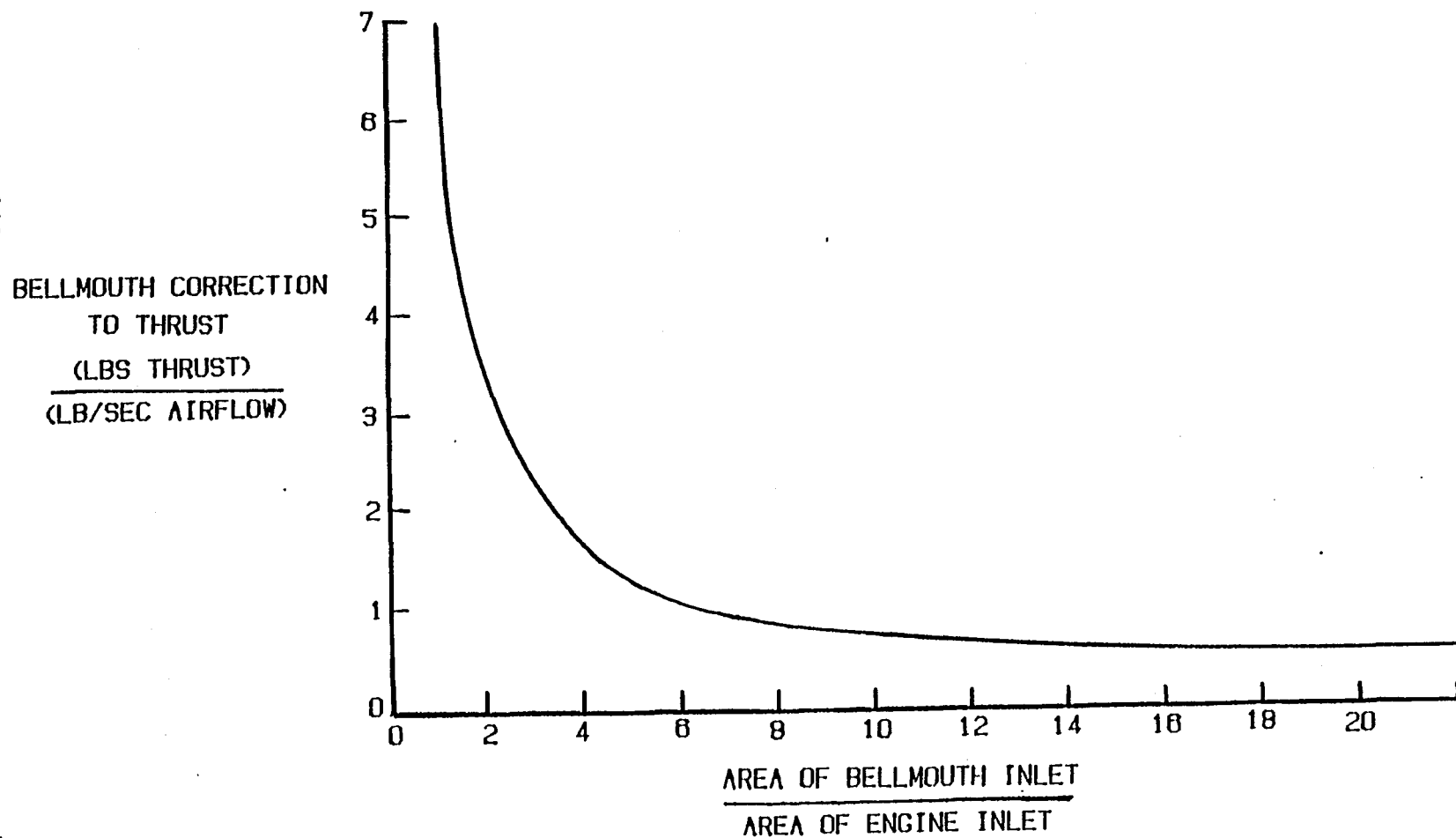


FIGURE 3

EFFECT OF BELLMOUTH SIZE ON MEASURED SEA LEVEL THRUST

ASSUMPTIONS :

- BELLMOUTH CONFIGURATION SHOWN IN FIGURE 3.2
- MACH NUMBER AT ENGINE INLET = 0.4
- NOSE CONE AREA NEGLECTED



-146-

6/17

## DUP PROJECT

Suggest a group size of 4 to 6 people with a provision that the group may split up if they cannot agree on an approach. Individual contributions are permitted. Each group or sub-group is required to complete the entire assignment.

- 1) Invent an exhaust nozzle that has the capability of vectoring gross thrust over a pitch range from  $5^\circ$  upwards to  $20^\circ$  downwards and also has all the capabilities of the JT11D-20 blow-in-door ejector nozzle.
- 2) Assumptions  
Design operating conditions Mach 3.0, 80,000 ft altitude.  
Ram Recovery 0.85  
10% Inlet bleed air discharged through ejector nozzle with a total pressure 5.0 times ambient pressure.  
Inlet aligned with the free stream velocity vector.  
Aircraft lift/drag ratio 5.0  
Exhaust nozzle temperature  $3200^\circ\text{F}$   
Exhaust pressure same as engine inlet total pressure  
Fuel lower heating value 18,500 BTU/lb  
Jet area 6 sq ft.  
Nozzle entry area 8 sq ft  
Constant cross sectional area between afterburner entry and nozzle entry.  
6% loss in total pressure between afterburner entry and nozzle exit.  
2500 psi hydraulic system  
If there is insufficient information to solve the problem then make additional assumptions as required. If there is too much information, then discard unnecessary information. Document additional assumptions and discarded information.
- 4) Define a bookkeeping system that accounts for thrust vector angle when describing lift, thrust and drag.
- 5) Define the thrust vectoring angle that will provide the best lift/drag ratio for cruise operation.
- 6) Write a report describing your invention that includes the following information:
  - Benefits
  - Problems or Penalties
  - Failure modes and the effect of failure
  - What is the effect on lift/drag ratio of 1% leakage from your nozzle into the secondary airstream?
  - Which are the key assumptions that affect your design? What happens if the assumptions are wrong? Is the design robust, i.e. is it still valid if the assumptions are not correct?
  - Size of thrust vector actuators
  - How are thrust vector loads transmitted to the airframe?
  - Will differential expansion cause thrust vectoring?
  - How will your thrust vector controls be integrated or coordinated with the engine controls? the airframe controls?
- 7) Prepare a verbal presentation limited to 10 slides and 15 minutes to sell your idea. Select one of the group to make the presentation.